

Contents lists available at ScienceDirect

Progress in Materials Science

journal homepage: www.elsevier.com/locate/pmatsci





The role of interstitial constituents in refractory complex concentrated alloys

Calvin H. Belcher*, Benjamin E. MacDonald, Diran Apelian, Enrique J. Lavernia

Department of Materials Science and Engineering, University of California, Irvine, Irvine, CA 92617, USA

ARTICLE INFO

Keywords:
Refractory Complex Concentrated Alloys
Interstitial impurities
Refractory Alloys
Refractory High Entropy Alloys
Metal Processing
Intrinsic Ductility

ABSTRACT

To meet the growing demand for transportation and energy consumption around the world, more efficient turbine engines and power generators with higher operating temperatures are needed, which require alloys with retained strength levels at elevated temperatures. In the past decade, refractory complex concentrated alloys (RCCAs) have gained prominence through numerous reports of superior strengths at higher homologous temperatures compared to those of conventional refractory and super alloys. However, these RCCAs, comprised of transition metals from subgroups IV, V, and VI, tend to be brittle at room temperature, hindering their broad applicability. Recent findings reveal that interstitial constituents may significantly contribute to, and convolute observations of, the ductility and strength of RCCAs at room temperature. This review of the literature examines and discusses the field's current understanding of the role of interstitial constituents, specifically oxygen and nitrogen, in the microstructure and mechanical behavior of RCCAs. Moreover, we provide context derived from the binary interactions of interstitial constituents with refractory metals and their contribution to the development and processing of conventional refractory alloys as a framework to gain insight into interstitial constituent mechanisms in RCCAs. In some cases, the mechanisms of interstitial constituents in RCCAs are similar to those of unalloyed subgroup VI transition metals and their dilute alloys, segregating to and embrittling grain boundaries. In other cases, interstitial constituents can be accommodated in solid solution, strengthening the RCCA, similar to interstitial constituents soluble in unalloyed subgroup IV and V metals and their dilute alloys. With the understanding of interstitial constituent element interactions with RCCA constituents, more holistic approaches to the design of RCCAs are suggested to engineer the mechanisms of intended and unintended interstitial constituents through alloy design and processing. For the development of strong and ductile RCCAs, the interactions between interstitial constituents and RCCA constituents and their resulting mechanisms must be understood and controlled.

1. Introduction

As the demand for global transportation and energy consumption grows, safer and more efficient turbine engines and power generators are needed. Significant improvements to the efficiency of engines and generators are readily achievable by increasing their maximum operating temperatures [1–5]. In turn, the operating temperatures of engines and generators are limited by the elevated

E-mail address: cbelcher@uci.edu (C.H. Belcher).

https://doi.org/10.1016/j.pmatsci.2023.101140

Corresponding author.

temperature strengths and stabilities of the structural materials comprising them. The development of alloys which retain their strengths at ever increasing high temperatures is necessary for more efficient global energy production and use. However, alloys with high temperature strength generally tend to be brittle and difficult to machine or fabricate into components at room temperature. So, historically, other turbine engine technologies, such as cooling channels, and high temperature coatings have been developed to extend the operating temperature ranges of conventional structural alloys and superalloys. In Fig. 1 below, the development trends for turbine engines and their theoretical maximum efficiency with respect to the turbine inlet temperature is shown, reprinted from Perepezko [1].

As shown in Fig. 1, while incrementally higher operating temperatures and efficiencies can be achieved through improvements in cooling and coating technologies, ultimately, alloys with higher temperature strengths are necessary to achieve closer to theoretical Carnot efficiency performance, meaning no inefficiencies due to heat losses [1,5]. Significant gains to engine efficiency were made in early development of Ni-based superalloys with improved alloy strengths at elevated temperatures and incremental gains to efficiency were made with cooling and coating technologies [1,6]. To bring turbine engines and power generators closer to theoretical performance efficiency, alloys with ideal combinations of high temperature properties and room temperature ductility are urgently needed. Given recent advances in metallic alloy development, a revived emphasis on alloy design for improved high temperature applications has emerged.

As a new class of metallic materials, high entropy alloys (HEAs) have significantly broadened the compositional space for alloy design [7]. HEAs were first discovered in 2004 and were originally defined as single phase, random solid solution alloys consisting of 5 or more constituent elements in equiatomic or near-equiatomic compositions [8,9]. Over time, some HEA systems were found to exhibit unique combinations of properties. For example, the CoCrNi system exhibited exceptional strain to failure and fracture toughness at room temperature and showed unexpected increased strength, ductility, and fracture toughness at cryogenic temperatures [10,11]. The exceptional macroscale properties of these HEA systems were attributed to unique mechanisms and thermodynamic properties of the non-dilute compositions of the alloys [12]. Eventually, the design and development of HEAs shifted toward the use of targeted mechanisms unique to non-dilute solutions of metal elements for improved mechanical behavior. With the shift in HEA design approaches, these non-dilute alloys came to be known as complex concentrated alloys (CCAs) for the complex mechanisms which could be targeted in their design for improved properties [13]. Within the broad variety of CCAs, refractory complex concentrated alloys (RCCAs) have been developed and studied for their potential use in high temperature applications.

Recently, a large focus has been directed at RCCAs to broaden the compositional design space to enable the development of alloys for high temperature applications. In general, RCCAs are made up of 3 or more refractory elements in equiatomic or near-equiatomic ratios and often have a body centered cubic (BCC) crystal structure [13,14]. A schematic diagram of a few BCC unit cells of a RCCA is shown below in Fig. 2.

The constituent refractory elements of a RCCA often form a single phase BCC random solid solution with some lattice distortions and equal probabilities of elements occupying the sites of the BCC cell, but interactions between the constituent refractory elements may also result in the formation of new phases or even short- or long-range ordering. In the BCC structure in Fig. 2 above, lattice distortions are depicted for clarity but are not necessarily to scale and do not imply severe lattice strain in RCCAs compared to conventional alloys [15]. However, differences in atomic sizes at each site may result in distortions to the lattice and thus may also

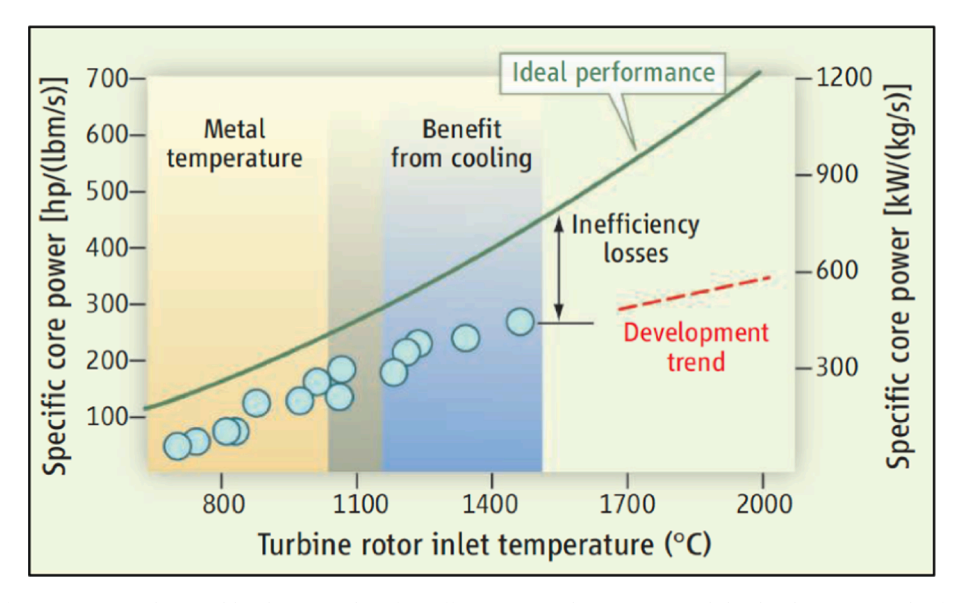


Fig. 1. Ideal performance curve, theorized by the principles of an efficient Carnot heat engine, and the development trends of turbine engines at increasing engine inlet temperatures, reprinted from Perepezko [1]. Each data point represents a specific engine and its power losses and the theoretical Carnot efficiency of the engine and development trend curves are sectioned by superalloy developments, increasing high temperature capabilities, and improvements to engine designs through cooling technologies.

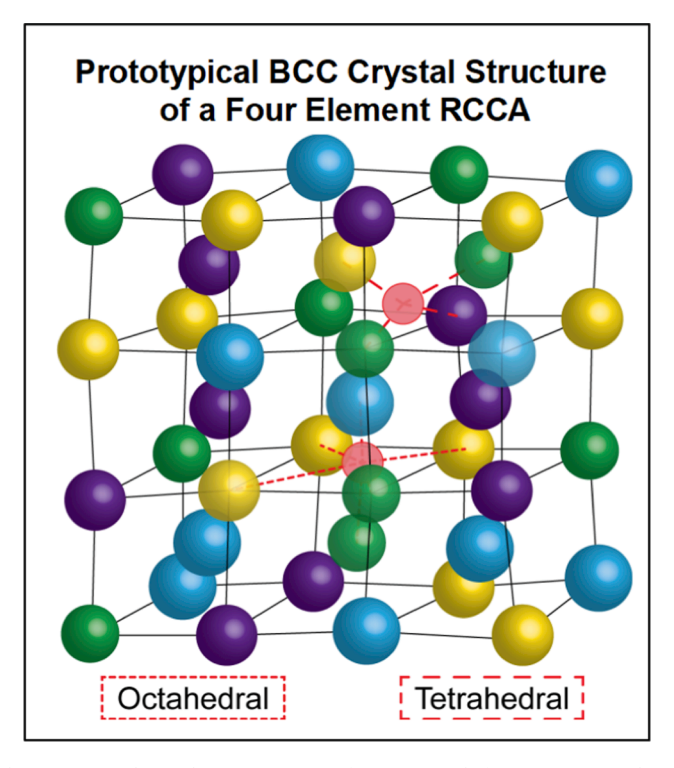


Fig. 2. A schematic diagram of the prototypical BCC lattice structure of a RCCA with four constituent elements with an equal probability of occupying any given lattice site; each color represents a different refractory transition metal element. The two distinct interstitial sites available in the BCC lattice are identified with red spheres as possible interstitial elements. (For interpretation of the references to color in this figure legend, the reader is referred to the web version of this article.)

result in a range of interstitial site sizes within the lattice. The term refractory elements typically refers to those with melting temperatures above 2000 °C and include Nb, Ta, Mo, W, and Re [3,16,17]. Broader definitions used when designing RCCAs often include metal elements from subgroups IV, V, and VI of the transition metals from the periodic table [18]. RCCAs have drawn significant attention for their capacity to achieve higher strengths at higher homologous temperatures than conventional refractory alloys, as shown in Fig. 3 (a) below from Wang et al. [19]. However, the application of many RCCAs studied to date has been limited by their relatively poor ductility at room temperature as shown by the trends in tensile elongation of RCCAs with high yield strengths in Fig. 3 (b) below from Senkov et al. [20].

The first RCCAs were discovered in 2010 and 2011 by Oleg Senkov et al. [14,21,22]. Since their discovery in 2010, nearly 1,400 studies related to RCCAs have been published as of the end of 2022 and the number of studies continues to grow. RCCAs stand out due to their unparalleled mechanical properties at temperatures over 800 °C, and even up to 1500 °C. Since RCCAs retain higher strengths at higher temperatures than conventional Ni-based superalloys and other conventional refractory alloys RCCAs appear to be promising candidates for high-temperature structural applications, [14,19,23]. By comparison, Ni-based superalloys, such as 718+, achieve strengths up to 1.5 GPa but steeply drop off beyond 600 °C, limiting their temperature ranges for application when compared to RCCAs [6]. However, Ni-based superalloys have undergone several decades of development and optimization to achieve alloys with cohesively balanced properties ideal for structural, high temperature turbine applications such as room temperature ductility, elevated temperature creep strength, moderate oxidation resistance, and density [6]. Though higher strength values at higher temperatures have been achieved in RCCAs, the only published creep strength of a RCCA, up to now, did not exceed those of Ni-based superalloys [24,25]. While RCCAs present opportunities to extend the operating temperatures beyond those currently achievable with conventional high temperature structural alloys, there are challenges that must be resolved before they can replace Ni-based superalloys; these include their relatively poor ductility at room temperature, and their less-than-optimum oxidation resistance at elevated temperatures. Extensive efforts in the development of RCCAs have focused on attaining room temperature ductility and defining the criteria and correlations necessary to achieve an alloy with room temperature ductility as well as high temperature stability and strength [20,26]. While a few RCCA systems have been found to have high strength and ductility, the criteria for the development and design of strong, ductile RCCAs is not fully understood.

As the field has grown, the criteria for strength and ductility in RCCAs has evolved. In conventional BCC alloys, high strength, brittle behavior is often attributed to sluggish screw dislocation motion and high Peierls stresses between atoms [19]. Compared to conventional BCC alloys, the strength of BCC RCCAs is thought to be dependent on increased solute strengthening and local chemical fluctuations which impede dislocation motion. The screw dislocations in RCCAs may readily form kinks due to compositional fluctuations in the lattice and the strength of RCCAs may depend on kink migration and cross-kink pinning and formation [19,23,27–29].

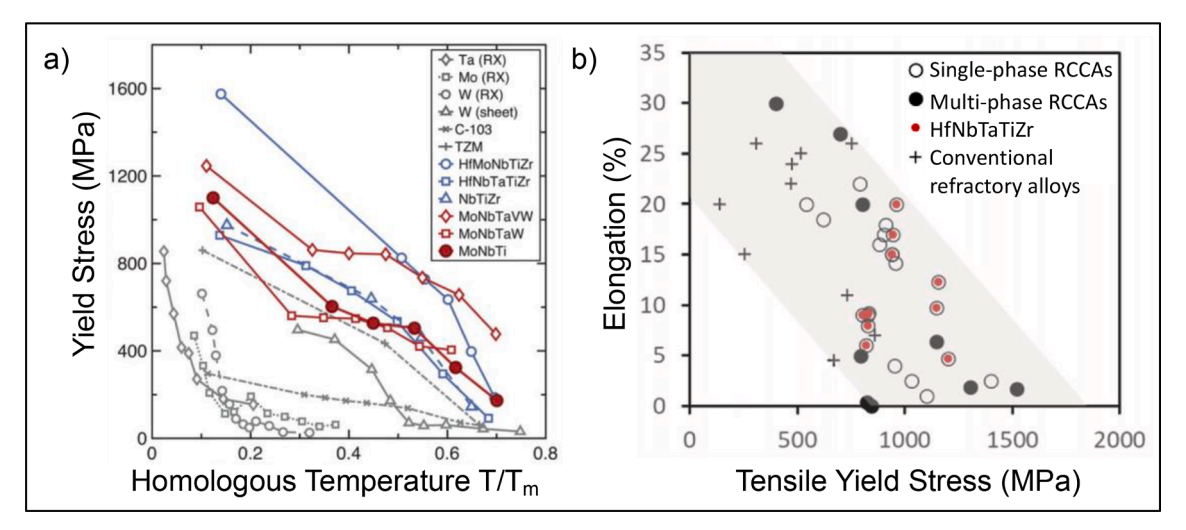


Fig. 3. Plots of RCCA mechanical properties, examining (a) strengths at elevated temperatures, relative to respective melting temperatures and (b) trends in tensile elongation to fracture with respect to the tensile yield strengths of respective RCCAs at room temperature, reprinted from Wang et al. and Senkov et al. [19,20]. In both, conventional refractory alloys are included for comparison to RCCAs.

Ultimately, the precise mechanisms of dislocation motion in RCCAs require additional research and are not the only criterion needed for the development of strong, ductile RCCAs. Initially, the intrinsic ductility of RCCAs was considered inherent to the constituent elements and their effects on dislocation motion in a single phase, random solid solution. One of the earliest proposed predictors of ductility in an RCCA is the alloy's valence electron concentration (VEC) [20,30]. This criterion suggests that an RCCA with VEC below 4.5 would have a ductile to brittle transition temperature (DBTT) at or below room temperature and would thus be intrinsically ductile [30]. Other recent predictions include Pugh-Pettifor, and Rice-Thomson criteria which considered the constituent elements and their resulting lattice parameters and thus Burgers vector lengths and shear moduli. Many of these criteria used in the predictions of intrinsic ductility assume the interactions between the RCCA constituent elements are in a single phase, solid solution and may not account for complex microstructural features or deformation mechanisms. Recently, Senkov et al. proposed that limitations to maximum yield strength may be necessary to develop RCCAs which still have high room temperature ductility [20,31]. However, this may prevent the opportunity to develop an RCCA with a superior combination of high strength and high ductility at room and elevated temperatures. Up to now, many of the proposed criteria have been based on assorted empirical data and from various studies of RCCAs with differences in microstructural features and unreported interstitial constituents in the RCCAs as well as idealized screw dislocation motions in BCC RCCAs. Observation of the DBTT of refractory BCC metals also depends on conditions such as loading rates, microstructural features, and impurities [32-35]. Impurities present in RCCAs may have a significant effect on the DBTT and thus the observed ductility [36]. By understanding the mechanisms by which interstitial impurities influence the mechanical behavior of RCCAs, high strength, ductile RCCAs can be developed. Since the determination of a high strength RCCA with intrinsic room temperature ductility is dependent on the constituent elements of the alloy, the interactions between the constituent elements and unintended interstitial impurities present in the alloy should be considered.

In recent literature, the importance of impurities in RCCAs has been underscored with respect to phase stabilities and mechanical properties. Specifically, focus has been toward the influence of interstitial oxygen and nitrogen impurities on the mechanical properties of RCCAs [37–46]. However, the precise mechanisms of various interstitial impurities in various RCCAs are often convoluted, not documented, and difficult to isolate and control. In some studies, interstitial impurities were inadvertently introduced due to steps required during synthesis and processing of the RCCAs. Initially, the unintended interstitial impurities in the range of 100 s of ppm were acknowledged and studied because they detrimentally segregated to grain boundaries (GBs) and embrittled the host RCCAs [45]. In other studies, unintended interstitial impurities did not contribute to detrimental mechanical properties in some RCCAs and the influence of interstitial impurities as constituents was studied when intentionally added in the range of several at. % [38,39,43]. Thus, for the development of strong and ductile RCCAs, the mechanisms by which impurities influence microstructural features and mechanical properties must be understood and established. The various microstructural features observed as the products of interstitial impurity interactions with RCCA constituents are schematically illustrated and summarized in Fig. 4 below.

As depicted in Fig. 4, some interstitial impurities intentionally added in RCCAs yield mechanisms which increased strength and ductility [39–41,46]. In other cases, trace amounts of interstitials in RCCAs were observed to segregate to grain boundaries and severely embrittle the alloys [37,44,45]. By understanding the mechanisms of interstitial impurities in RCCAs, and the influence of the various mechanisms on mechanical properties, additional criteria for more holistic design of strong and ductile RCCAs can be formulated. Compared to the state-of-the-art knowledge of impurities in RCCAs, the thermodynamics and kinetics of interstitial impurity interactions in conventional BCC refractory metals are well understood and have been used in the development of conventional refractory alloys [1–4]. With the context of impurity interactions in conventional refractory metals and alloys, a close examination of recent RCCA publications can yield an understanding of the influence of impurities on mechanical properties and can be utilized for

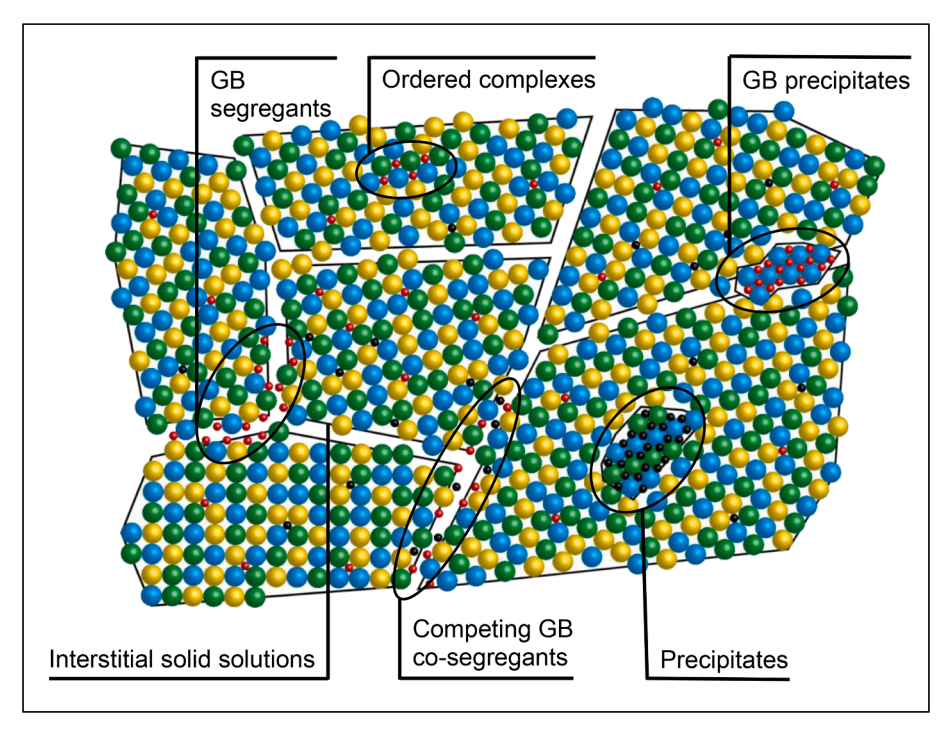


Fig. 4. A schematic diagram of the various microstructural features which have been observed in RCCAs with interstitial impurities. The microstructural features depicted in this figure have not all been observed in the same microstructure or same RCCA, but each feature has an observed influence on the mechanical behavior of an alloy.

more holistic design of RCCAs with high strength and ductility.

In view of the above discussion, the objective of this review is to establish our current understanding of the influence of interstitial impurities on the mechanical behavior of RCCAs for the holistic design of ductile RCCAs. By examining published studies focused on RCCAs with intended and unintended interstitial impurities, considerations to design RCCAs with intrinsic ductility will be developed. In the first section of this review, the sources of interstitial impurities in conventional refractory alloys and in RCCAs will be presented and the mechanisms driving interstitial impurity absorption are discussed. Then, state-of-the-art understanding of the mechanisms of interstitial impurities, specifically oxygen and nitrogen, in pure refractory metals, defined as the transition metals in subgroups IV, V, and VI, will be presented and established through examination of conventional synthesis and processing techniques and previously published experimental and computational results. The development of dilute conventional refractory alloys with respect to interstitial impurity element interactions will also be described. In the following section, the observations of interstitial impurities in two RCCA systems, MoNbTaW and HfNbTaTiZr, will be contextualized from the knowledge of conventional refractory metals and alloys. This will be followed by criteria for more holistic design of strong and ductile RCCAs based on an understanding of the influence of interstitial impurities on the mechanical properties of various RCCAs. Finally, the scientific gaps in the current knowledge of interstitial impurities in RCCAs are identified and future directions for possible research are proposed. In this review, a majority of the discussions will be focused to oxygen and nitrogen as interstitial impurity elements since these interstitials have pronounced effects on the microstructures and mechanical properties of RCCAs and hence there is a substantial amount of published data available, MoNbTaW and HfNbTaTiZr will be examined as the two model RCCA systems since these systems have the most extensive published research to date, especially with regard to interstitial impurities, and have historically driven the exploration of additional RCCA compositional spaces. Throughout the rest of this review, the interstitial impurity solvent elements, such as oxygen and nitrogen, will be referred to as interstitial constituents and the substitutional metal solute elements comprising RCCAs will be referred to as RCCA constituents since the interstitials can be thought of as expected constituent elements in alloys. Ultimately, by understanding the mechanisms by which $oxygen\ and\ nitrogen\ influence\ the\ mechanical\ properties\ of\ the\ model\ MoNbTaW\ and\ HfNbTaTiZr\ RCCAs,\ more\ holistic\ design\ criteria$ of strong and ductile RCCAs for high temperature applications can be established.

2. Sources of interstitial constituents

The interstitial constituents which end up in refractory alloys, and influence their mechanical behavior, often exist in relatively high abundance as diatomic gaseous molecules in the atmosphere. During the synthesis and processing of refractory alloys, the interstitial constituents can be introduced from the atmosphere into the alloys. Through some processing methods, especially solid-state processes such as powder metallurgical techniques, significant interstitial constituents may be inadvertently introduced and may unexpectedly alter the alloy's mechanical properties. Since such solid-state powder metallurgical techniques introduced

impurities into alloys during processing, conventional refractory alloys with lower sensitivities to impurities were developed to enable the use of powder metallurgical techniques. For example, molybdenum-hafnium alloys were developed for commercial production using conventional powder metallurgical techniques. The addition of hafnium accounted for interstitial oxygen constituents introduced into molybdenum during powder metallurgical processing, and improved the ductility of the alloy. On the other hand, some molten state processing techniques, such as vacuum melting, have been developed to degas or remove interstitial constituents from refractory alloys intended for high temperature structural applications. Such processing techniques which degas and purify alloys in the molten state have enabled the application of several refractory alloys which are relatively sensitive to interstitial constituents today. By understanding how interstitial constituents were introduced during processing, the development and use of a variety of conventional refractory alloys could be achieved. Ultimately, an understanding of the sources of interstitial constituents in RCCAs and their influence on mechanical behavior of RCCAs is necessary for the design of RCCAs with high strength and room temperature ductility.

2.1. Sources of interstitial constituents in conventional refractory alloys

During the synthesis and processing of conventional BCC refractory metals and alloys, the absorption of interstitial constituents into the metals is dictated by the thermodynamic and kinetic interactions between the metals and gases in the atmosphere at various temperatures [47–51]. To that end, refractory metal vacuum melting processes, such as consumable electrode vacuum arc remelting, (VAR) have been developed to remove gas impurities during the ingot casting process of conventional refractory alloys. VAR processes were first utilized in 1902 and have enabled the development of components for high temperature aerospace applications [52–54]. A schematic diagram of a VAR unit is shown below in Fig. 5, reprinted from Knight et al. [53].

In the consumable electrode VAR process, the electrode is melted to produce the final refractory metal or alloy to be further processed. VAR utilizes an electrical arc between the consumable electrode and the crucible floor, melting the electrode into the crucible. As the electrode is melted, the molten pool fills the crucible and the electrode is continuously lifted, maintaining a consistent arc gap between the rising molten pool and electrode. The metal vapor pressure from the melting electrode and molten pool sustain the arc and a relatively short arc gap between the melt and the electrode can be maintained. Often an external magnetic field, produced by an induction field coil, is also used to help sustain and stabilize the arc. At such short gaps in consumable electrode VAR, the arc is relatively stable and an ultra-high vacuum, around 10^{-13} Torr, can be achieved while melting the metal, effectively degassing the melt [52]. At the extremely high melting and superheat temperatures achieved during VAR, interstitial constituents may volatize as gases and be completely removed from the alloy through the vacuum pumps of the VAR process. Consumable electrode VAR processes can often achieve as few as 10 s of ppm of oxygen and nitrogen interstitial constituents left in the cast alloy [52]. At an industrial scale, this process typically requires automated movements of the electrode and crucible to maintain short arc gaps under high vacuum. Other processes used to produce refractory metals and alloys, especially solid-state techniques such as powder metallurgical approaches, do not inherently have degassing steps involved and may even be the source of interstitial constituents through mechanisms of absorption and may result in alloys with an order of magnitude more interstitial constituents. Many refractory metals still contain trace amounts of

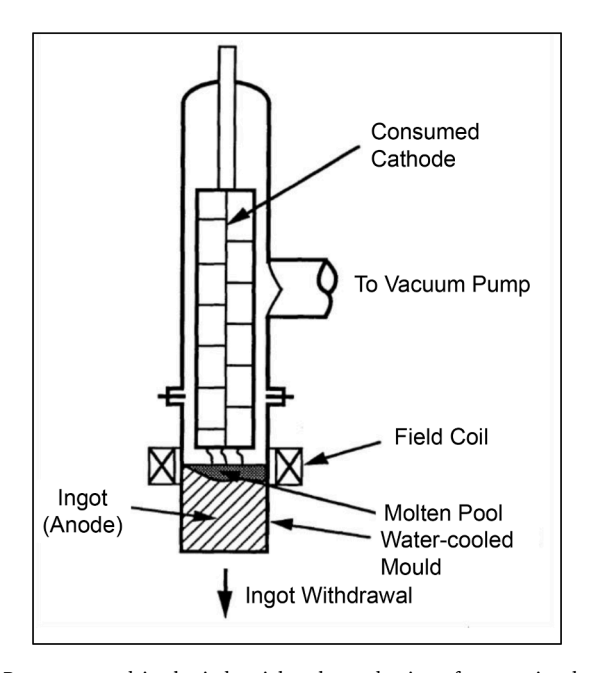


Fig. 5. Schematic diagram of the VAR process used in the industrial scale production of conventional refractory alloys for high temperature structural applications, reprinted from Knight et al. [53]. The VAR process can remove interstitial constituents and is necessary in the purification of some refractory alloys.

impurities introduced during processing steps which may influence their mechanical properties. During synthesis and processing, the absorption or degassing of interstitial constituents into the alloy are dictated by reversible reactions between the metal in its solid or molten state with gases in the environment.

The reversible reactions of gases with BCC metals initially occur by the decomposition of the various gases from the environment at the surface of the metal into individual atoms of that element. The liberated oxygen or nitrogen atoms can then diffuse into the metal lattice, interstitially, to form solid solutions or metal-nonmetal compounds [47,48,51]. In Fig. 6 (a) below, a schematic diagram of the reactions of oxygen and nitrogen gases at the surface of a metal are depicted and an Ellingham Diagram plotting the standard Gibbs free energy change (ΔG_f°) of the formation of various metal oxides, reprinted from Ellingham, is shown in Fig. 6 (b) [51].

These reactions may occur in both the solid and molten state of BCC refractory metals, but the temperature of the metal and atmospheric pressure can dictate the direction and rate of the reaction. At the surface of the metal, the reversible decomposition of the gas and reaction with the metal surface is thermodynamically driven by the temperature of the metal surface, the partial pressures of the gases in the atmosphere and metal, the possible metal-nonmetal compounds which may form, and the energetics necessary for the dissociation of the gases in the environment, as illustrated in the schematic diagrams in Fig. 6 (a). The kinetics of the reactions are limited by the physical impingement of gases at the surface of the metal, controlled by the partial pressure of the gas in the atmosphere, and the diffusion of the interstitial gas elements through the lattice of the metal [47,48,51]. Using a straight edge, the Ellingham Diagram shown in Fig. 6 (b) from H. J. T. Ellingham can be used to determine the partial pressures of oxygen and the temperatures necessary for the formation of oxides and absorption or for the degassing of oxygen from the refractory metals [51]. A straight line drawn from $\Delta G_f^{\circ} = 0$ through the temperature of a suspected oxide, e. g. Cr_2O_3 at 2000 °C, and beyond crosses through the partial pressure of oxygen necessary for oxides to form [55]. To plot Ellingham Diagrams, ΔG_f° is calculated with the assumption that all the reactants are in their standard states, limited by 1 mol of the reacting gas and is often idealized by Eqs. (1) and (2) below.

$$\Delta G_f^c = \Delta H^\circ - T \Delta S^\circ \tag{1}$$

$$\Delta G^{\circ} = -RT \ln K \tag{2}$$

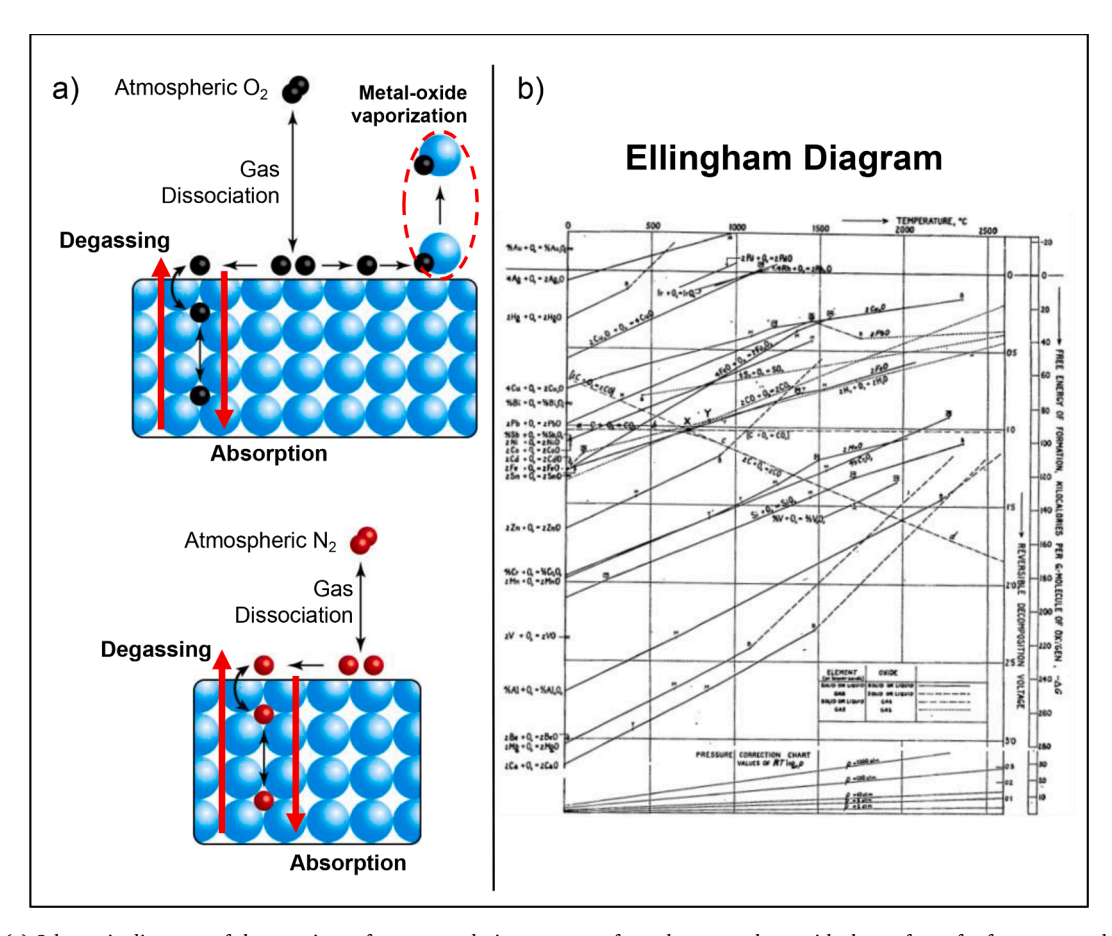


Fig. 6. (a) Schematic diagrams of the reactions of oxygen and nitrogen gases from the atmosphere with the surface of refractory metals and an Ellingham Diagram, first created by Harold J. T. Ellingham, which plots ΔG_f° of various oxides versus temperature and can be used to quantify the absorption or degassing of interstitial constituents from the atmosphere [51].

Where ΔH° is the enthalpy of the reaction, ΔS° is the entropy, R is the ideal gas constant, T is temperature, and K is assumed to be equivalent to the partial pressure of oxygen limiting the reaction. So, when observing the Ellingham Diagrams, the slope of the plotted ΔG_1° is the ΔS° , the y-intercept is the ΔH° of the reaction, and at specified temperatures, the partial pressures of gases needed to prevent or drive the reaction can be approximated. Ellingham Diagrams depicting ΔG_f° with respect to temperature of other metal-nonmetal compounds are also useful for understanding the sources of other impurities [55]. Though the ΔG° used to plot Ellingham Diagrams is specific to the formation of a compound from 1 mol of gas, in the standard state, the ΔG° of the dissociation of the gas into its individual constituents must also be considered. From Ellingham Diagrams, at intermediate temperatures and at high enough partial pressures, the gases can decompose at metal surfaces, and the individual elements can form compounds on the metal surface or diffuse throughout the metal. At high enough temperatures, such as when the metal is molten, some compounds which may form on the surface of the metal, especially oxides, may decompose and volatilize into gases. Additionally, at relatively high temperatures, and at relatively low partial pressures of gases, such as under ultra-high vacuum, the compounds within the metal may decompose, freeing interstitial constituents which can then volatize into the atmosphere. This has enabled refractory metals in the solid and molten state to be degassed at relatively high temperatures under ultra-high vacuum (10⁻¹³ Torr) [48]. Whereas at moderate temperatures and with higher partial pressures of gases (10⁻³ Torr), the gas decomposition and diffusion into the refractory metal proceeds causing the absorption of interstitial constituents into refractory metals and alloys. Because refractory alloys require such high temperatures to melt and the environments around the molten metal can be controlled, solidification processes can be useful in the degassing of refractory alloys. However, upon cooling, if the environment during various processes is not precisely controlled, interstitial constituents can inadvertently absorb into the refractory metal or alloy. By exploiting these degassing and gas absorption mechanisms, solidification processing techniques can produce metals and alloys purified of most interstitial constituents. Furthermore, the reactions between gases and metal alloys at low and moderate temperatures may result in relatively high concentrations of interstitial constituents in alloys produced through solid state techniques which generally require low temperature.

2.2. Sources of interstitial constituents in RCCAs

Just as synthesis and processing is necessary in the development of conventional refractory alloys, the synthesis and processing of RCCAs, may be utilized to control the bulk compositions and mechanisms of interstitial constituents in RCCAs. In the past decade, RCCAs have been synthesized via solidification processes, powder metallurgical techniques, and thin film deposition techniques to understand and develop RCCAs. Each of these synthesis techniques has its own advantages and disadvantages for controlling interstitial constituents and their mechanisms in RCCAs. Vacuum arc melting (VAM) has enabled the exploration of RCCA compositions with industrially representative microstructures and is one of the most common methods to produce RCCAs. Unlike industrial-scale consumable electrode VAR, VAM processes in laboratory-scale settings use a non-consumable tungsten electrode in an inert gas atmosphere to conduct a plasma arc which melts the feedstock constituent elements in a water-cooled copper crucible. Since non-consumable electrode VAM processes are not actually melting under a vacuum, it may be misleading to refer to them as VAM. Instead, the term plasma arc melting (PAM) is often used in industry and conventional refractory alloy development literature to refer to non-consumable electrode arc melting processes in inert atmospheres. Through the rest of this review, PAM will be used to refer to the non-consumable electrode arc melting process often used to produce laboratory scale RCCAs with industrially representative microstructures. A schematic diagram and photograph of the PAM process is presented below in Fig. 7 (a) and (b).

During the non-consumable electrode PAM process, the temperature of the plasma arc is controlled by the electrical current conducted between the electrode and feedstocks in the crucible. The feedstocks are homogenously melted to form an alloy by moving the electrode, directing the arc and melt pool across the feedstocks. Once consolidated into an alloyed ingot, or button, the alloy is flipped and remelted several times to fully homogenize the constituent element feedstocks. Unlike consumable electrode VAR, the electrode in PAM is not being consumed, and the arc gap is not maintained at a constant distance, so a medium through which the arc is conducted is required. During non-consumable electrode PAM, the melting chamber environment is evacuated using vacuum pumps and then backfilled with an inert gas such as argon to minimize interstitial constituent absorption before striking an arc and melting the alloy. PAM has enabled the molten state preparation of RCCAs because extremely high temperatures, greater than 3000 °C, can be achieved relatively quickly and can yield industrially representative microstructures and sample sizes. Through the use of high purity feedstocks and clean vacuum and gas system practices, the introduction of impurities to the RCCAs is relatively low. However, the feedstocks typically have some low amounts of interstitial constituents, 100–1000 s of ppm, which can be retained in the final RCCA. Because the RCCAs produced via PAM are not actually melted under a constant vacuum, vaporized oxides and dissolved gases may reabsorb into the metal alloy as it cools, leaving interstitial constituents in the PAM RCCAs [52]. Despite this, PAM processes are necessary for the development of RCCAs for industrial applications and have enabled RCCA development and experimentation.

Although the PAM process can be used to produce RCCAs with industrially representative sizes and microstructures and relatively low amounts of interstitial constituents, in most cases, PAM processes do not directly remove impurities or degas the molten alloys, so interstitial constituent contents are relatively higher than those achieved in VAR. However, further removal of the interstitial constituents may be possible through degassing processes during PAM. For example, in recent literature studying the PAM process, by melting titanium in an atmosphere of Ar with 10 vol% H₂, the concentration of oxygen and nitrogen impurities could be reduced by an order of magnitude [56]. The hydrogen in the atmosphere during arc melting can react with degassing impurities, reducing the melt, and prevent their absorption into the final alloy [56]. Often, after PAM of RCCAs, post processing techniques are required to break down dendrites formed during solidification and to achieve homogenous microstructures. Because of the segregation of elements during solidification of PAM processed RCCAs, secondary thermomechanical processing techniques such as cold rolling (CR) or hot isostatic pressing (HIP) are often implored which may introduce more interstitial constituents into the alloy, especially on exposed

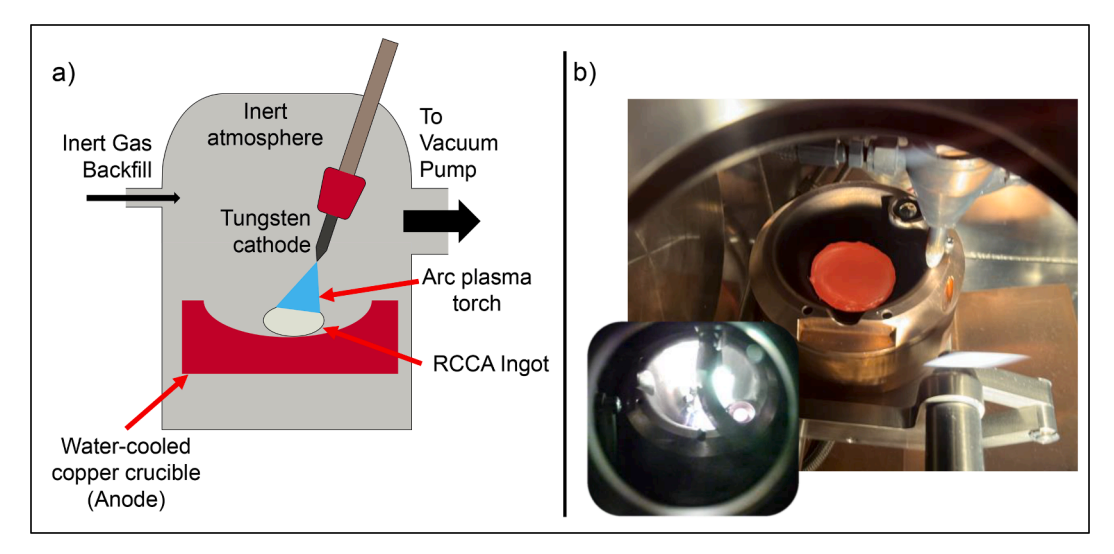


Fig. 7. (a) A schematic diagram of the PAM process used in the synthesis of RCCAs with industrially representative microstructures and (b) a photograph of a RCCA ingot in a PAM unit as it cools in an inert atmosphere after melting. A photograph taken through a darkened weld lens of a PAM arc during melting is shown in the inset in (b). Unlike VAR, before melting in the PAM process, the environment in the chamber is evacuated via vacuum pumps and subsequently backfilled with an inert gas such as argon.

surfaces. Other molten metal synthesis techniques such as vacuum induction melting (VIM) have also been used for the production of industrially representative RCCAs but often may not achieve the temperatures necessary to fully melt some RCCAs and also cannot reach the high temperatures necessary to degas molten RCCAs. In some studies of RCCAs, PAM has been used to add oxygen, nitrogen, and carbon interstitial constituents by melting oxide, nitride, or carbide feedstocks with the RCCA constituents [37,39]. While conventional VAR alloys can reach as low as 10 s of ppm of interstitial constituents, PAM RCCAs tend to contain on the order of 100 s of ppm of interstitial constituents. For now, the relatively low amounts of interstitial constituents may not be completely removed and must be considered in the development of PAM processed RCCAs.

Unlike PAM, powder metallurgical techniques such as mechanical alloying and sintering may introduce significant impurities into RCCAs during synthesis. Due to the high surface area to volume ratios of powder metals, it is possible for interstitial constituents to be introduced to the final RCCAs through compounds formed on the surfaces of the powders. Mechanical alloying (MA) of elemental feedstock powders has been used to produce well alloyed, RCCA powders since atomization of RCCAs can be challenging due to the high melting and super heat temperatures needed. The severe plastic deformation of the elemental feedstock powders during MA causes fracturing and cold welding of the feedstocks, eventually refining grains to ultrafine and nanocrystalline sizes and inducing elemental diffusion and mixing of the powders to produce well-alloyed powders with non-equilibrium microstructures [57,58]. The severe plastic deformation during MA can also introduce and mix impurities into the alloyed powders from the mechanical alloying media, process control agents, compounds on the surface of the powders, and the environment around the powders [58]. The use of no process control agent and inert gas environments can help to minimize impurity introduction, but relatively high concentrations of introduced impurities are inevitable. In RCCAs synthesized via MA and subsequent sintering, a range of several at. % of impurities were introduced in the final RCCAs [59]. In many cases, non-equilibrium, rapid, consolidation techniques, such as spark plasma sintering (SPS), are subsequently used to produce bulk RCCAs from MA powders while minimizing further introduction of impurities to the RCCAs and retaining ultrafine and nanocrystalline grain sizes produced during MA of the powders [60]. It is possible that in some RCCAs, the ultrafine and nanocrystalline grain sizes may enable the distribution of interstitial constituents across many more GBs, preventing embrittlement, similar to ductile, fine-grain tungsten alloys [34]. In addition to grain growth, consolidation techniques and other secondary processing may also drive the formation of equilibrium phases, especially intermetallic compounds. For example, Smeltzer et al. synthesized MoNbTaW alloy powders by MA of elemental feedstocks in liquid nitrogen to introduce nitrogen interstitial constituents into the powders [59]. Through MA in liquid nitrogen, 24 at. % nitrogen and 8 at. % carbon were introduced to the RCCA powders as well as ~ 4 at. % iron from the stainless-steel MA media. The MA powders were then consolidated through uniaxial pressing between tungsten carbide dies and subsequent annealing in argon. Upon annealing at 1100 °C for 1000 h, lath-like complex carbonitride ceramic phases and complex nitride phases were found to form. The complex carbonitride ceramic phases were found to have coherent orientation relationship with the BCC matrix they were surrounded in and significantly improved the hardness of the RCCA compared to the same alloy MA in argon which contained significantly less nitrogen and carbon [59]. Because the use of powder metallurgical techniques may result in RCCAs with inherently higher amounts of interstitial constituents, RCCA design should consider controlling the inherent interstitial constituents through targeted mechanisms in the RCCAs.

Recently, some RCCAs have also been studied as thin films, deposited through processes such as magnetron sputtering. Magnetron sputtering (MS) of thin films is a useful method for producing and studying RCCAs because relatively low amounts of interstitial constituents, on the order of 100 s of ppm, may be achieved during deposition and the thin films can be utilized in the studies of the

atomistic and nanoscale mechanisms of interstitial constituents in RCCAs. Because of the nanocrystalline grain sizes achieved through MS, GB events may be kinetically easier to achieve and study [61]. As shown by several researchers, the addition of interstitial constituents to RCCAs is possible by selecting specific sputtering targets for thin film deposition [40,61]. Controlled amounts of interstitial constituents may be added to RCCA thin films by using oxide or nitride based sputtering targets. However, the MS nanometer thin films and columnar, nanocrystalline grains may not be fully representative of microstructures of RCCAs needed for structural applications [62]. Furthermore, the nanocrystalline grains and nanometer thickness of the RCCA thin films may provide more nucleation for reactions with interstitial constituents from the environment during secondary processing.

The use of additive manufacturing (AM) techniques has shown promise to produce net-shaped RCCAs without the need for conventional subtractive manufacturing techniques and to produce aerospace components with greater complexity. Laser powder bed fusion (LPBF) and selective laser melting (SLM) AM processes utilize a high energy laser, rastered across a bed of pre-alloyed powders melting the powders in its pathway, forming a solid layer of the part, A subsequent bed of powders is spread over the previous layer and the laser continues to raster, building the part layer by layer [63–65]. Direct energy deposition (DED) and laser metal deposition (LMD) AM processes utilize a laser rastered across a substrate, creating a molten pool of metal. Metal feedstock powders are blown into the melt pool by a carrier gas which then solidify, forming a layer of the part [66–69]. The process is repeated to build a net-shaped part layer by layer. Through the layer by layer rapid melting and solidification, AM processing of metal parts with nearly full density can be achieved. The repeated melting and solidification of subsequent layers in AM processes can enable some control over microstructural features such as porosity, grain morphology, and phase transformations. Further, by varying the compositions and feedrates of the metal feedstock powders in some AM processes, complex components with functionally graded microstructures can be fabricated [65,69,70]. Other AM processes can use other sources of heat to melt and deposit metal such as an arc or electron beam melting (EBM) [71]. Despite the latest advances in AM processes, and their promising application for the production of refractory alloys, improvements to AM processes are still necessary. The thermal cycling caused by the repeated melting and solidification of subsequent layers of an AM fabricated part often lead to high residual strain left in the part, requiring secondary processing to relieve the strain. In some alloys not designed for AM processes, the rapid solidification of the layers and the residual strain from thermal cycling can cause severe cracking in the fabricated part. Because of these phenomena, producing parts with high dimensional accuracy and low surface roughness through AM processes is often challenging. As of yet, the interstitial constituents introduced during AM processes are not well characterized in published literature. Furthermore, for AM processes to successfully produce RCCAs for industrial applications, the synthesis of spherical RCCA feedstock powders is required. For AM techniques to successfully produce RCCAs, the solidification pathways of the RCCAs and the sources and mechanisms of interstitial constituents in the RCCAs during powder synthesis and AM processes need to be carefully considered.

As more RCCAs are studied and developed, improvements to processing techniques are needed to further minimize and control unintended interstitial constituents and their interactions and mechanisms in RCCAs. Secondary degassing processes may also need to be utilized and developed to help bring designed RCCAs to industrial applications. However, there may be a minimum threshold of interstitial constituents achievable in RCCAs through conventional processing methods so more holistic RCCA design must consider the low, but irremovable trace amounts of interstitial constituents in RCCAs, inherent to certain processing techniques. In Table 1 below, the common techniques used to synthesize and process conventional refractory alloys and RCCAs are summarized along with their nomenclature, a brief description of the type of process, and the range of interstitial constituents.

By considering the synthesis and processing of RCCAs the interstitial constituent interactions can be controlled to activate specific mechanisms to target unique mechanical properties. To develop some RCCAs, lower contents of interstitial constituents may need to be achieved, requiring specific processes or additional process developments.

Prior to 1925, zirconium and titanium were considered intrinsically brittle elemental metals. The development of the van Arkel-de Boer process enabled the production of zirconium and titanium, free of impurities. In the van Arkel-de Boer process, zirconium and titanium tetraiodides were formed and subsequently thermally decomposed to the base metal. The high ductility of the metal produced demonstrated that impurities were the cause of embrittlement in titanium and zirconium [72–74]. In the 1950 s and 1960 s, it was verified that impurities caused premature, catastrophic failure of steel turbine disks during operation [75]. And in recent years, interstitial constituents have been revealed as a contributing factor in the embrittlement of tungsten [33,34]. It is now understood that

Table 1A summary of the common techniques utilized in the development and processing of refractory metals and alloys, presented with their nomenclature, a brief description of the process type, and the range of interstitial constituents resulting in the processed metals and alloys.

Technique	Nomenclature	Type of Process	Range of interstitial constituents [ppm]
Vacuum Arc Remelting	VAR	Vacuum melting and solidification	10 – 100
Plasma Arc Melting	PAM	Inert environment melting and solidification	100 – 10,000
Magnetron Sputtering	MS	Inert environment solid-state thin film deposition	100 – 1,000
Mechanical Alloying & Spark Plasma Sintering	MA & SPS	Solid-state severe plastic deformation	10,000+
Additive Manufacturing	AM	Inert environment melting and solidification	

impurities can influence the DBTT of some BCC refractory metals when segregating to GBs. The segregation of interstitial constituents to GBs can cause detrimental decohesion of the boundaries, which leads to brittle, intergranular fracture in some metals and alloys [33,34]. Recently, the understanding that interstitial constituents influence the mechanical behavior of RCCAs has begun to emerge as well. Different BCC refractory metals have varying degrees of sensitivity to interstitial constituents, so processing techniques to control the introduction of interstitial constituents and the binary interactions of the refractory metals and interstitial constituents had to be considered for conventional refractory alloy development and should be considered for RCCA development as well. Ultimately, the solubility and segregation of impurities are highly dependent on the chemical interactions of interstitial constituents with the RCCA constituents and thus the electrons of the different interacting and competing atomic species. To understand the mechanisms of the influence of interstitial constituents on the mechanical behavior of conventional BCC refractory alloys and eventually RCCAs, the interactions between the pure transition metal elements of subgroups IV, V, and VI and interstitial constituents are examined.

3. Interstitial constituents in refractory metals

Generally, trends can be found in the columns and rows of the periodic table to describe atomic features of elements such as size, electronegativity, electron configurations, and more. Within the columns, or subgroups, of the periodic table, elements have the same number of valence electrons and tend to interact and bond similarly, but because there are more total electrons, neutrons, and protons per atom in descending rows, differences in their interactions are observed. The trends in the interactions between the refractory metals and interstitial constituents follow trends in the subgroups of the periodic table. By understanding the trends in the interactions between the refractory transition metals and interstitial constituents, the development of conventional refractory alloys can be used to provide a framework for the development of strong, ductile RCCAs. The binary interactions between interstitial constituents and refractory metals can help to guide the design of RCCAs by targeting mechanisms induced by the interactions between the interstitial constituents and RCCA constituents. In Table 2 below, thermodynamic properties of interstitial nitrogen and oxygen constituents in refractory metals from subgroups IV, V, and VI of the periodic table are shown.

In general, the solubilities of oxygen and nitrogen in transition metal elements from subgroup IV, in other words with VEC of 4, are much greater than the elements of subgroups V or VI, which have greater VEC. The general trends in nitrogen and oxygen solubilities can be related to the comparisons between the enthalpies of solution and formation of metal-nonmetal compounds, the atomic structures of the elemental metals, the elemental metal's electronegativity, and the electron affinity of the elemental metals. Oxygen and nitrogen are not exactly the same in their atomic sizes or electronic interactions and may have slightly different interactions with refractory metals. However, since oxygen and nitrogen are both relatively small, highly electronegative nonmetal elements, they often result in similar mechanisms in metals and alloys.

Other interstitial constituent elements such as boron, carbon, and hydrogen are also well understood to contribute to the deformation mechanisms and the mechanical behavior of BCC metals and alloys. Boron and carbon have been studied extensively as GB strengthening and hard precipitate forming elements to improve strength and ductility of many alloys [104,105]. Separately, understanding the role of hydrogen in the embrittlement of metals and alloys has demanded an entire field of research. Because hydrogen is so small and diffusive, even at room temperatures, observing and controlling hydrogen is extremely challenging [106,107]. One of the major theories of hydrogen embrittlement suggests that hydrogen diffuses ahead of crack tips, allowing the crack to propagate and the metal to experience brittle failure [108,109]. Other studies suggest that hydrogen may form hydrides in some metals and alloys which results in embrittlement of the alloys [110]. While hydrogen embrittlement and boron and carbon strengthening have demanded significant fields of research fields for conventional alloys, these interstitial elements have not been studied extensively in BCC RCCAs. Thus far, there is little literature focused on boron, carbon, and hydrogen interstitials in RCCAs and more understanding is needed. So, this review of interstitial constituents in RCCAs and the context provided from conventional alloys will mainly focus on oxygen and nitrogen in BCC RCCAs which is more available in the current literature.

The trends in atomistic properties are ultimately related to the electron configurations of each specific individual metal and interstitial constituent and can aid the understanding of the binary interactions between the interstitial constituents and the refractory transition metals. Within each respective group, although the VEC does not change, the size and electron density of the atom does, changing the electron configurations and resulting in electron shells which become less stable and more likely to ionize with highly electronegative elements. The trends of atomic radii and electron density in the periodic table are dependent on numbers of neutrons, protons, and electrons in individual elements and can be visualized in Table 2 above. In 1990, Cottrell reported that hybridization of both the metal and nonmetal elements can lead to more covalent or more ionic bonds in the material, especially at grain boundaries, which can ultimately lead to cohesion or decohesion [96,111]. The hybridization of bonding elements is dependent on the respective electron configurations and dictates the sharing of electrons between bonding atoms. To understand how the refractory elements may interact with interstitial constituents in conventional dilute alloys and in RCCAs, a closer examination of each individual subgroup of elements is presented.

3.1. Subgroup IV pure refractory metals

The transition metals of subgroup IV have the highest solubilities of oxygen of any transition metals from the periodic table and can result in relatively low sensitivity of the subgroup IV transition metals to interstitial constituents. Titanium specifically has the highest oxygen solubility. In fact, the main strengthening mechanisms of commercially pure titanium are attributed to minor changes in interstitially alloyed oxygen up to 0.25 at. %, beyond which oxygen embrittles titanium [112–115]. The high solubilities of interstitials in titanium, zirconium, and hafnium can be attributed to the accommodation of strain fields in the lattices of the subgroup IV elements.

Table 2
Thermodynamic properties of the interactions between nitrogen and oxygen interstitial constituents and refractory transition metals from subgroups IV, V, and VI on the periodic table. The data for this table were collected from references [76–95,97–99,101–103].

Transition Metals		Maximum solubility limit		Nitrogen		Oxygen		Pauling Electronegativity	Electron Affinity [kJ/ mol]	Atomic Radius [pm]
	Nitrogen [at. %]	Oxygen [at. %]	ΔH ^o _s [kJ/ mol]	ΔH_f° [kJ/mol]	$\Delta H_s^{\rm o}$ [kJ/mol]	$\Delta H_f^{ m o}$ [kJ/mol]				
0 1	α-Ti (HCP)	21	32	-385	-334	-606	-542	1.54	-7.6	176
	β-Ti (BCC)	7	8							
	α-Zr (HCP)	25	26	-374	-364	-619	-541	1.33	-41.1	206
β-Zr (BCC) α-Hf (HCP) β-Hf (BCC)		5	11							
		27	20	-218*	-368	-552	-553	1.33	0	208
		5								
Nb	V (BCC)	11	17	-269	-109	-422	-432	1.63	-50.6	171
	Nb (BCC)	9	1.7	-178	-272	-386	-418	1.6	-86.1	198
	Ta (BCC)	10.5	5.7	-182	-204	-398	-2047	1.5	-31	200
Subgroup VI	Cr (BCC)	4.4	0	+37	-362		-1128	1.66	-64.3	166
	Mo (BCC)	1.1	0	+14.4	-32*		-580	2.16	-71.9	190
	W (BCC)	0	0	+156	-71		-840	2.36	-78.6	193

^{*} values from Miedema Model calculations [87].

Compared to the metal-nonmetal compounds of other refractory metal elements, the metal-nonmetal compounds of the subgroup IV elements are highly stable and do not readily volatize at high temperatures making removal of interstitial constituents from subgroup IV elements through degassing processes more challenging [48,73]. Because nitrogen has a larger atomic size than oxygen and nitride formation in these metals tends to be thermodynamically more favorable than oxide formation, nitrogen tends to be less soluble than oxygen in subgroup IV refractory metals. As shown in Table 2, nitrogen has a lower solubility than oxygen, and embrittles titanium, zirconium, and hafnium metals and their alloys at lower atomic fraction values than oxygen [73]. Unlike the refractory elements of subgroups V and VI, at room temperature, the subgroup IV elements stabilize in the HCP structure. The α -HCP structures of the subgroup IV elements have higher solubilities of interstitial constituents than their high temperature β -BCC structures as shown in Table 2. The higher solubility of the α -HCP allotropes of the subgroup IV elements is attributed to the higher packing density and larger interstitial site sizes compared to the BCC structures of the subgroup IV elements.

In the past few decades, many experimental and computational studies have been carried out in an effort to understand the mechanisms of interstitial constituents in the HCP lattice of the subgroup IV elements [113,115–123]. The subgroup IV elements tend to have relatively low electron affinity, causing stable attractive interactions with highly electronegative elements such as oxygen and nitrogen which have higher electron affinities [116–119,122,124]. Because the HCP lattice has relatively large interstitial sites, the strong attractive forces between highly electronegative interstitial elements and subgroup IV elements can be accommodated as a solid solution in the HCP lattice [113,116–122,124,125]. In fact, it is also suggested that oxygen stabilizes the HCP structure of subgroup IV elements by bringing the c/a ratio of the respective lattices closer to an ideal 1.633 [116–119,122,124]. The strengthening and embrittlement of polycrystalline HCP titanium by oxygen interstitials is due to the suppression of deformation twins and the shuffling of oxygen atoms from metastable to stable interstitial sites during deformation, increasing planar slip [113]. Using density functional theory (DFT) Nayak et al. showed that highly electronegative elements can energetically stabilize configurations at interstitial octahedral sites in HCP titanium and may form impurity dimers. The stable configurations of the interstitial constituents are dependent on the chemical hybridization and charge transfer between the interstitial constituents and transition metal host [122]. In Fig. 8 (a) below, the relationships between charge transfer of impurities and titanium and the formation energies of various interstitial and substitutional impurities are plotted, adapted from Nayak et al. [122].

The presence of the electronegative impurity elements at other interstitial sites induces strain fields on the lattice, making those configurations energetically less stable. In oxygen alloyed BCC β - titanium alloys, a stress induced reordering of oxygen interstitials resulted in mechanical energy dissipation of the material during deformation, improving the plasticity of the alloys [126]. This

mechanism is known as a Snoek relaxation and is characterized as the reversible relaxation of the lattice during deformation through interstitial element jumps between stable interstitial configurations and sites [100]. In subgroup IV elements, Snoek relaxation mechanisms are enabled by the relatively large interstitial site sizes and the stable electronic interactions between the non-metal interstitial constituents and metal constituent elements. A plot comparing the damping capacity, enabled by Snoek relaxation mechanisms, of various BCC β - titanium alloys with respect to interstitial oxygen is shown in Fig. 8 (b), reprinted from Yin et al. [126]. In both the HCP and BCC lattices of subgroup IV elements, substitutionally alloyed transition metal elements produce strain fields in the lattice resulting in repulsive forces acting on interstitial constituent elements and may induce structural transformations in the form of complexes [112,119-122,124,127-130]. It has been suggested that the sensitivity of the HCP subgroup IV elements to oxygen embrittlement is attributed to short range ordering of interstitials with the metal elements. In the BCC structure, the interstitial sites are smaller and are unable to accommodate as many strain fields induced by the interstitial elements in solid solution. The solubility of interstitial constituent elements is attributed to attractive electron interactions between subgroup IV metals and interstitial constituent solute elements and the accommodation of the interstitial constituents in the interstitial sites of the subgroup IV metal lattice. The stable attractive forces and high solubilities of interstitials in subgroup IV metals produce strain fields in the metal lattices which can induce structural transformations, strengthening and eventually embrittling subgroup IV-based alloys. Ultimately, the transition metals of subgroup IV have high affinities and high solubilities of interstitial oxygen and nitrogen resulting in relatively low sensitivities to interstitial constituents. The relatively low sensitivities of the subgroup IV elements and their high affinities for interstitial constituents can provide useful interactions and mechanisms for the development of strong and ductile alloys.

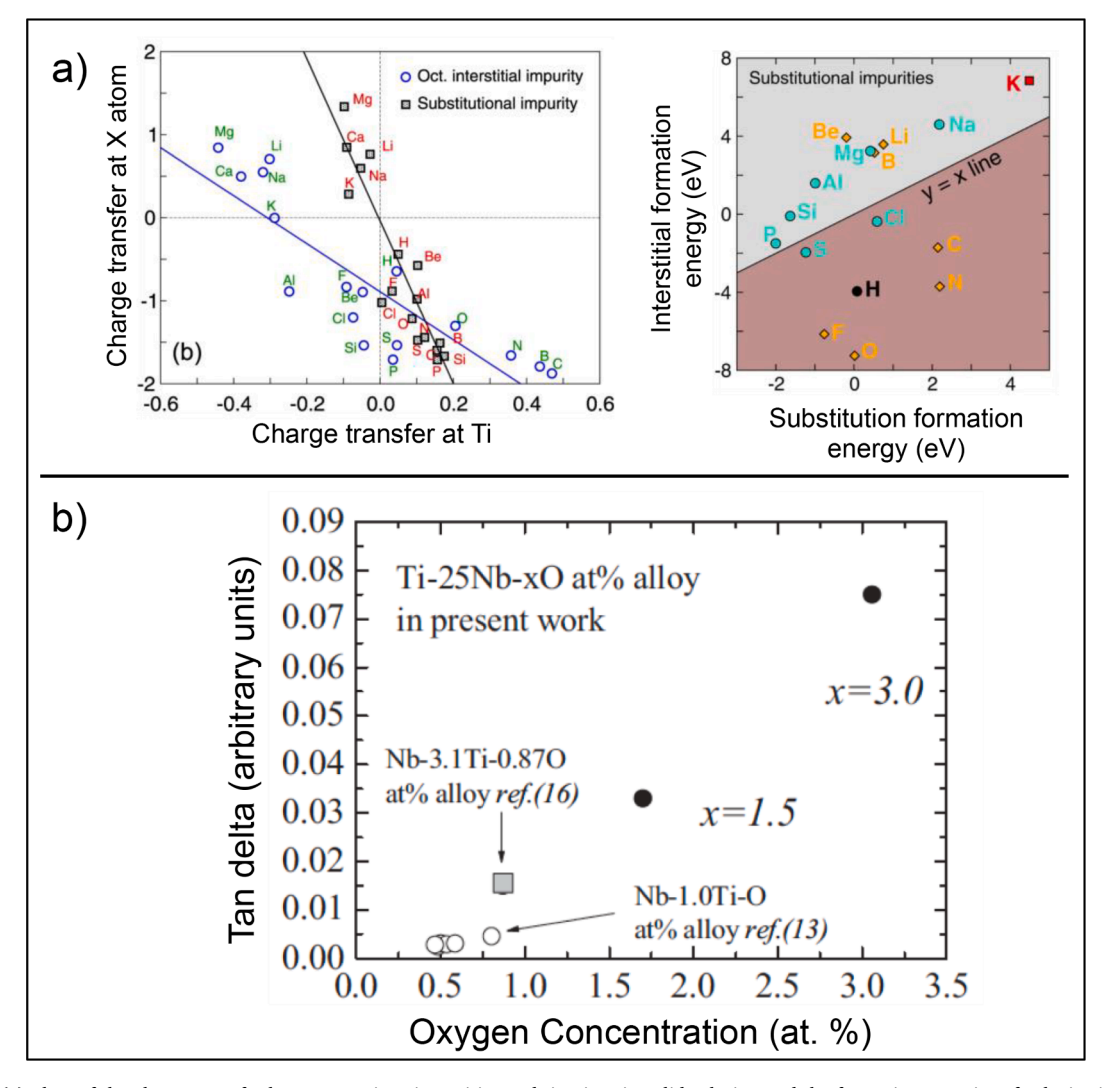


Fig. 8. (a) Plots of the charge transfer between various impurities and titanium in solid solution and the formation energies of substitutional and interstitial point defects of various elements as calculated using DFT, adapted from Nayak et al. [122] and (b) a plot relating the Snoek-type damping capacity of various BCC β - titanium alloys to interstitial oxygen concentration, reprinted from Yin et al. [126].

3.2. Subgroup V pure refractory metals

The subgroup V elements, niobium, vanadium, and tantalum have moderate solubilities of interstitial constituents and like the elements of subgroup IV, undergo strengthening and eventual embrittlement by interstitial constituents. At room temperature, the subgroup V elements are stable in the BCC structure and oxygen and nitrogen impurities relax in the larger octahedral interstitial sites of the BCC lattice [131–135]. At room temperature, the pure elements of subgroup V are considered relatively ductile, with strain to failure reaching nearly 50 %. Since subgroup V metals have moderate interstitial solubilities, additions of oxygen and nitrogen impurities have shown to be an effective interstitial strengthening mechanism of subgroup V metals, but can cause detrimental embrittlement of subgroup V elements above 1 at. % oxygen or nitrogen [132,136–142]. While the BCC lattice and electron configurations of subgroup V elements are able to accommodate higher concentrations of interstitials in solid solution, it is thought that the interaction between dislocations and the interstitials in solution drives strengthening and embrittlement.

While historically it is well known that interstitial constituents such as oxygen and nitrogen strengthen and eventually embrittle subgroup V elements, the exact mechanisms of strengthening and embrittlement have only recently been revealed. It was initially believed that interstitials would strengthen subgroup V elements due to attractive interactions between the interstitials and dislocation cores, impeding the motion of the dislocations [143]. Using DFT calculations and molecular dynamic (MD) simulations to corroborate experimental studies, the mechanism of interstitial oxygen strengthening and embrittlement in niobium was identified [138]. Yang et al. showed that a repulsive field around oxygen interstitials caused passing screw dislocations to emit clusters of vacancies and interstitials. The oxygen interstitials would then stabilize the vacancies, forming vacancy-oxygen complexes which obstruct additional screw dislocation motion, significantly hardening niobium. Furthermore, a "pinch-off" of cross kinks produced more vacancies which were also stabilized by oxygen interstitials forming complexes and eventually forming nano-cavities which coalesce and initiate failure [138]. In Fig. 9 below, the results of in-situ nanomechanical tests performed on a submicron Nb-O alloy are shown, reprinted from Yang et al. [138].

From the in-situ nanomechanical tests shown above in Fig. 9 and MD simulations of the deformation of a single crystal of niobium with 1 at. % oxygen, the mechanisms of oxygen-initiated deformation and failure in niobium were demonstrated. These findings were later corroborated experimentally in nanocrystalline vanadium with 1.7 at. % oxygen showing screw dislocation interactions with oxygen-vacancy complexes [137]. While these studies were mainly focused to oxygen interstitials in niobium and vanadium, it is expected that this understanding of embrittlement mechanisms can be extended to other interstitial constituents, such as nitrogen, in subgroup V metals. Having moderate solubility of interstitial constituents, subgroup V elements tend to have a relatively moderate sensitivity to embrittlement by interstitial constituents compared to subgroup IV and subgroup VI metals.

3.3. Subgroup VI pure refractory metals

The elements of subgroup VI have the lowest solubilities of interstitial oxygen and nitrogen compared to any of the refractory metals and readily form metal-nonmetal compounds, stable at room temperature. At high enough temperatures, while there is kinetic availability for the formation of metal non-metal compounds on the surfaces of subgroup VI metals, the formation reaction is reversible and the compounds are thermally unstable and readily volatize [47,73]. This allows the subgroup VI elements to be easily degassed under high vacuum at high temperatures and limits their use in high temperature applications in atmospheric environments. The attractive interactions between interstitial constituents and subgroup VI metals, indicated by the low formation enthalpies and electron affinities in Table 2, cannot be accommodated by the small interstitial site sizes and dense electron configurations of the subgroup VI metals. Because the interstitials cannot be accommodated in solution in the BCC lattices of the subgroup VI metals, there is a tendency for the interstitial elements to either form compounds such as oxides and nitrides or to segregate to GBs. The segregation of interstitial constituents to GBs may be a more stable configuration for interstitial elements in subgroup VI metals [33,35,36,50,105,144–149]. The segregation of impurities to the GBs of subgroup VI metals can severely reduce the cohesion of the

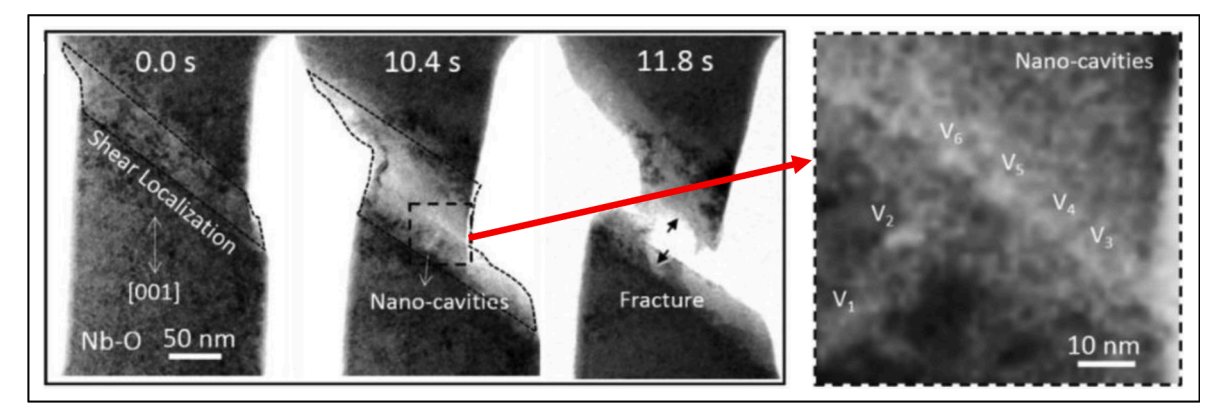


Fig. 9. In-situ nanomechanical tests of a submicron Nb-O alloy, revealing the mechanisms of shear localization, leading to vacancy formation and the coalescence of nano-cavities, reprinted from Yang et al. [138]. The nano-cavities formed by the coalescence of vacancies are labeled $V_1 - V_6$.

GBs, causing embrittlement. Because of the thermally activated dislocation character, limited dislocation mobilities, poor GB cohesion, and limited solubility of interstitial elements, the BCC subgroup VI metals are highly susceptible to embrittlement by impurity segregation [33,146]. Trace amounts as low as 100 ppm of oxygen or nitrogen can embrittle subgroup VI elements [35,36,149]. Recent studies have shown that the cohesion of the GBs in subgroup VI metals is highly dependent on the chemistry at the GBs [111]. Through DFT calculations studying GB sites in tungsten, Setyawan et al. suggest that d-orbital occupation of elements in GB sites can dictate the cohesion of the GBs [144]. The segregated interstitial constituents may bond and hybridize, forming compounds with the GB atoms, resulting in disruptions to the d-orbital electrons around GB sites, which causes decohesion along the GBs. With nearly no solubility of interstitial constituents, subgroup VI metals are highly sensitive to embrittlement by interstitial constituents.

3.4. Conventional refractory alloys

In many conventional refractory alloys, dilute solutions of the transition metals from subgroups IV, V, and VI have been developed to control interactions between interstitial constituents and substitutional alloying elements. For example, because of the strong interactions between subgroup IV elements and interstitial constituents which drive unique mechanisms, the subgroup IV elements have shown effective use as substitutional alloying additives to prevent detrimental interactions between interstitials and other transition metal elements. In powder metallurgically processed molybdenum, the addition of 2 at. % hafnium in solid solution prevents embrittlement by trace interstitial constituents and promotes transgranular fracture at room temperature by scavenging oxygen from GBs and through minor oxide formation in the bulk grain interiors [105]. In the TZM alloy, titanium and zirconium in molybdenum effectively allow internal oxidation, but prevent the direct segregation of oxygen impurities to GBs, which would embrittle molybdenum [150]. Titanium and zirconium are also effective in TZM at forming stable complex carbides which restrict the growth of grains improving hardness and strength of the TZM alloy [151]. The elements of subgroup IV have strong interactions with interstitial constituents and form relatively stable metal-nonmetal compounds and are especially useful in preventing detrimental interstitial constituent embrittlement in more sensitive refractory metals. Because of their strong interactions with interstitial constituents and unique atomic structures and transformations, the development of RCCAs may utilize subgroup IV metals to control interstitial constituents.

The high melting temperatures and relatively low densities of the subgroup V metals, compared to other refractory metals, have shown promise as principal elements for high temperature structural alloys. Recent conventional refractory alloy development has aimed to use subgroup V metals, especially niobium, as the principal alloying elements for their high melting points and high ductility at room temperature. However, the high temperature oxidation of the subgroup V metals has posed a major challenge to the industrial application of niobium-based alloys. For example, the addition of hafnium and titanium to niobium in the C-103 alloy and silicon to eutectic niobium silicide alloys helps to prevent the oxidation at high temperatures. However, in the C-103 alloy, at oxygen concentrations above 0.04 at. % or 400 ppm, hafnium oxides can form at grain boundaries, embrittling the alloy [4,152,153]. Subgroup V elements have also shown use as alloying elements for their strong, stable compound formation, useful for strengthening alloys. In nickel super alloys, niobium and tantalum are added to improve the thermal stability of the γ and γ phases and to improve the strength of the alloys through carbide formation [16,154]. The metals of subgroup V have high ductility without the presence of interstitial constituents and can have moderate sensitivities to the presence of interstitial constituents. The interactions between interstitial constituents and subgroup V metals can be targeted in dilute alloys and RCCAs for strengthening mechanisms and can help control an alloy's sensitivity to interstitial constituents.

Subgroup VI elements tend to have the highest melting temperatures and retain exceptionally high strengths at elevated temperatures but are highly sensitive to interstitial constituent embrittlement, so conventional alloying techniques are used to improve their ductility and decrease DBTT. In some cases, the addition of certain transition metal elements to subgroup VI metals can improve their ductility [144]. The additions of solute transition metal elements with both lower and higher VEC to molybdenum and tungsten GBs may have improved cohesion at certain GB sites [144]. In arc melted tungsten, rhenium additions as low as 1 at. % and as high as 35 at. %, near the solid solubility limit, have been shown to reduce the DBTT of tungsten to near room temperature, enabling the mechanical processing of tungsten [34]. Rhenium additions to molybdenum have shown similar effects [145,155]. While the exact effects of rhenium are still debated, theories suggest rhenium may improve ductility of subgroup VI metals through modification of dislocation core structures, through GB cohesion strengthening via d-orbital interactions at GB sites, or through possible interstitial constituent scavenging, preventing the segregation of embrittling interstitial constituents to GBs [34,144,146]. The possible mechanisms and the high cost of rhenium has initiated the research of other rare earth and rare earth-like metals to improve ductility of subgroup VI BCC alloys. For example, improvements to strength and ductility of molybdenum were achieved through rare earth element lanthanum-oxide dispersions in the grains of nanostructured molybdenum, lowering the DBTT to well below room temperature [146]. Furthermore, the addition of 2 at. % hafnium to powder metallurgically processed molybdenum prevents the GB embrittlement of molybdenum by oxygen at room temperature. Using atom probe tomography (APT) and DFT calculations, Leitner et al. showed that the addition of hafnium to molybdenum improves ductility by modifying the GB chemistry in molybdenum. The hafnium in solid solution prevents the segregation of trace amounts of oxygen impurities to GBs during the powder metallurgical processing, and allows the trace amounts of carbon and boron to compete for and occupy GB sites, improving GB cohesion [105]. Although the hafnium does not prevent the absorption of oxygen into molybdenum during processing, hafnium's strong attraction to oxygen causes the scavenging of oxygen away from molybdenum GBs and allows the segregation of boron and carbon to GB sites, improving ductility. Fig. 10 below depicts the 3D APT reconstruction of a bicrystal of the alloy and a compositional line profile across the GB, revealing the segregation of boron and carbon, adapted from Leitner et al. [105].

By now, it is well understood that GB cohesion can be the limiting factor in the ductility of subgroup VI metals and that segregated

impurities can exacerbate the poor cohesion of the GBs. Subgroup VI metals with highly refined grain sizes, down to the nanometer regime, have also shown markedly improved ductility and reduced DBTT [34,156,157]. By reducing grain sizes and increasing the volume fraction of GBs, segregated impurities are more distributed, effectively reducing the interstitial constituent concentrations at each GB and limiting the effects of GB decohesion. Ultimately, the subgroup VI metals are relatively sensitive to interstitial constituents and are susceptible to impurity embrittlement because of their inherently poor GB cohesion and low solubilities of interstitials, causing GB segregation, and necessitate alloying and processing techniques to control interstitial constituents. Ductile subgroup VI-based alloys can be achieved through conventional alloying and processing techniques which aim to prevent the segregation of impurities to GBs or by directly strengthening the GBs. The methods by which subgroup VI-based alloys are designed and processed can help guide the development of more ductile RCCAs with subgroup VI elements.

The interactions and mechanisms between interstitial constituents and refractory metal elements are dependent on trends in the periodic table. Electron configurations and atomic sizes of the various elements dictate the strength and stability of their interactions with highly electronegative interstitial elements. Because interstitial constituent absorption is sometimes inevitable through necessary processing routes, their interactions with refractory metals may be unavoidable. However, the mechanisms by which interstitial constituent elements interact with refractory metals can be controlled to beneficially influence the mechanical properties of refractory alloys. Since the trends in the binary interactions between pure refractory metals and interstitial constituents are predictable and similar in dilute alloys, mechanisms such as scavenging, and site competition can be exploited to combat impurity embrittlement and even strengthen refractory alloys. By considering the processing of RCCAs and the interactions of interstitial constituent elements with the constituent refractory metals, more holistic RCCA development approaches can be adopted. The mechanisms by which interstitial constituents influence mechanical behavior of RCCAs can be controlled by targeting interstitial constituent mechanisms for stronger, more ductile RCCAs.

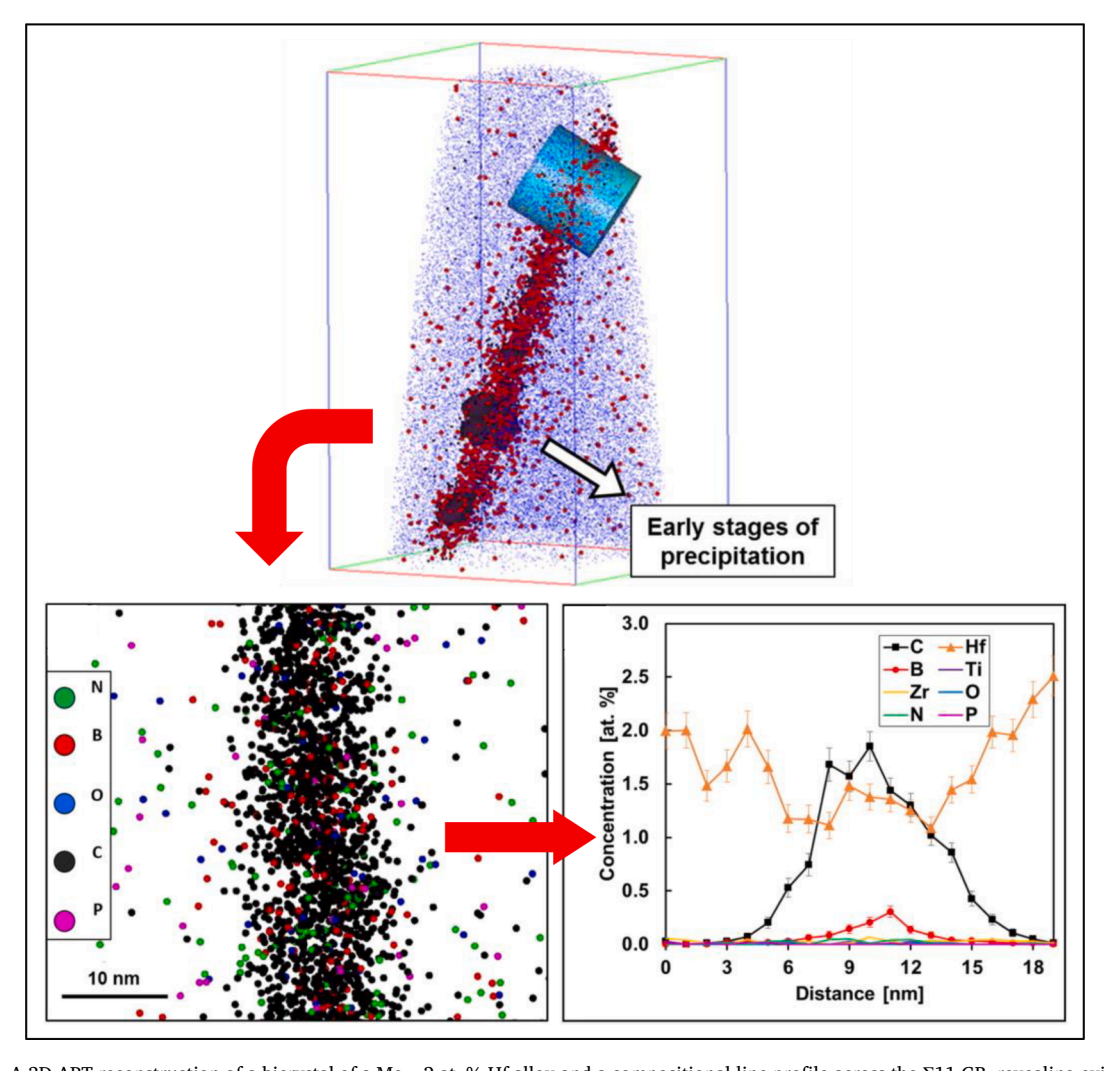


Fig. 10. A 3D APT reconstruction of a bicrystal of a Mo – 2 at. % Hf alloy and a compositional line profile across the Σ 11 GB, revealing evidence of the strong segregation of boron and carbon, competing with oxygen to improve the ductility of molybdenum, adapted from Leitner et al. [105].

4. Interstitial constituents in RCCAs

Just as the interactions between interstitial constituents and refractory metal elements are utilized and modified through developments of conventional refractory alloys, RCCA development can capitalize on the interactions between interstitial constituents and the RCCA constituent elements to achieve strong, ductile RCCAs. As the field of RCCAs has grown to develop more unique alloy systems with their own microstructural and mechanical characteristics, the realization that interstitial constituents influence the behavior of RCCAs has grown too. Lately, in studies of RCCAs, the influence of interstitial constituents has begun to be characterized to remove uncertainty in the understanding of their thermodynamic and mechanical properties. By reviewing the RCCA literature examining the role of interstitial constituents in RCCAs with context from pure refractory metals and conventional refractory alloys, more holistic design approaches to RCCAs can be developed.

In previous criteria for the design of RCCAs, the interactions between constituent elements and interstitial constituents were not intentionally considered. In some cases, RCCAs designed with low VEC tended to contain more constituent elements from subgroups IV and V which have fewer d and s electrons and by coincidence the subgroup IV and V elements also have high interstitial element solubilities due to their electronic configurations [30,158,159]. The high interstitial solubilities and relatively low sensitivities to interstitials in the RCCAs with low VEC may have contributed to recent observations of low DBTT. By understanding mechanisms of interstitial constituents in RCCAs, holistic approaches to RCCA design can be implemented to effectively develop high strength, ductile RCCAs for targeted applications. Although many early publications of mechanical behavior of RCCAs did not directly focus on the influence of interstitial constituents, recent studies have acknowledged and varied the presence of interstitial constituent elements in RCCAs. Many of the studies describing the influence of interstitial constituents on RCCA mechanical behavior have used model systems such as MoNbTaW and HfNbTaTiZr to understand fundamental interactions and mechanisms. The MoNbTaW and HfNbTaTiZr systems represent the far ends of the spectrum of sensitivity to interstitial constituents, and variations to these systems have been studied to predict and develop other RCCAs. The data from several recent publications of RCCAs with assessed interstitial constituents are summarized below in Table 3 and are organized in descending VEC.

It is important to note the data in Table 3 is comprehensive, but limited in that there is more information published but not included in the above table. The data has been specifically selected from the literature to compare and examine recently published RCCAs with observed presence of interstitial constituents and the influence of interstitial constituents on mechanical behavior. In some cases, the interstitial constituents were intentionally added and in other cases, the interstitial constituents were inherent to the synthesis and processing methods employed. Some data from RCCAs without studied interstitial constituents are also provided in Table 3 to compare the effects of constituent elements with unknown concentrations of interstitial constituents. Table 3 includes data from RCCAs synthesized via a variety of techniques to compare variations in interstitial constituent contents and microstructural features. It is also important to note that variability in microstructural features may convolute the mechanical properties contained in Table 3, but the existence of complex phases, especially those driven by interstitial constituent interaction, are necessary for the development of RCCAs and the prediction of future phases and mechanical behavior.

Further examinations by this review paper will focus on the influence of interstitial constituents, specifically oxygen and nitrogen, on the mechanical properties of the MoNbTaW and HfNbTaTiZr systems using context provided from analyses of the interactions between the RCCA constituents and the interstitial constituents. By examining the influence of interstitial constituents on the mechanical behavior of these systems the fundamental understandings can be established to suggest future holistic design of RCCAs.

4.1. The MoNbTaW system

The MoNbTaW RCCA system was first reported by Senkov et al. and over time, research has shown this RCCA system to be highly susceptible to interstitial constituent embrittlement. In 2010 the MoNbTaW RCCA was first developed and in 2011 was quickly followed by the observation of relatively high strength, around 500 MPa, retained at elevated temperatures of 1600 °C with elongation of more than 25 %, outperforming some nickel based super alloys [14,21]. Compressive stress strain curves of the MoNbTaW RCCA at room and elevated temperatures are shown below in Fig. 11 (a), adapted from Senkov et al. [21].

In these initial studies, Senkov et al. showed that at room temperature, the MoNbTaW RCCA systems undergo brittle, intergranular fracture [21]. Microstructural characterization of the alloy showed that during solidification, the alloy formed a single BCC phase but also underwent severe dendritic segregation. From X-Ray Diffraction (XRD) results, the lattice parameter of the alloy was extrapolated to be 0.3213 nm [14]. At the time, the low DBTT was intrinsically attributed to the MoNbTaW RCCA system [21]. It was later shown through a variety of mechanical tests, such as compression, tension, bending, shearing, and microhardness testing, that the as-cast MoNbTaVW RCCA underwent cleavage, not shear, as the dominant fracture mechanism of the alloy suggesting brittle behavior [190]. In tension, the RCCA would mostly fracture through interdendritic cracking, but in compression and in low-load microhardness testing, slip bands and intragranular cracks were present suggesting the potential for plasticity in the MoNbTaVW RCCA at room temperature [190]. By compressing columnar nanocrystalline pillars in a magnetron sputtered thin film of the MoNbTaW RCCA at room temperature, plasticity of up to 15 % strain and extremely high strengths of up to 6.5 GPa were observed by Zou et al. [191]. The same authors later showed through compression of micropillars in an arc melted and annealed MoNbTaW RCCA that within single grains of the alloy, high strength and ductility were achievable and dependent on size [44]. By compressing a bicrystal micropillar of the RCCA Zou et al. showed that brittle fracture occurs along the GB of the alloy [44]. The fractured bicrystal pillar from Zou et al. is shown in Fig. 11 (b) depicting the brittle fracture along the GB [44]. Zou et al. then conducted in situ notched micro cantilever experiments on specimens ion beam milled from the arc melted and annealed MoNbTaW RCCA to compare the fracture toughness of a single crystal and bicrystal. The bicrystal sample of the MoNbTaW was found to have a fracture toughness an order of magnitude lower

Table 3
Summarized microstructural features, processing methodologies, room temperature (RT) mechanical properties, and interstitial constituent contents of recently published RCCAs. The data in this table are organized in descending VEC values to visualize correlations in sensitivity to interstitial constituent elements and ductility.

RCCA	Ref.	Microstructure	Processing	VEC	RT Yield Strength [MPa]	RT Elongation [%]	Oxygen [at. %]	Nitrogen [at. %]	Other non-metal impurities [at. % X]
NbRe _{0.3} TiZr	[160]	BCC + FCC	PAM + HIP	6.08	1220 ± 24*	53 ± 7*	0.0090	0.0020	0.0016C
Re _{0.3} TaTiZr		BCC + BCC	PAM + HIP	6.08	$1715\pm30^*$	$10\pm1^*$	0.0110	0.0020	0.0017C
MoNbTaW	[37]	BCC + GB Segregants	PAM	5.50	1074-1095*	1.4-1.7*	0.0147		
		BCC + GB Segregants	PAM	5.50	1175-1207*	5.8-6.2*			0.040B**
		BCC + GB Segregants	PAM	5.50	1255-1325*	7.6-7.8*			0.100B**
		BCC + GB Segregants	PAM	5.50	1262-1372*	10.3-11.5*			0.500B**
		BCC + GB Segregants	PAM	5.50	1243-1369*	7.6-9.1*			0.800B**
		BCC + GB Segregants	PAM	5.50	1132-1190*	5.7-6.5*			0.050C**
		BCC + GB Segregants	PAM	5.50	1323-1416*	7.6-8.7*			0.150C**
		BCC + GB Segregants	PAM	5.50	1507-1567*	5.5-6.3*			0.500C**
	[161]	BCC + FCC + HCP	PAM	5.50	1285*	6.5*			10.0000C**
		BCC + FCC	PAM	5.50	1753*	4.6*			20.0000C**
		BCC + FCC + HCP	PAM	5.50	1972*				30.0000C**
	[61]	BCC + Amorphous	Magnetron Sputtered +	5.50			1.1000		
		Intergranular Films	Annealed						
	[59]	BCC + Nitrides + Carbonitrides	MA + Sintered	5.50				23.8000	
CrNb	[162]	BCC + Laves	PAM + HIP	5.50	1670*	0.95*	0.3020	0.3800	0.0120C
MoNbTaW	[63]	BCC	LPBF	5.50	1196*	4.6*			
		BCC + Nb Carbides	LPBF	5.50	1725*	7.0*			0.5000C**
MoNbTaW	[71]	BCC	EBM	5.50	1173*	8.82*			
		BCC + Nb, Ta Carbides	EBM	5.50	1221*	7.23*			5.8900C
MoNbTaVW	[163]	BCC + GB Oxides	MA + SPS	5.40	2612*	18*	1.4100		1.1200C
		BCC + GB Oxides	MA + SPS	5.40	2514*	12.5*	1.3300		1.5200C
		BCC + GB Oxides	MA + SPS	5.40	2491*	9.5*	0.9600		1.7700C
MoNbTaVW	[164]	BCC	LPBF	5.40					
MoNbTaV	[165]	BCC	PAM	5.25	1256*	35*			
	[166]	BCC	PAM	5.25	1500*	21*			
NbTaVW	[167]	BCC	PAM	5.25	1530*	12.5*			
MoNbTaTiW	[168]	BCC	PAM	5.20	1343*	14.1*			
MoNbTiVW	[169]	BCC + BCC	PAM	5.20	2136*	15.31*			
		BCC + BCC	PAM	5.20	2150*	14.25*			0.0250Si
		BCC + BCC	PAM	5.20	2175*	12.75*			0.0500Si
		BCC + BCC	PAM	5.20	2250*	12.25*			0.0750Si
		BCC + BCC + M ₅ Si ₃ Eutectic	PAM	5.20	2298*	12.02*			0.1000Si
CrTaTiVW	[170]	BCC + Ti ₃ O ₅ Precipitates	VIM	5.20	1628	8.5			
MoNbTaTiVW	[168]	BCC	PAM	5.17	1515*	10.6*			
CrNbTi	[162]	BCC + Laves	PAM + HIP	5.00	1353*	6*	0.1370	0.0230	0.0270C
CrNbTaTi		BCC + Laves	PAM + HIP	5.00	515*		0.1610	0.0330	0.0460C
MoNbTiV	[171]	BCC	PAM	5.00	1747*	18*			
		$BCC + M_5Si_3$	PAM	5.00	1869*	33*			0.2500Si
MoNbTaTiV	[172]	BCC	PAM	5.00	1400*	30*			
NbTaTiVW	[167]	BCC	PAM	5.00	1420*	20*			
HfMoNbTaTi	[173]	BCC + Hf-N Nanoparticles	PAM	4.80	1713*	12*		0.0300	
HfMoNbTaZr	[174]	BCC	PAM	4.80	1524*	13.5*			
$Hf_{0.51}Mo_{0.3}0Ta_{0.19}$	[175]	BCC + Eutectic + HCP + Laves	PAM + HIP	4.79	1672*	2.7*	0.1100 ± 0.006	0.0300 ± 0.002	$0.1700 \pm 0.005C$
CrNbTa5TiZr	[176]	BCC + Laves	PAM	4.76	1800*	2.9*			

Table 3 (continued)

RCCA	Ref.	Microstructure	Processing	VEC	RT Yield Strength [MPa]	RT Elongation [%]	Oxygen [at. %]	Nitrogen [at. %]	Other non-metal impurities [at. % X]
Hf ₁₅ Mo ₂₅ Nb ₂₀ Ta ₅ Ti ₃₅	[177]	BCC	PAM + Homogenized	4.75			0.0800	0.0200	0.0100C
NbTaTiV	[167]	BCC	PAM	4.75	965*	50*			
NbTaTi	[178]	BCC + Ti rich GB Compounds	PAM + HIP	4.67	724*	35.4*	0.1120	0.3910	0.1320C
NbTaZr	[178]	BCC + BCC + HCP + Zr rich GB Compounds	PAM + HIP	4.67	1027*	16.9*	0.1450	0.2790	0.1220C
HfMoNbTaTiZr	[174]	BCC	PAM	4.67	1512*	11*			
Cr ₁₆ NbTa ₅ TiZr	[176]	BCC + Laves	PAM	4.63	1514*	8.3*			
Hf _{0.58} Mo _{0.21} Ta _{0.21}	[177]	HCP + BCC + Eutectic	PAM + HIP	4.63	1496*	5.3*	0.0400 ± 0.006	0.1500 ± 0.005	$0.0900 \pm 0.005C$
HfMoTaTiZr	[174]	BCC	PAM	4.60	1600*	3*			
HfMoNbTiZr		BCC	PAM	4.60	1351*	17*			
Hf ₃₀ Mo ₅ Nb ₂₅ Ta ₂₅ Ti ₁₅	[179]	BCC	PAM	4.60	$964 \pm 16*$	50*			
Nb ₄₀ Ti ₄₀ V ₂₀	[180]	BCC	PAM + CR + Annealed	4.60	650*	37.2*	0.0450	0.0032	
Cr ₁₂ NbTa ₅ TiZr	[176]	BCC + Laves	PAM	4.57	1340*	15.69*			
Hf _{0.61} Mo _{0.16} Ta _{0.23}	[175]	HCP + BCC + Eutectic	PAM + HIP	4.55	1468*	5.8*	$\begin{array}{c} 0.1200 \; \pm \\ 0.006 \end{array}$	0.0100 ± 0.002	$0.1800\pm0.005\text{C}$
NbTaTiZr	[38]	BCC	PAM	4.50	1013 ± 7	13.2 ± 0.5			
	[00]	BCC	PAM	4.50	1115 ± 10	14.7 ± 0.8		0.3000**	
		BCC	PAM	4.50	1196 ± 8	17.5 ± 0.3		0.6000**	
		BCC + GB Zr-N Nanoparticles	PAM	4.50	1242 ± 15	1710 ± 010		0.9000**	
NbTaTiZr	[38]	BCC + BCC	PAM + Annealed	4.50	1238 ± 9	18.8 ± 0.3		0.6000**	
	[181]	BCC + Nanoparticles	PAM + Annealed	4.50	1004	16.1	$\begin{array}{c} 0.3494 \ \pm \\ 0.0891 \end{array}$	0.0105 ± 0.0021	0.0042 ± 0.0004 C, 0.0457 ± 0.0025 Si
	[182]	BCC	PAM	4.50	958*	50*	0.0031	0.0021	± 0.002001
	[102]	BCC + FCC Carbides	PAM	4.50	1048*	50*			10.000C**
		BCC + FCC Carbides	PAM	4.50	1076*	44.8*			20.000C**
HfNbTiV	[182]	BCC + FCC Carbides	PAM	4.50	1115*	37.8*			30.000C**
Cr ₈ NbTa ₅ TiZr	[176]	BCC + Laves	PAM	4.50	1354*	25.08*			30.0000
Cr ₄ NbTa ₅ TiZr	[176]	BCC	PAM	4.43	1224*	60*			
Hf ₂₃ Nb ₂₂ Ti ₃₇ V ₁₅ W ₃	[183]	BCC + FCC + HCP	PAM	4.43	980 ± 18	19.8 ± 0.55			
Hf ₁₆ Nb ₁₆ Ti ₄₁ V ₂₇	[184]	BCC + FCC + FICE	PAM	4.43	953	25	0.3300		
1111614016114142/	[101]	BCC + BCC	PAM	4.43	1517	12	2.6800		
HfNbTaTiZr	[185]	BCC + BCC	VIM	4.40	875 ± 11	16.5 ± 0.2	2.0000		
HfNbTatiZr	[68]	BCC	LMD	4.40	0/3 ± 11	10.5 ± 0.2			
Hf ₂₄ Nb ₂₃ Ti ₃₈ V ₁₅	[181]	BCC	PAM	4.38	774	20.6	$\begin{array}{c} 0.2540 \; \pm \\ 0.0818 \end{array}$	$\begin{array}{c} 0.0110 \; \pm \\ 0.0034 \end{array}$	0.0026 ± 0.0011 C, 0.0302 ± 0.0025 Si
		BCC + Nanoparticles	PAM + Annealed	4.38	802	22.5	0.3570 ± 0.1051	0.0108 ± 0.0026	0.0045 ± 0.0038C, 0.0318 ± 0.0038Si
NbTa6.25TiZr	[176]	BCC	PAM	4.38	1368*	60*	0.1001	0.0020	_ 0.000001
Hf _{0.69} Mo _{0.05} Ta _{0.26}	[175]	HCP + BCC + Eutectic	PAM + HIP	4.36	1647*	26*	$\begin{array}{c} 0.1100 \; \pm \\ 0.006 \end{array}$	$\begin{array}{c} 0.0100 \; \pm \\ 0.002 \end{array}$	$0.1700 \pm 0.005 C$
Hf ₅ Nb ₂₀ Ta ₁₅ Ti ₂₅ Zr ₃₅	[41]	BCC	PAM	4.35	1200*	45*	5.0000	0.002	
5.4D2010151125Z135	[41]	BCC + BCC + HCP	PAM + Annealed	4.35	1700*	25*	5.0000		
NbTiZr	[40]	BCC	Magnetron Sputtered	4.33	$1300\pm100^*$				
NbTiZr	[40]	BCC	Magnetron Sputtered + Annealed	4.33			8.0000**		
		BCC	Magnetron Sputtered	4.33	$2900\pm200^*$	65*	5.7000	0.5000	0.9000C
		BCC + GB Segregants	Magnetron Sputtered +	4.33	$4200 \pm 200^*$	65*	11.6000	0.5000	0.8000C
		0 -0	Annealed			-			

Table 3 (continued)

Ref.	Microstructure	Processing	VEC	RT Yield Strength [MPa]	RT Elongation [%]	Oxygen [at. %]	Nitrogen [at. %]	Other non-metal impurities [at. % X]
[28]	BCC	PAM + CR + Annealed	4.33	630	18	0.0214	0.0011	0.0080C
[160]	BCC	PAM + HIP	4.33	$920\pm18^{\color{gray}*}$	60*	0.0120	0.0063	0.0021C
	BCC + BCC	VAM + HIP	4.33	$1670\pm30^*$	$2.5\pm0.5^{*}$	0.0070	0.0020	0.0021C
[186]	BCC + TiB ₂ Whiskers	PAM	4.33	740*	50*			0.20 wt% TiB ₂
	$BCC + TiB_2$	PAM	4.33	905*	50*			2.0 wt% TiB ₂
	BCC + Coarse and Thin TiB ₂ Fibers	PAM	4.33	1010*	9*			4.4 wt% TiB ₂
[180]	BCC + B2	PAM + CR + Annealed	4.30	750*	45.6*	0.0445	0.0030	
[160]	BCC + BCC	PAM + HIP	4.33	$1670\pm30^*$	$2.5\pm0.5^{*}$	0.0070	0.0020	0.0021C
[175]	HCP + Eutectic	PAM + HIP	4.27	1738*	13.7*	0.1100 ± 0.006	0.1300 ± 0.005	$0.1500 \pm 0.005 C$
[187]	BCC	PAM	4.26	690	13	0.2260		
-	BCC	PAM	4.26	900	14	1.2580		
	BCC	PAM	4.26	1075	15	2.4040		
	BCC	PAM	4.26	1200	15	3.3010		
	BCC	PAM	4.26	800	1.5	3.7120		
	BCC	PAM		525	1			
[39]					14.21 ± 1.09			
	BCC + Ordered Interstitial					2.0000**		
		PAM	4.25	1300 ± 20	9		2.0000**	
[43]	BCC	PAM + Homogenized + CR	4.25			2.0000**		
	BCC	${\sf PAM} + {\sf Homogenized} + {\sf CR}$	4.25				2.0000**	
[46]	BCC		4.25	1138	10.8	0.3770	0.0420	
2.03	$BCC+Ordered\ Interstitial$	PAM	4.25	1138	23	2.2410	0.0390	
	BCC + Ordered Interstitial	PAM	4.25	1362	15	0.3830	2.2870	
[188]	BCC + HCP	LMD	4.25	1034	18.5			
	BCC	LMD	4.20	782	13.1			
[189]	BCC	PAM	4.20	907	14.9			
[180]	B2	PAM + CR + Annealed	4.20	795*	0.3*	0.0448		
[189]	BCC	PAM	4.15	821	9.1			
[188]	BCC	LMD	4.15					
		PAM		600	9	0.1340		
2 2				800				
	BCC	PAM	4.14	950	18	2.1370		
	BCC	PAM	4.14	1075	25.1	3.3550		
	DCC							
	BCC	PAM	4.14	1150	8.5	3.8660		
	BCC	PAM			8.5 2			
[189]			4.14 4.14 4.10	1150 1200 647	8.5 2 7.9	3.8660 4.3520		
	[28] [160] [186] [180] [160] [175] [187] [39] [39] [43] [46] [188] [189] [180] [189]	[28] BCC [160] BCC BCC + BCC [186] BCC + TiB ₂ Whiskers BCC + TiB ₂ BCC + Coarse and Thin TiB ₂ Fibers [180] BCC + BCC [175] HCP + Eutectic [187] BCC BCC BCC BCC BCC BCC BCC GCC BCC GCC BCC [39] BCC + Ordered Interstitial Complexes BCC BCC BCC BCC BCC BCC [43] BCC [46] BCC BCC BCC BCC [48] BCC BCC BCC BCC BCC BCC [48] BCC	[28] BCC	[28] BCC PAM + CR + Annealed 4.33 [160] BCC PAM + HIP 4.33 BCC + BCC VAM + HIP 4.33 BCC + TiB ₂ Whiskers PAM 4.33 BCC + Coarse and Thin TiB ₂ PAM 4.33 Fibers [180] BCC + BC PAM + CR + Annealed 4.30 Fibers [180] BCC + BC PAM + HIP 4.37 [175] HCP + Eutectic PAM + HIP 4.27 [187] BCC PAM + HIP 4.27 [187] BCC PAM + HIP 4.27 [187] BCC PAM 4.26 BCC PAM 4.25 [39] BCC PAM 4.25 [39] BCC PAM 4.25 [40] BCC PAM 4.25 [41] BCC PAM 4.25 [42] BCC PAM 4.25 [43] BCC PAM 4.25 [44] BCC PAM 4.25 [45] BCC PAM 4.25 [46] BCC PAM 4.25 [46] BCC PAM 4.25 [47] BCC PAM 4.25 [48] BCC PAM 4.26 [48] BCC PAM 4.11 [48] BCC PAM 4.11	Table Tabl	Each	128	Cast BCC

^{*} Mechanical properties tested in compression, ** Targeted impurity concentrations.

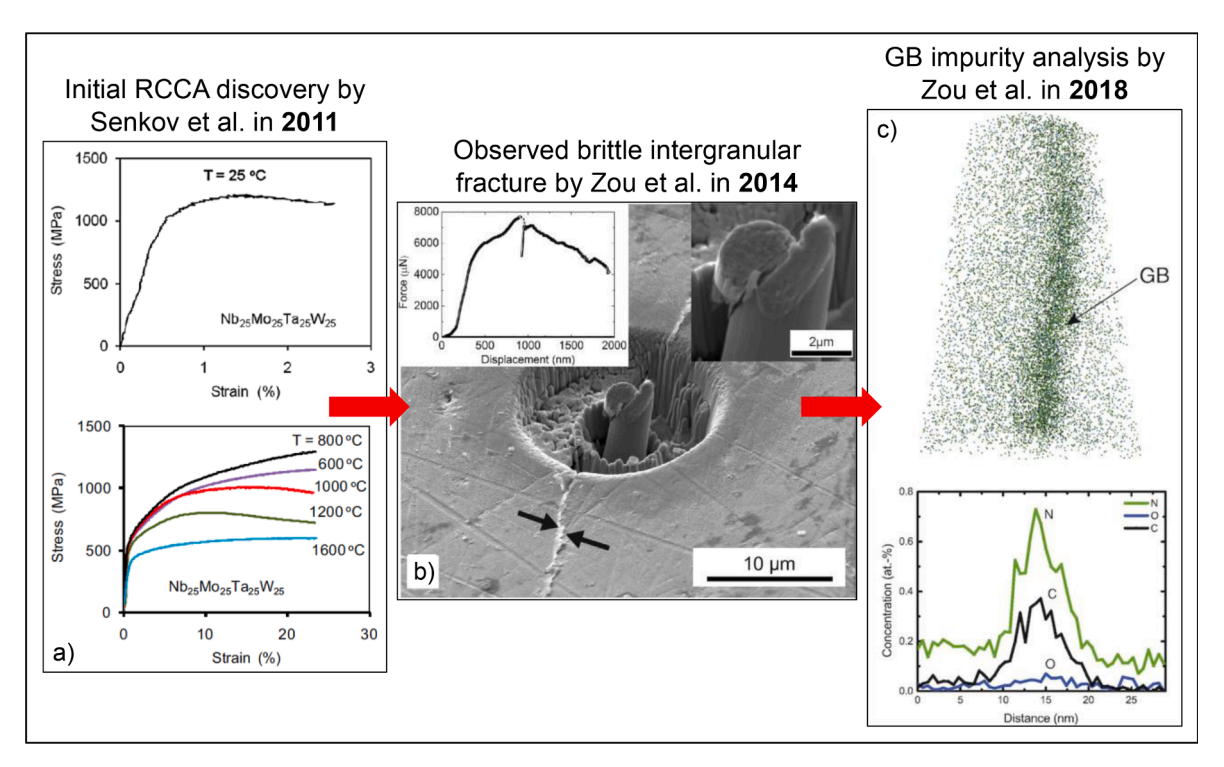


Fig. 11. The progression of understanding of the embrittlement in the MoNbTaW RCCA, starting from (a) the compressive stress–strain curves of the alloy at elevated and room temperature from Senkov et al. [21], then (b) observation of brittle fracture along a GB in a bicrystal micropillar from Zou et al. [44], and finally (c) APT reconstruction of a GB in the MoNbTaW RCCA and concentration profiles taken across the GB, showing presence of interstitial constituent elements and metal-nonmetal compounds segregated at GBs from Zou et al. [45].

than the fracture toughness of the single crystal MoNbTaW microcantilever specimen. Upon further investigation of the GBs using APT, Zou et al. found that oxygen, nitrogen, and carbon impurities had segregated and formed compounds along the GBs. The APT reconstruction of a bicrystal of the MoNbTaW RCCA from Zou et al. is shown in Fig. 11 (c) along with concentration profiles taken across the GB, revealing segregated impurities along the GB [45]. The concentration profile from APT revealed that concentrations of 0.75 at. % nitrogen, 0.35 at. % carbon, and 0.05 at. % oxygen had segregated to the GBs. The low fracture toughness and embrittlement of the bicrystal microcantilever specimen are attributed to the segregation of impurities and formation of intermetallic compounds at the GB [45]. This APT experiment of the MoNbTaW RCCA was the first observation of interstitial constituents in an RCCA. Through this APT study, the influence of interstitial constituents on the mechanical behavior of the MoNbTaW RCCA could be assessed. Although the interstitial constituent elements were not intentionally introduced into the MoNbTaW RCCAs described above, their presence, on the order of ~ 100 s of ppm is inherent to the processing techniques used and can affect the GB cohesion of the MoNbTaW RCCAs as in conventional BCC metals and alloys. The MoNbTaW RCCA is still considered intrinsically brittle with high DBTT, but the mechanism by which it is embrittled by GB segregated interstitial constituents can be appreciated. The reason for segregation and ultimately embrittlement of the MoNbTaW RCCA system can be understood through context from the interactions between the interstitials and the constituent elements of the RCCA.

In the MoNbTaW RCCA system, segregation of interstitial constituent elements and poor GB cohesion of the RCCAs contribute to the embrittlement of the alloy. Much like conventional BCC metals and alloys, the embrittlement and DBTT of the MoNbTaW RCCAs can be controlled by dislocation motion and cohesion of the GBs [19,27,192]. Although the exact atomistic mechanisms of the motion of dislocations in non-dilute BCC alloys such as RCCAs may be debated, poor GB cohesion can prevent the transmission of dislocations, limiting the plasticity of the alloys. The MoNbTaW RCCA with VEC of 5.50 is made up of constituent elements from subgroups V and VI. The subgroup VI elements molybdenum and tungsten are likely significant contributors to both poor cohesion of GBs and segregation of interstitial constituents to GBs in the MoNbTaW RCCA systems. From the APT observations, subgroup V elements, especially tantalum contribute to the formation of intermetallic compounds along GBs, where interstitial constituents have diffused and segregated. Due to the relatively small experimentally determined lattice parameter (0.3213 nm) of the MoNbTaW RCCA, the alloy also has relatively small effective radii and interstitial sites, especially with respect to the high electron density of the elements, much like the subgroup VI elements. From the lattice parameter found by Senkov et al., an effective atomic radius could be calculated to then approximate the octahedral and tetrahedral interstitial site sizes of the MoNbTaW RCCA. From the lattice parameter determined by Senkov et al., the effective atomic radius of the MoNbTaW RCCA is calculated to be 0.1391 nm and the octahedral and tetrahedral sites were then approximated to be 0.0215 and 0.0405 nm respectively. These interstitial sites are approximated to be smaller compared to the subgroup VI elements, but more quantified and direct observations of the interstitial sites are necessary. Similar to subgroup VI

elements, the MoNbTaW RCCA cannot accommodate the electronic interactions with interstitial constituents in the interstitial sites of the lattice. Despite the strong interactions between the interstitial constituent elements and the constituent elements in the MoNbTaW RCCA as shown by the low formation enthalpies in Table 2, the stable configuration of the interstitial constituents may be segregated at GBs where the interstitial constituent atoms can be accommodated. The relatively fast diffusion of the interstitial constituents and relatively slow diffusion of the constituent elements may prevent the formation of new intermetallic structures in the grain interiors and can kinetically allow the segregation of the impurities to GBs where compound formation can then occur. After segregating to GBs, the impurity elements may then further interact with the constituent refractory metal elements distributed at and near the GBs.

At the GBs, the interactions can be driven by the formation of compounds with the lowest formation enthalpies, in this case subgroup V tantalum and niobium intermetallic compounds with oxygen and nitrogen, shown in Table 2. The segregated impurities and intermetallic compounds at the GBs can then disrupt the d orbital electrons along the GBs and contribute to decohesion. Additionally, distributions of both subgroup V and VI elements may cause disruptions in the d orbital electrons along the GB which causes poor GB cohesion. Just as in conventional subgroup VI refractory metals and alloys, the GBs of the MoNbTaW RCCAs have poor GB cohesion and the decohesion can be exacerbated by segregated interstitial constituents and intermetallic compounds along the GBs. This mechanism of segregation and intermetallic compound formation at the GBs in the MoNbTaW RCCA in the previously discussed studies is most likely driven by the long annealing times and high annealing temperatures needed to produce a homogenous, equiaxed microstructure in the alloy. The interstitial constituents are likely unintentionally introduced to the RCCA from the feedstock materials during the synthesis processes and are driven to segregate and diffuse during secondary processing steps. Ultimately, interstitial constituent interactions with the RCCA constituents led to the mechanisms which embrittled the MoNbTaW RCCA system but can be mitigated to achieve RCCAs with improved strength and ductility.

Computational methods provide an effective tool to address the issue of embrittlement of the MoNbTaW RCCA system by interstitial constituents, and can greatly enhance efforts in developing strong, ductile RCCAs. So far, in the continued development of MoNbTaW based RCCAs, DFT calculations paired with experiments have been applied to understand and control interstitial constituent interactions to improve the plasticity of the MoNbTaW RCCA. Most recently, Wang et al. used DFT to show that the interactions between oxygen and the constituent elements of the MoNbTaW RCCA, at GBs, lead to reduced cohesion and strength of the GBs, embrittling the alloy [37]. Through experiments, Wang et al. showed that additions of up to 8000 ppm of boron and carbon, could improve the ductility of the MoNbTaW alloy by competing with oxygen for GB sites and improving the strength and cohesion of the GBs. With additions of boron, a maximum compressive strain to failure of 11 % in a polycrystalline sample could be achieved. APT experiments were used to observe segregation of oxygen to GBs in the MoNbTaW RCCA without additions of boron. After the addition of boron, APT experiments revealed greater compositions of boron segregated to GBs than oxygen. A 3D APT reconstruction of the RCCA with boron is shown below in Fig. 12 (a), reprinted from Wang et al. [37].

Using DFT calculations, Wang et al. found that boron and carbon have lower segregation energies than oxygen, suggesting a greater propensity for boron and carbon to segregate to GBs, preventing oxygen from segregating and occupying GB sites, as shown in Fig. 12 (b) from Wang et al. [37]. The DFT calculations also showed that the segregated interstitial boron and carbon impurities could improve the strengthening of the GBs of the RCCA. Wang et al. then studied the types of bonding and charge density distributions between the interstitial constituents segregated at GBs and the RCCA constituents of the alloy. The charge density distributions of the segregated interstitial constituents, calculated using DFT, are shown in Fig. 12 (c), reprinted from Wang et al. [37]. It was found that stronger bonds with greater sharing of electrons between boron and carbon impurities and the constituent elements at GBs were formed which helped to strengthen and improve the cohesion at GBs, revealing ductile behavior of the RCCA at room temperature [37]. In this study, boron and carbon were intentionally added, but as shown in conventional alloys with trace amounts of boron and carbon, these interstitial constituents energetically favor segregation to GB sites and can compete with other interstitial constituents which may segregate to GBs [105]. Unlike oxygen and nitrogen, boron and carbon segregated to the GBs of some alloys can enhance the cohesion of the GBs, improving the ductility of the alloy. In both RCCAs and conventional refractory alloys, the segregation energies of boron and carbon and their contributions to the cohesion of the GB could be studied and quantified using DFT [37,105]. Through the use of DFT calculations, experimental results can be validated and mechanistically understood for future development of ductile RCCAs.

However, this method is not necessarily predictive or driven by specifically intended mechanisms. Thus far, few computational techniques have been utilized to understand the influence of interstitial constituents in the MoNbTaW RCCA system, Although the ductility of the MoNbTaW RCCA could be improved by the addition of boron or carbon and the mechanisms by which interstitial constituents embrittle the GBs are being understood, it is still not yet fully known how individual constituent elements may directly contribute to the interactions with the interstitial constituents. For example, the additions of other constituent elements, such as titanium or rhenium, can improve the ductility of the MoNbTaW RCCA, and have been attributed to changes in dislocation motion, but titanium and rhenium likely have strong interactions with trace interstitial constituent elements in the alloy but have not yet been characterized in the MoNbTaW RCCA [168,193-197]. In another study using DFT calculations to support experiments, Tong et al. showed that by removing molybdenum from the MoNbTaW RCCA, ductile transgranular fracture could be achieved [198]. The improved ductility was attributed to improved GB strength by removing molybdenum but the interactions between interstitial constituents and RCCA constituents at the GBs were not characterized. The exact roles of each of the subgroup V and VI constituent elements in the MoNbTaW RCCA require further understanding. Through DFT calculations, a recent study has suggested there are attractive interactions between subgroup V elements and oxygen in the lattices of the MoNbTaW RCCAs, but further studies especially considering interfacial defects are necessary [199]. Through the use of computational techniques, the interactions between interstitial constituents and the constituent elements of RCCAs can be understood to help guide and justify experimental findings. The use of computational techniques can also aid the development of predictive models to develop more ductile RCCAs.

Experimental and computational results reveal that the MoNbTaW RCCA system is particularly sensitive to interstitial constituents

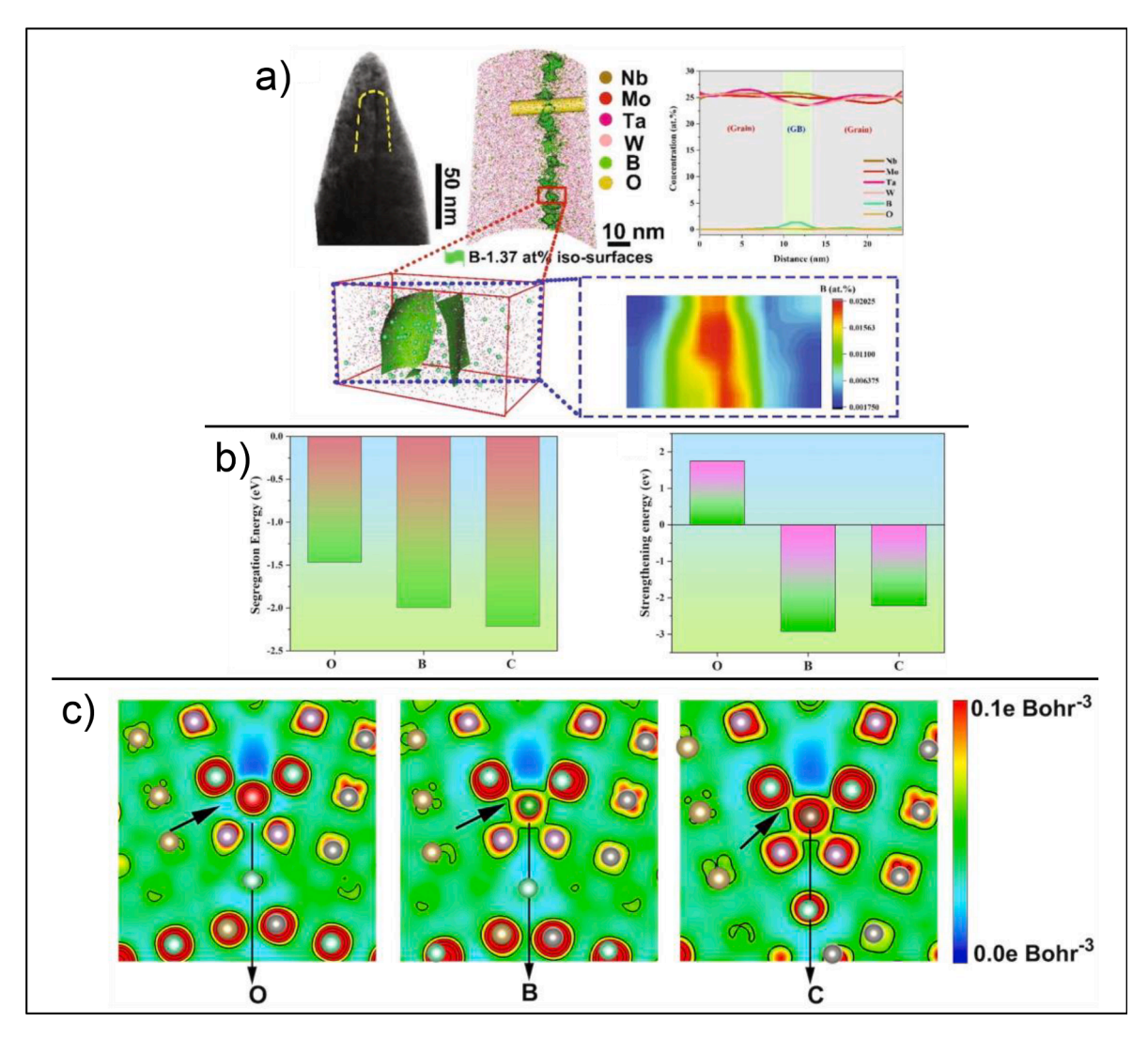


Fig. 12. (a) An APT reconstruction of the MoNbTaW RCCA with additions of boron along with a 1D compositional line profile taken across the GB, and higher magnification analysis of the GB showing 1.37 at. % boron *iso*-surfaces which revealed the segregation of boron to GBs, competing with oxygen, (b) the DFT results of the segregation energy and strengthening energy of various interstitial constituents in the MoNbTaW RCCA, with negative values suggesting greater segregation tendency and greater GB strengthening respectively, and (c) charge density distribution maps of various interstitial constituents segregated along the GBs of the MoNbTaW RCCA, reprinted from Wang et al. [37].

and susceptible to embrittlement by the segregation of trace amounts of interstitial constituents to GBs. The MoNbTaW RCCA appears to have a limit of approximately 100 ppm of oxygen and nitrogen interstitial constituents which embrittle the alloy. The segregation and resultant bonding of oxygen and nitrogen atoms with the RCCA constituent elements along GBs caused the weakening and decohesion of the GBs. DFT calculations proved useful in predicting the segregation energies and bonding of interstitial constituents at GBs. Future work regarding the MoNbTaW RCCA system should aim to understand the role of each of the subgroup V and VI constituent elements in the interactions with interstitial constituents, especially at interfacial defects such as GBs or secondary phase boundaries. By better understanding these interactions, holistic design of RCCAs with high strength and room temperature ductility can be achieved.

4.2. The HfNbTaTiZr system

In 2011, around the same time the MoNbTaW RCCA was initially discovered, the equiatomic HfNbTaTiZr RCCA was also studied for the first time. After arc melting, the HfNbTaTiZr alloy solidified into a single phase BCC microstructure with dendritic microsegregation. Through XRD, the lattice parameter of the single phase BCC alloy was found to be 0.3403 nm [22]. Unlike the MoNbTaW RCCA system however, the HfNbTaTiZr RCCA was found to have high ductility at room temperature. After arc melting and HIP consolidation to close porosity, the HfNbTaTiZr RCCA had a compressive yield strength of 929 MPa and greater than 50 % strain to

failure [22]. The room temperature compressive stress strain curve of the HfNbTaTiZr RCCA is shown below in Fig. 13 (a), from Senkov et al. [22].

The compressive stress strain curves of the MoNbTaW and MoNbTaVW RCCAs are shown in Fig. 13 (a) for comparison. The HfNbTaTiZr RCCA has much higher strain to failure and work hardening behavior than the MoNbTaW RCCA at room temperature. The high room temperature ductility of the HfNbTaTiZr RCCA was attributed to enhanced dislocation motion and twins which reduced stress along GBs. However, upon high loading, cracks were observed to form along GBs. Like conventional BCC metals and alloys, the GBs of the HfNbTaTiZr RCCA most likely have relatively low cohesion, compared to the bulk grain interiors, but the RCCA appeared to be less sensitive to trace amounts of interstitial constituents.

The high ductility of the HfNbTaTiZr RCCA led to its use as the basis for the development of many other RCCAs with high room temperature ductility and inspired theories of ductility prediction in RCCAs. From this system, several non-equiatomic HfNbTaTiZr based RCCAs have been developed with high deformability and cold rolling capabilities [185,200,201]. Because of the relatively low sensitivity of the HfNbTaTiZr RCCA system to interstitial constituents, the influence of interstitial constituents on the mechanical properties of the RCCA systems were not directly studied until more recently. In 2018, Lei et al. arc melted HfNbTiZr alloys with additions of 2 at. % oxygen and 2 at. % nitrogen [39]. The addition of 2 at. % nitrogen increased the strength of the HfNbTiZr alloy to above 1200 MPa but reduced the tensile elongation to 10 % and was attributed to the larger atomic radius of nitrogen, compared to oxygen. However, the addition of 2 at. % oxygen resulted in increased strength and an anomalous increase in ductility of the alloy. Using high angle annular dark field (HAADF) and annular bright field (ABF) techniques in scanning transmission electron microscopy (STEM), Lei et al. observed regions described as having chemical short range ordering (CSRO) [39]. CSRO is the preferential accommodation of lattice sites at relatively short length scales, such as nearest neighbors, and has been observed in several CCAs and is predicted in some RCCAs as well [12,202-204]. CSRO is suggested to be due to the preference or avoidance of an element with other element species or with itself. In the HfNbTiZr RCCA, some regions of CSRO were enriched in titanium and zirconium, and some were enriched in hafnium and tantalum. From STEM-ABF, oxygen was shown to occupy both tetrahedral and octahedral interstitial sites and showed preference for interstitial sites near the titanium and zirconium enriched CSRO regions, forming ordered oxygen complexes (OOCs). Using APT, Lei et al. showed the OOCs could reach up to 10 at. % oxygen and internal friction measurements were used to detect the ordered structural state of oxygen in the OOCs. An APT reconstruction of the alloy with OOCs is shown in Fig. 13 (b), reprinted from Lei et al. [39]. 3 at. % oxygen isocompositions were highlighted to visualize the oxygen enriched complexes on the nanometer scale in the matrix of the alloy [39]. The occupation of oxygen atoms in the titanium and zirconium rich complexes in an orderly manner is attributed to the increased plasticity and work hardening of the alloy. It was suggested that the OOCs can distort the local lattice, creating a strain field around them and can promote cross slip. Ultimately, Lei et al. showed that interstitial elements in solution may interact with each constituent element in an RCCA preferentially, resulting in new ordered complex structures which improved strength and ductility by 50 and 100 % of the original RCCA strength and ductility, respectively.

In another study of interstitials in 2020, Lei et al. arc melted $HfNb_{0.5}Ta_{0.5}TiZr$ alloys with additions of 2 at. % oxygen and 2 at. % nitrogen [46]. In both cases, the added oxygen and the added nitrogen interstitials contributed to the formation of ordered interstitial complexes (OICs) and resulted in improvements to both the strength and ductility of the starting alloy [46]. Using internal friction measurements, Lei et al. were able to deconvolute the contributions to mechanical properties of the ordered complexes and randomly distributed interstitial constituents. Furthermore, through internal friction measurements, Lei et al. observed Snoek-type stress induced switching of interstitial site configurations. The final and intermediate Snoek-type jumps by interstitials between

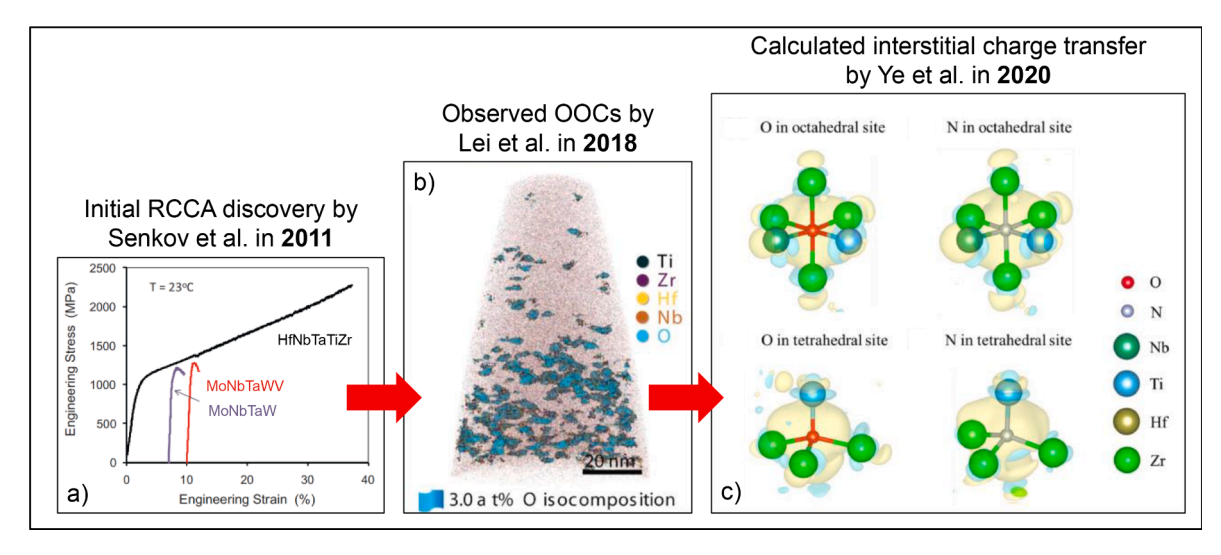


Fig. 13. The progression of understanding of the HfNbTaTiZr RCCA system over time, starting from (a) the compressive stress strain curve of the RCCA at room temperature, reprinted from Senkov et al. [22], (b) APT reconstruction of the HfNbTiZr RCCA which led to the observation and assessment of OOCs from Lei et al. [39], and finally (c) mapping of localized charge transfer distribution between interstitial constituents and RCCA constituents in a HfNbTaTiZr RCCA determined through DFT from Ye et al. [43].

configurations yielded high damping performance in the alloy [46]. The damping behavior of the HfNb_{0.5}Ta_{0.5}TiZr alloys with OICs are compared to conventional interstitially doped alloys below in Fig. 14 (a), reprinted from Lei et al. [46].

The OICs of the alloys were identified through APT experiments and the resulting reconstruction is shown in Fig. 14 (b), from Lei et al. [46]. These findings showed that constituent elements in RCCAs can dictate the mechanisms by which interstitial constituent elements influence the mechanical properties of the RCCAs and could potentially be controlled to target exceptional combinations of strength and ductility in RCCAs.

Recently, many more studies of the interstitial constituents in HfNbTaTiZr based alloys have been published [38,41,43,184,187,205]. In 2022, Liu et al. developed and studied a BCC single phase massive interstitial solid solution (MISS) alloy from an equiatomic NbTiZr RCCA with additions of up to 12 at. % oxygen. The initial equiatomic NbTiZr RCCA constituent elements were chosen for their high solubilities of oxygen interstitials. Calculated phase diagrams (CALPHADs) were used to analyze the binary phase diagrams of the constituent elements with oxygen to approximate and design for high solubility of oxygen in the alloy. In addition to the 12 at. % oxygen interstitials, 1 at. % carbon, and 1 at. % nitrogen were also added to the alloy to segregate to and strengthen and stabilize the GBs of the alloy without detrimental formation of carbides or nitrides along the GBs. The segregation of nitrogen and carbon to GBs suppressed localized deformation and embrittlement of the GBs and the 12 at. % oxygen in solution significantly improved the strength of the alloy. It is also possible the addition of the carbon and nitrogen helped compete with and prevent the segregation of oxygen to the GBs of the alloy. The (NbTiZr)₈₆O₁₂C₁N₁ MISS alloy was magnetron sputtered and subsequently annealed to allow diffusion of interstitials and formation of any thermodynamically stable intermetallic compounds. Upon annealing, no new phases formed; a single phase BCC massive solid solution was retained. Through micropillar compression testing, the yield strength of the MISS alloy was found to be 4.2 GPa, near the theoretical limit of ~ G/10 and more than 65 % strain to failure with significant strain-hardening behavior. A stress strain curve from microcompression tests of the NbTiZr alloys is shown below in Fig. 15 (a), reprinted from Liu et al. [40].

Upon deformation, Liu et al. found that the oxygen interstitials promoted dislocation multiplication. The dislocation multiplication during deformation and enhanced strength of the GBs promoted deformation-driven grain refinement in the alloy, owing to the high strain-hardening [40]. Through intentional RCCA design, interstitial constituents can be exploited to improve strength and deformation mechanisms of RCCAs. Although the HfNbTaTiZr RCCA system and similar RCCAs are not highly sensitive to embrittlement by

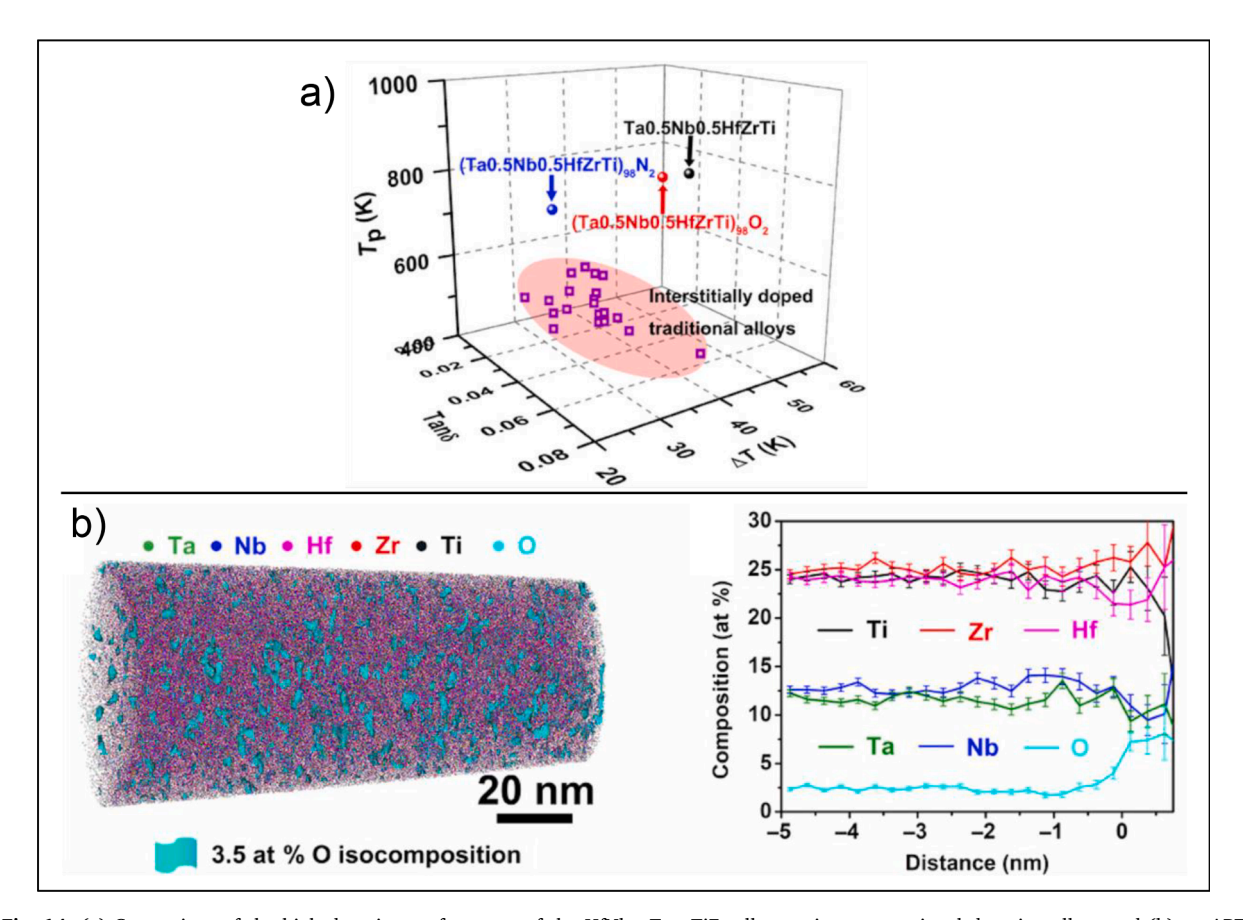


Fig. 14. (a) Comparison of the high damping performance of the $HfNb_{0.5}Ta_{0.5}TiZr$ alloy against conventional damping alloys and (b) an APT reconstruction of a sample of the $HfNb_{0.5}Ta_{0.5}TiZr$ alloy revealing OICs presented with a 1D compositional line profile taken across the boundary between the alloy matrix and an OIC, reprinted from Lei et al. [46].

interstitial constituents as in the MoNbTaW RCCA system, interstitial constituents still play an important role in contributing to the strength and ductility of the alloys. Because of the solubility of interstitials in the HfNbTaTiZr RCCAs, interstitial alloying is an effective strengthening strategy for the HfNbTaTiZr based RCCAs. The mechanisms by which the interstitial constituents influence the HfNbTaTiZr based RCCA systems can be understood and controlled by considering the interactions between the interstitial constituent elements and the RCCA constituent refractory metal elements.

Unlike the MoNbTaW RCCA systems, the HfNbTaTiZr based RCCAs are much less sensitive to interstitial constituent elements and the interactions between the RCCA constituent refractory metal elements and the interstitial constituent elements can be accommodated in the lattice. The BCC lattice of the HfNbTaTiZr RCCA can accommodate the interactions with oxygen and nitrogen impurities in solid solution interstitial sites as stable configurations. The subgroup IV and V elements have relatively large atomic radii with respect to their relatively low electron density which enables stable attractive forces between the RCCA constituents and interstitial elements and the accommodation of the impurities in interstitial sites. Since the HfNbTaTiZr RCCA has a relatively large lattice parameter (0.3403 nm) compared to the MoNbTaW RCCA, the associated large interstitial sites may be able to accommodate the attractive electronic interactions with interstitial constituents. From the lattice parameter found by Senkov et al., an effective atomic radius could be calculated to then approximate the octahedral and tetrahedral interstitial site sizes of the HfNbTaTiZr RCCA. From the lattice parameter determined by Senkov et al., the effective atomic radius of the HfNbTaTiZr RCCA is calculated to be 0.14735 nm and the octahedral and tetrahedral sites were then approximated to be 0.0228 and 0.0429 nm respectively. These interstitial sites are calculated to be smaller than those of subgroup IV, V, and VI metals. Using an average of the atomic radii of the HfNbTaTiZr RCCA constituents, the octahedral and tetrahedral interstitial sites are approximated to be 0.0306 and 0.0575 nm, respectively and are potentially more representative of the interstitial site sizes calculated in the subgroup IV and V refractory metals. Further research to precisely observe, measure, and quantify the interstitial sites in RCCAs is still needed. Much like conventional BCC refractory metals and alloys, the HfNbTaTiZr RCCA may have relatively lower cohesive forces at the GB compared to the bulk grain interiors. Because any inherent interstitial constituent elements are accommodated in solid solution, they may have less direct impact on the GB cohesion. Furthermore, the bonding between the RCCA constituents and interstitial constituents at GBs may improve the cohesion of the GBs as suggested by Liu et al. [40]. Just as in conventional subgroup IV metals and alloys, oxygen and nitrogen can occupy interstitial sites and tend to prefer sites near titanium and zirconium. In conventional titanium based alloys, repulsive forces produced by substitutional solutes caused preferential occupation of interstitial sites near titanium [122]. In the HfNbTaTiZr based RCCAs, a similar phenomenon may be occurring, suggested by the observation that OOCs are titanium and zirconium rich and separate CSRO regions of hafnium and tantalum were also observed, depleted of oxygen. The non-dilute solid solution of subgroup IV and V metals may have reduced repulsive interactions with interstitials since not all the interstitial constituents contributed to the formation of ordered complexes and some are still randomly distributed. It is possible that in the HfNbTaTiZr based RCCAs, titanium and zirconium

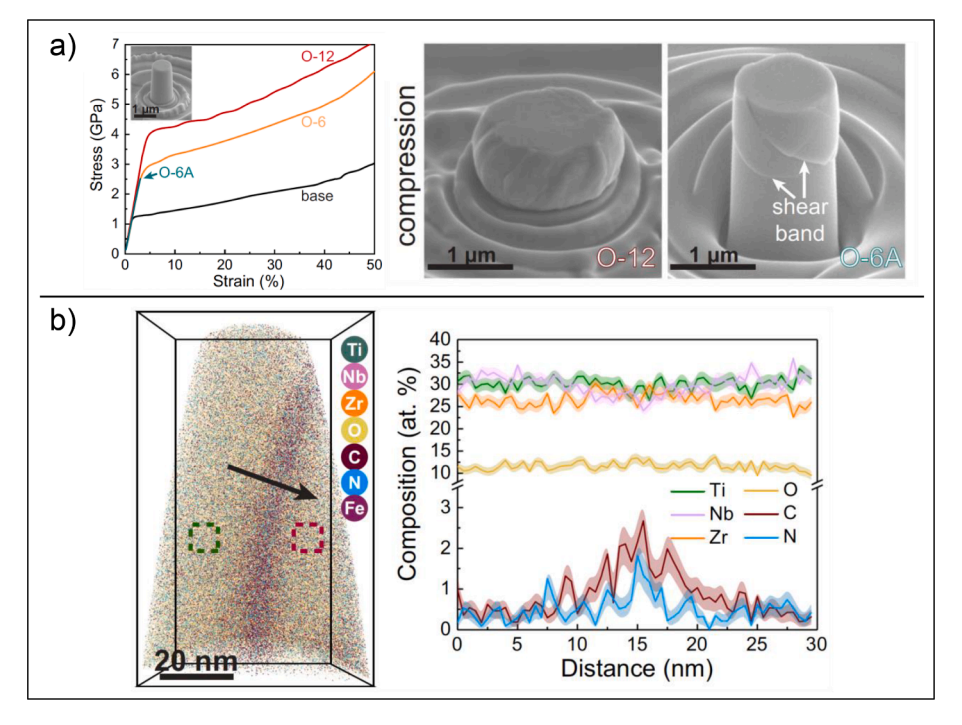


Fig. 15. (a) Stress strain curves from the microcompression tests of the MISS NbTiZr alloy, compared to the NbTiZr alloy with no interstitial constituents intentionally added along with electron micrographs of the compressed alloys, revealing high deformability and shear bands in the alloys. (b) An APT reconstruction of the MISS NbTiZr alloy before deformation and a 1D compositional line profile across the GB of the alloy, revealing carbon and nitrogen at GBs and oxygen in solution, not segregated to GBs, reprinted from Liu et al. [40].

may form more attractive cohesive bonding with interstitial elements than hafnium and tantalum. Because they can be accommodated in the lattice, the interstitial oxygen and nitrogen atoms in solution significantly contribute to the interstitial solid solution strengthening of the alloy. Nitrogen's larger atomic radius than oxygen yields a larger impact on the increase in strength of the alloy and induces embrittlement and may form nitrides more easily and at lower concentrations than oxygen. In the HfNbTaTiZr based RCCAs, OICs also contribute to the strength and the ductility of the alloy. The strong cohesive forces between the constituent metals and interstitials in the complexes require higher energy to initiate deformation. The accommodation of dislocations by the ordered complexes can contribute to the ductility and work hardening of the alloy. Furthermore, the Snoek-type stress induced jumps by interstitials between stable interstitial configurations may produce the high work hardening and ductility of the alloy. A more complete understanding for why OICs tended to contain more titanium and zirconium as opposed to hafnium is still needed. It may be that the titanium and zirconium elements have greater attractive forces for oxygen and nitrogen due to a lower electron density and that the other substitutional solutes hafnium, niobium, and tantalum, may produce repulsive forces due to strain fields and higher electron densities in the lattice. Further studies understanding the interactions between RCCA constituents and interstitial constituent elements are needed. Ultimately the interactions of interstitial constituents with the constituent RCCA elements can produce beneficial influences on the mechanical properties of RCCAs. By understanding the mechanisms of the interactions between impurities and RCCA constituents, RCCAs can be designed to have low sensitivity to interstitial constituent elements and to even take advantage of the mechanisms for more holistic design of RCCAs.

Computational techniques can be useful tools in the understanding of interstitial constituent element interactions in HfNbTaTiZr based RCCAs and the understanding of the influence of interstitial constituents on the mechanical behavior of the RCCA. In 2020, Ye et al. studied the influence of interstitial constituents on the dislocation motion of the HfNbTiZr RCCA using nanoindentation experiments paired with DFT calculations [43]. Equiatomic HfNbTiZr RCCAs were arc melted without intentional interstitial constituents and with additions of 2 at. % oxygen and 2 at. % nitrogen. The arc melted alloys were then homogenized, cold rolled to 80 % reduction in thickness, and finally annealed achieving homogenous, equiaxed grains in the size range of 30 to 350 µm for nanoindentation experiments. The load versus displacement curves obtained from the nanoindentation experiments of the HfNbTiZr RCCA are shown below in Fig. 15, reprinted from Ye et al. [43].

From the nanoindentation experiments of the alloys, a linear, elastic load–displacement relationship was observed [43]. From the linear, elastic region, the Young's modulus was found to increase in the RCCAs with additions of 2 at. % oxygen and 2 at. % nitrogen compared to the RCCA without intentionally added interstitial constituents. Following the linear, elastic region of the load displacement curve, a "pop-in" event caused by a displacement burst was observed, as shown in Fig. 16 above, reprinted from Ye et al. [43]. The "pop-in" event is indicative of the onset of yielding and plastic deformation of the alloy. From the "pop-in" loads, shear moduli (G) on the order of 3 GPa were calculated, and the maximum shear stress was found to be near the theoretical strength of $\sim G/10$. Most likely due to the larger atomic radius of nitrogen, the RCCA alloyed with 2 at. % nitrogen had a larger increase in shear stress than the 2 at. % oxygen alloyed RCCA. By the Frank-Read source model, it was assumed that the "pop-in" displacement burst is due to the sudden nucleation and multiplication of dislocations. However, the deformed volume under the nanoindentation depth is too small to accommodate the nucleation and multiplication of dislocations at the scale described by the Frank-Read model. So, Ye et al. used DFT calculations to understand the "pop-in" event and the influence of interstitial constituents on the "pop-in". From the DFT calculations and TEM characterization of the indented samples, Ye showed that the plastic deformation of the alloy with and without interstitials is mediated by $\{1\,1\,0\}\$ $\langle 1\,1\,1\rangle$ slip and that the oxygen and nitrogen atoms may occupy both the octahedral and tetrahedral

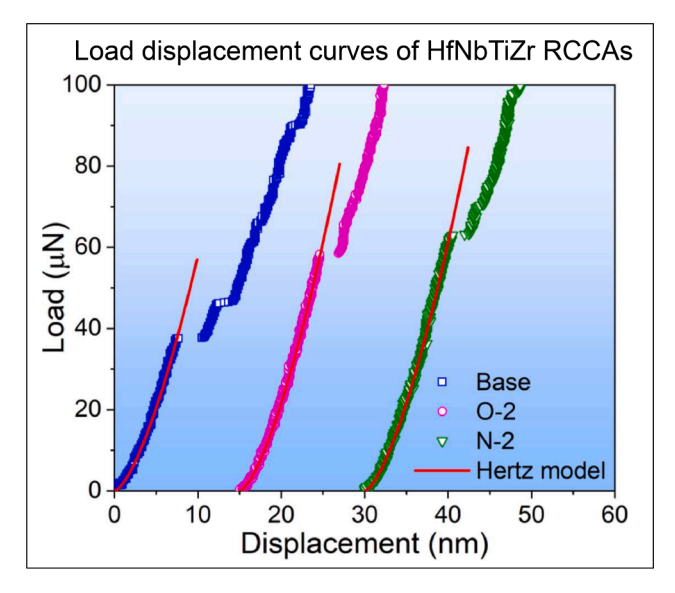


Fig. 16. Load versus displacement curves of the HfNbTiZr RCCAs, revealing "pop-in" events during the nanoindentation of the alloys, reprinted from Ye et al. [43].

interstitial sites of the alloy [43]. Ye et al. used DFT calculations to analyze the local charge transfer between the interstitial constituents and neighboring RCCA constituents. It was found that the interstitial oxygen and nitrogen elements draw more charge from their respective nearest neighbor metal atoms [43]. The localized Bader charge distribution map of the interstitial constituent elements, surrounded by neighboring metal elements from DFT calculations are shown in Fig. 13 (c), reprinted from Ye et al. [43]. From the charge distribution DFT calculations, oxygen and nitrogen are found to attract significant electrons from their local environments. The observed charge transfer results in more ionic-like bonding between the metals and interstitials in solution, increasing the atomic cohesion between them. This ionic-like bonding of the interstitial constituents and RCCA constituents resulted in the formation of metal-interstitial complexes. The enhanced cohesion between the interstitial constituents and RCCA constituents in the complexes required higher energy and stress to shear the bonds of the interstitial complexes. The increase in shear strength caused by the presence of interstitial constituents and associated charge transfer agreed well with the experimental results. In the study by Ye et al., DFT calculations paired with nanoindentation experiments were used to develop an understanding of the influence of interstitial constituents on the mechanical behavior of the HfNbTiZr RCCA. The use of computational techniques, especially when paired with experimental findings, can aid the understanding of the mechanisms by which interstitial constituents influence mechanical properties of RCCAs. By understanding the mechanisms of interstitial constituents in RCCAs through computational models and simulations, RCCAs can be designed to achieve high strength and high ductility.

Most recently, CSRO and ordered complexes in the NbTiZr alloy have been intentionally manipulated through compositional design of both the RCCA constituents and the interstitial constituents. Jiao et al. synthesized NbTiZr alloys with varying amounts of 14 – 30 at. % niobium and 0 to 4 at. % oxygen through PAM [187]. The contents of oxygen were near the targeted concentrations and could be used to suggest trends in OOC formation with respect to the compositional design of the RCCA constituents. In the NbTiZr alloy with 26 at. % niobium, the addition of oxygen increased the lattice parameter nearly linearly from 0.3392 nm with 0 at. % oxygen to 0.3401 nm with 4 at. % oxygen [187]. In the alloys with only 14 at. % niobium, the addition of oxygen would lead to increased strength and increased ductility, up to 3.5 at. % oxygen, while in the alloys with 30 at. % niobium, additions of oxygen would lead to increased strength but not ductility [187]. Jiao et al. attributed this phenomenon to CSRO and OOC formation. In Fig. 17 below, reprinted from Jiao et al., contributions to CSRO and OOC formation from the RCCA constituents and interstitial constituents are summarized [187].

As depicted in Fig. 17, Jiao et al. showed that niobium stabilized the BCC structure in the NbtiZr alloy and further niobium additions would cause titanium and zirconium rich CSRO in the alloy. Jiao et al. used DFT to determine that in the NbTiZr alloy, the CSRO was caused by niobium atoms preferring niobium nearest neighbor atoms [187]. At 30 at. % niobium and above, the amount of CSRO would reduce. In the NbTiZr alloys with CSRO, the addition of oxygen would lead to the formation of OOCs and above 3 at. % oxygen would lead to GB segregation and eventually embrittlement. The high affinity for oxygen of titanium and zirconium in the CSRO regions would cause the formation of the OOCs but no phase transformation was observed via XRD or HRTEM [187]. Ultimately, Jiao et al. used experimental and DFT studies to design RCCAs by considering the interactions between RCCA constituents and interstitial constituents to achieve alloys with both high strength and high ductility.

Through both experimental and computational studies, the HfNbTaTiZr RCCA and similar systems have shown to have relatively low sensitivity to interstitial constituents which can improve the strength and ductility of the RCCA. The HfNbTaTiZr RCCA appears to have a sensitivity limit of nearly 3 at. % oxygen in the alloy before detrimental embrittlement occurs. The electronic interactions between the RCCA constituents and the interstitial constituents and the relatively large interstitial sites enable the accommodation of interstitial constituents in the lattice, reducing the sensitivity of the RCCA to interstitial constituents. The interactions between the RCCA constituents and the interstitial constituents may lead to the formation of nanometer scale OICs. The charge distributions and bonding in the OICs and their interfaces with the surrounding matrix can impede the motion of dislocations and cause the nucleation of more dislocations improving both strength and ductility of the RCCAs. The use of computational methods such as DFT proved useful in understanding the charge distributions which lead to the mechanisms and microstructural features observed in the HfNbTaTiZr RCCAs. CALPHAD modeling may also be useful in designing similar RCCAs which have high solubilities of interstitial elements and have extremely low sensitivities to interstitial constituents. More computational and experimental studies are clearly needed to properly establish an in-depth understanding of the role of interstitial constituents in RCCAs and how RCCAs can be developed to take advantage of inherent interstitial constituents through holistic design approaches.

5. Holistic design of interstitial constituents in RCCAs

RCCAs can be designed to target alloys with specific properties for intended performance across an entire industrial application, from synthesis to use. Just as many conventional alloys are designed with intended processing conditions, deformation mechanisms, and performance limits, holistic approaches to the design of RCCAs should consider the synthesis of RCCAs, mechanisms which influence the properties of the RCCAs, and the final properties needed for intended applications. Since many processing techniques were developed to enable the application of specific conventional alloys, further process developments may be required to bring RCCAs to full industrial scale applications. For now, conventional processing techniques need to be used with alloy design criteria to control mechanisms and interactions of interstitial constituents in RCCAs.

To design RCCAs with improved ductility at room temperature and high strength at elevated temperatures, the interactions of interstitial constituents with the RCCA constituent elements and the effects of processing on those interactions need to be considered. Specific synthesis and processing techniques can control the introduction and mechanisms of interstitial constituents in RCCAs. The use of specific synthesis and processing methods and the targeting of intended interstitial constituent mechanisms should drive the design of RCCAs with certain constituent elements. The selection of certain RCCA constituents may in turn also drive the need for

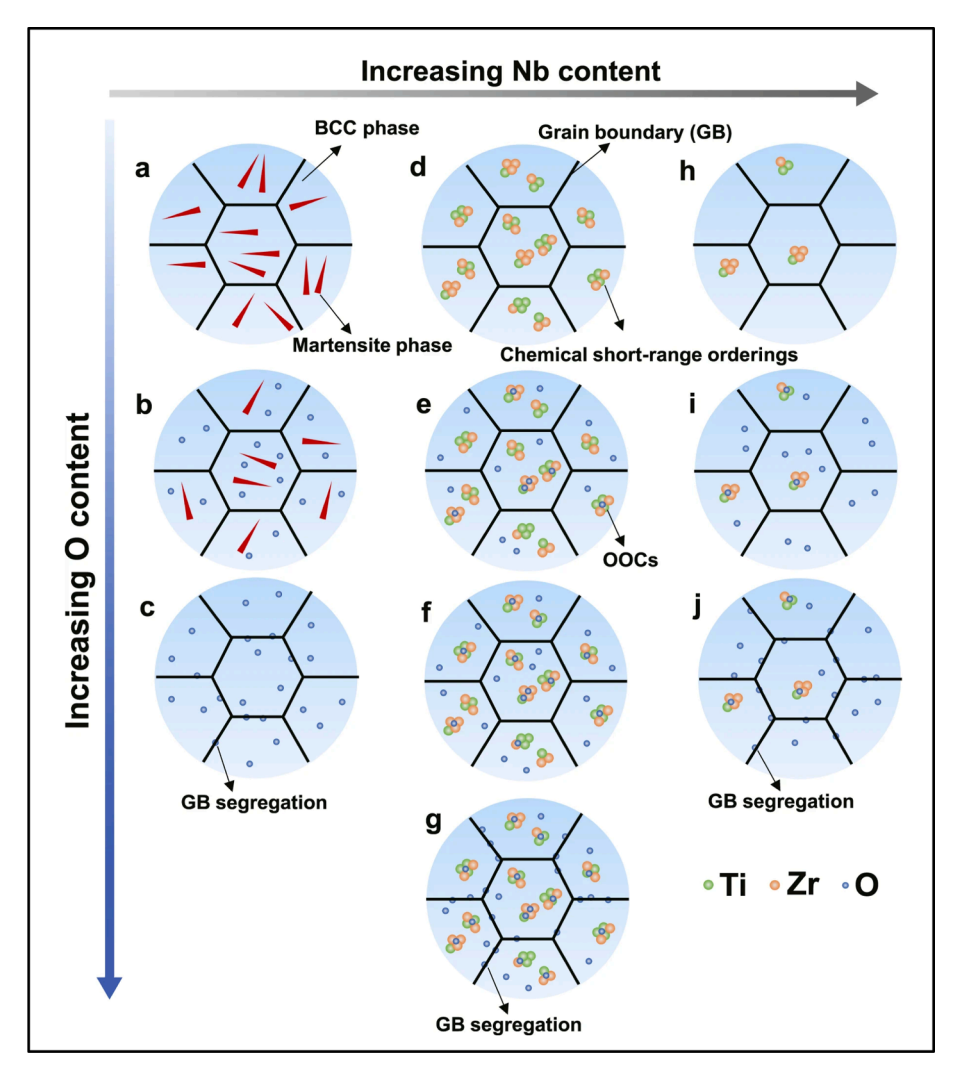


Fig. 17. A schematic diagram of the variations in CSRO and OOCs, which can be manipulated by compositional design of the NbTiZr RCCA, reprinted from Jiao et al. [187].

specific processing techniques and interstitial constituent interactions. A schematic diagram of an example of selection criteria for more holistic RCCA design, driven by targeted properties, is proposed below in Fig. 18.

By intentionally choosing specific selection criteria, intended mechanisms or effects in designed RCCAs can be targeted to influence mechanical properties such as strength and ductility. For example, powder metallurgical techniques may be needed to develop molybdenum based RCCAs to offset the costs of solidification processes and other secondary processing to achieve a ductile, homogenous alloy. Because powder metallurgical techniques introduce significantly more interstitial constituents and subgroup VI elements such as molybdenum are highly sensitive to interstitial constituents, the RCCA constituents and other powder metallurgical processing conditions should be intentionally designed to control the mechanisms of the interstitial constituents which are inherently expected in the molybdenum based RCCA. Since molybdenum and other subgroup VI elements are highly sensitive to interstitial constituents, mechanisms need to be discovered and controlled to design RCCAs which utilize subgroup VI elements, but have lower sensitivities to interstitial constituents. It may be possible that the OOCs observed in HfNbTaTiZr-based RCCAs can be achieved in MoNbTaW-based RCCAs through intentional compositional design and may lower the MoNbTaW RCCA's sensitivity to interstitial constituents resulting in improved room temperature ductility. Up to now, several design criteria and guidelines for RCCAs with room temperature ductility have been suggested but may not fully account for the unintended interactions between interstitial constituents and RCCA constituents. More holistic design approaches to RCCAs can encapsulate previously suggested design criteria, such as VEC, as starting points for RCCA design to fully develop industrial application specific RCCAs with targeted properties by considering how interstitial constituents influence RCCAs. Since interstitial constituent interactions with RCCA constituents may be driven by electron configurations and atomic sizes, average VEC and electron densities may be useful criteria for initial design of RCCAs with intended interstitial constituent mechanisms to account for expected amounts of inherent interstitial constituents. Ultimately, designing RCCAs by considering interstitial constituents and the processing routes necessary to produce them can result in more ductile RCCAs for targeted industrial

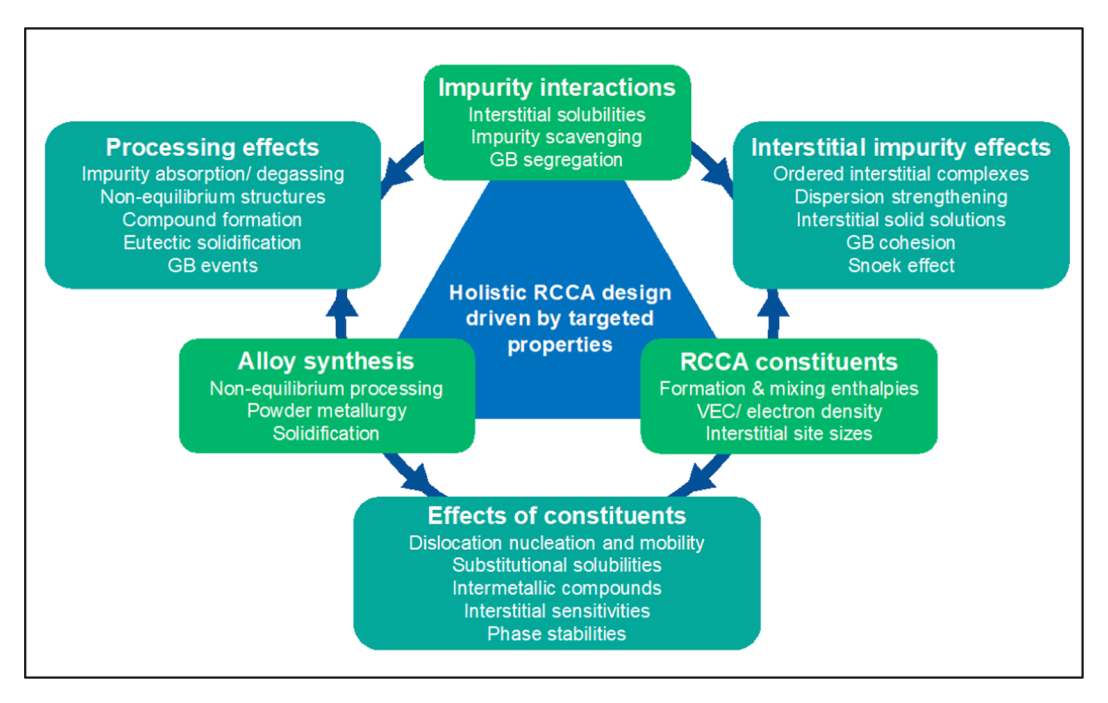


Fig. 18. A schematic diagram of considerations for holistic RCCA design to target properties and intended industrial applications. At the points of the triangle are selection criteria which can drive mechanisms and effects which influence the mechanical properties of the final RCCA.

applications.

Furthermore, for RCCAs to compete with the applications of conventional refractory and Ni-based superalloys, RCCAs must also have high temperature creep strength, oxidation resistance, and relatively low density. So, achieving RCCAs with high ductility at room temperature is only part of the holistic design challenge. To achieve high temperature strengths in RCCAs, certain elements and phases with high temperature strengths and stabilities are necessary, but may be highly sensitive to interstitial constituents, so further processing and alloy design are needed to achieve low sensitivity to interstitial constituents and room temperature ductility. Since some of the subgroup VI elements are ideal for achieving high temperature creep strength but are also severely sensitive to interstitial constituents, highly dense, and not resistant to oxidation, RCCA design must make use of subgroup IV and V elements as well as other transition metal elements not conventionally used in the design of refractory alloys.

6. Key takeaways and future directions

By now it is well understood that the mechanical behavior of RCCAs is influenced by the interactions between interstitial constituents and RCCA constituents. Just as in conventional refractory metals and alloys, the fracture of BCC RCCAs can be controlled by dislocation motion and cohesion at GBs. The observation of the DBTT in RCCAs can be influenced by interstitial constituents. If not characterized, the interactions between interstitial constituent elements and RCCA constituent elements may convolute the understandings, observations, and predictions of mechanical properties of RCCAs. In this review, the mechanisms by which interstitial constituents influence the mechanical properties of RCCAs are summarized and examined in depth with context from understandings of conventional refractory metals and alloys. The key findings from this review of the current state-of-the-art literature are summarized below:

- As a result of both experimental and computational techniques, we now have a better understanding of the interactions between interstitial constituents and RCCA constituents. The interactions have been shown to be driven by electron configurations which dictate valency, bonding, atomic size, and electron density of the RCCA constituents.
- RCCAs can have a wide range of mechanical properties and the MoNbTaW and HfNbTaTiZr systems represent distinct sensitivities
 to interstitial constituents in RCCAs. The MoNbTaW RCCA is highly sensitive to interstitial constituents, above 100 ppm, which
 segregate to GBs and contribute to brittle or ductile failure. The HfNbTaTiZr RCCA has low sensitivity to interstitial constituents
 and can form solid solutions up to approximately 3 at. % oxygen or nitrogen and even OICs which can improve both strength and
 ductility of the alloy.
- By understanding how interstitial constituents may influence mechanical properties and deformation mechanisms of RCCAs, more
 holistic RCCA design can be achieved. Holistic RCCA design approaches must also consider the interactions between RCCA constituents and interstitial constituents and the use of synthesis and processing techniques to control those interactions for desired
 mechanisms and thus mechanical properties.

Ultimately, holistic approaches to the design of RCCAs can help achieve high temperature structural alloys with low sensitivities to
interstitial constituents and thus high strength and room temperature ductility. In addition to room temperature ductility, RCCAs
must also have high temperature creep strength, relatively low density, and oxidation resistance to outcompete conventional refractory and Ni-based superalloys.

This review of recent literature has highlighted several studies which have reported on the influence of interstitial constituents on the mechanical properties of RCCAs, but further research is needed if deeper understandings of the governing mechanisms are to be established. Areas which require further advancements to better understand and control interstitial constituents in RCCAs are summarized below:

- Some computational techniques such as DFT and CALPHAD calculations have been used to better understand and predict the interactions between interstitial constituents and RCCA constituents. However, further understanding is needed to better predict how constituent elements may compete and interact with interstitial constituents in RCCAs. To better characterize the interactions and driving forces between interstitial constituents and RCCA constituents, and to aid holistic design of RCCAs, computational modelling and simulations continue to be necessary. Additional use of DFT calculations will benefit the understandings of interactions between interstitial constituents and competing RCCA constituents to understand what types of mechanisms may influence the mechanical properties of an RCCA. Further CALPHAD calculations can also be used to aid predictions of interstitial constituent mechanisms in RCCAs to drive holistic RCCA design targeting intended mechanisms, but more binary and ternary interactions with interstitial constituents need to be assessed to accurately compute phase diagrams. MD simulations may also be useful in developing the understanding of interstitial constituent interactions with RCCA constituents during synthesis and in the presence of GBs to aid holistic design considerations to control and target intended mechanisms. More interatomic potentials which include interstitial constituents need to be developed for MD simulations.
- In some literature, the influence of processing techniques on the interactions and mechanisms of interstitial constituents in RCCAs was reported and examined but is still not fully characterized. Further understandings of the influence of synthesis and processing techniques are also required to accurately characterize the influence of interstitial constituents in RCCAs. Processing techniques may require further developments to produce RCCAs with more industrially representative contents of interstitial constituents. A closer look at the use of advanced processing techniques for RCCAs, such as additive manufacturing and molten alloy degassing, may be necessary to bring RCCAs to industrial application.
- To understand the mechanisms and interactions of interstitial constituents in RCCAs, the continued use of nanoscale and atomistic characterization techniques becomes more necessary. As described in this review, nanoscale characterization techniques such as APT and various TEM, STEM, and HRTEM techniques were necessary to observe the structural features resulting from interstitial constituents in RCCAs. In some cases, microanalysis characterization techniques such as electron backscattered diffraction, energy dispersive x-ray spectroscopy, and XRD may be useful in identifying changes to phases, microstructural features, and lattice parameters due to changes in interstitial constituents. Though changes to lattice parameters in RCCAs with interstitial constituents have been noted and quantified, it is not yet clear to what degree the interstitial constituents in RCCAs may result in further distortion or straining of the BCC lattice. Furthermore, the interstitial site sizes in RCCAs may differ in size and range of sizes from conventional refractory alloys and may not yet be fully understood. The existence of CSRO in RCCAs may further disrupt and contribute to the possible ranges and distributions of interstitial site sizes in RCCAs.
- Furthermore, interstitial constituents will likely play significant roles in the elevated temperature properties of RCCAs. In addition to understanding processing of RCCAs at elevated temperatures, more extensive data to describe service life of RCCAs such as creep rates, oxidation resistance, and phase stabilities need to be understood and considered in the design of RCCAs. Additionally, further understanding of interstitial constituents beyond oxygen and nitrogen are necessary, especially for elevated temperature properties. The behaviors of boron, carbon, and hydrogen in RCCAs must also be understood for the development of high temperature structural materials.
- Due to the nature of the challenges associated with controlling and measuring interstitial constituent elements, advanced modeling, synthesis, and characterization continue to be necessary for the design of RCCAs from an atomistic level.

In some RCCAs which have been shown to have high ductility at room temperature, it is possible that the specific combinations of constituent elements of the RCCA are not sensitive to inherent interstitial constituents, but the influence of the impurities is not addressed. Therefore, in many RCCAs developed and studied thus far, the precise interactions of interstitial constituents and constituents are not yet fully understood or predictable. As new RCCA compositional space is explored, the interstitial constituents inherent to specific processing techniques and their interactions should be considered and reported. In non-dilute solutions of metals, the activities and chemical potentials of the elements likely change, thereby changing their interactions with interstitial constituents, especially during processing, but are not yet fully characterized. More holistic approaches to RCCA design still require additional understanding of how interstitial constituents interact with the non-dilute RCCA constituent elements and how their mechanisms influence mechanical properties. With further characterization of the mechanisms by which interstitial constituents influence mechanical behavior of RCCAs, holistic design approaches can be used to develop strong, ductile RCCAs.

Author Contributions.

Calvin H. Belcher participated in conceptualization, validation, formal analysis, investigation, resources, writing the original draft, and visualization. Benjamin E. MacDonald took part in methodology, validation, resources, writing, reviewing, and editing. Diran Apelian took part in conceptualization, writing, reviewing, editing, supervision, and funding acquisition. Enrique J. Lavernia

contributed to conceptualization, resources, writing, reviewing, editing, supervision, and funding acquisition.

Declaration of Competing Interest

The authors declare that they have no known competing financial interests or personal relationships that could have appeared to influence the work reported in this paper.

Data availability

Data will be made available on request.

Acknowledgements

This research was primarily supported by the National Science Foundation Materials Research Science and Engineering Center program through the UC Irvine Center for Complex and Active Materials (DMR-2011967). The authors acknowledge the use of facilities and instrumentation at the UC Irvine Materials Research Institute (IMRI) supported in part by the National Science Foundation Materials Research Science and Engineering Center program through the UC Irvine Center for Complex and Active Materials (DMR-2011967).

References

- [1] Perepezko JH. The hotter the engine, the better, Science 2009;(80-.), 326;1068-9, https://doi.org/10.1126/science.1179327.
- [2] Zhang T, Deng HW, Xie ZM, Liu R, Yang JF, Liu CS, et al. Recent progresses on designing and manufacturing of bulk refractory alloys with high performances based on controlling interfaces. J Mater Sci Technol 2020;52:29–62. https://doi.org/10.1016/j.jmst.2020.02.046.
- [3] D. Rowe, Refractory Metals, 2003. https://www.asminternational.org/c/portal/pdf/download?articleId=HTP00307P056&groupId=10192.
- [4] Snead LL, Hoelzer DT, Rieth M, Nemith AAN. Refractory Alloys: Vanadium, niobium, molybdenum, tungsten. Elsevier Inc.; 2019. 10.1016/B978-0-12-397046-6.00013-7.
- [5] Curzon FL, Ahlborn B. Efficiency of a Carnot engine at maximum power output. Am J Phys 1975;43:22-4. https://doi.org/10.1119/1.10023.
- [6] Cemal M, Cevik S, Uzunonat Y, Diltemiz F. ALLVAC 718 Plus[™] Superalloy for Aircraft Engine Applications. Recent Adv Aircr Technol 2012;718. https://doi. org/10.5772/38433.
- [7] Miracle DB, Senkov ON. A critical review of high entropy alloys and related concepts. Acta Mater 2017;122:448–511. https://doi.org/10.1016/j.
- [8] Yeh JW, Chen SK, Lin SJ, Gan JY, Chin TS, Shun TT, et al. Nanostructured high-entropy alloys with multiple principal elements: Novel alloy design concepts and outcomes. Adv Eng Mater 2004;6:299–303. https://doi.org/10.1002/adem.200300567.
- [9] Cantor B, Chang ITH, Knight P, Vincent AJB. Microstructural development in equiatomic multicomponent alloys. Mater Sci Eng A 2004;375–377:213–8. https://doi.org/10.1016/j.msea.2003.10.257.
- [10] Gludovatz B, Hohenwarter A, Catoor D, Chang EH, George EP, Ritchie RO. A fracture-resistant high-entropy alloy for cryogenic applications. Science 2014;345 (6201):1153-8.
- [11] Gludovatz B, Hohenwarter A, Thurston KVS, Bei H, Wu Z, George EP, et al. Exceptional damage-tolerance of a medium-entropy alloy CrCoNi at cryogenic temperatures. Nat Commun 2016;7:1–8. https://doi.org/10.1038/ncomms10602.
- [12] Bajpai S, MacDonald BE, Rupert TJ, Hahn H, Lavernia EJ, Apelian D. Recent progress in the CoCrNi alloy system. Materialia 2022;24:101476. https://doi.org/10.1016/j.mtla.2022.101476.
- [13] George EP, Raabe D, Ritchie RO. High-entropy alloys. Nat Rev Mater 2019;4:515-34. https://doi.org/10.1038/s41578-019-0121-4.
- [14] Senkov ON, Wilks GB, Miracle DB, Chuang CP, Liaw PK. Refractory high-entropy alloys. Intermetallics 2010;18:1758-65. https://doi.org/10.1016/j.intermet.2010.05.014.
- [15] Owen LR, Pickering EJ, Playford HY, Stone HJ, Tucker MG, Jones NG. An assessment of the lattice strain in the CrMnFeCoNi high-entropy alloy. Acta Mater 2017;122:11–8. https://doi.org/10.1016/j.actamat.2016.09.032.
- [16] Wadsworth J, Nieh TG, Stephens JJ. Recent advances in aerospace refractory metal alloys. Int Mater Rev 1988;33:131–50. https://doi.org/10.1179/imr.1988.33.1.131.
- [17] Jaffee RI. A Brief Review of Refractory Metals. Columbus, Ohio: Battelle Memorial Institute; 1959.
- [18] Senkov ON, Miracle DB, Chaput KJ, Couzinie JP. Development and exploration of refractory high entropy alloys A review. J Mater Res 2018;33:3092–128. https://doi.org/10.1557/jmr.2018.153.
- [19] Wang F, Balbus GH, Xu S, Su Y, Shin J, Rottmann PF, et al. Multiplicity of dislocation pathways in a refractory multiprincipal element alloy. Science (80-) 2020;370:95–101. https://doi.org/10.1126/science.aba3722.
- [20] Senkov ON, Miracle DB, Rao SI. Correlations to improve room temperature ductility of refractory complex concentrated alloys. Mater Sci Eng A 2021;820: 141512.
- [21] Senkov ON, Wilks GB, Scott JM, Miracle DB. Mechanical properties of Nb25Mo25Ta 25W25 and V20Nb20Mo 20Ta20W20 refractory high entropy alloys. Intermetallics 2011;19:698–706. https://doi.org/10.1016/j.intermet.2011.01.004.
- [22] Senkov ON, Scott JM, Senkova SV, Miracle DB, Woodward CF. Microstructure and room temperature properties of a high-entropy TaNbHfZrTi alloy. J Alloys Compd 2011;509:6043–8. https://doi.org/10.1016/j.jallcom.2011.02.171.
- [23] Lee C, Maresca F, Feng R, Chou Y, Ungar T, Widom M, et al. Strength can be controlled by edge dislocations in refractory high-entropy alloys. Nat Commun 2021;12:6–13. https://doi.org/10.1038/s41467-021-25807-w.
- [24] Gadelmeier C, Yang Y, Glatzel U, George EP. Creep strength of refractory high-entropy alloy TiZrHfNbTa and comparison with Ni-base superalloy CMSX-4. Cell Reports Phys Sci 2022;3(8):100991.
- [25] Liu CJ, Gadelmeier C, Lu SL, Yeh JW, Yen HW, Gorsse S, et al. Tensile creep behavior of HfNbTaTiZr refractory high entropy alloy at elevated temperatures. Acta Mater 2022;237:118188. https://doi.org/10.1016/j.actamat.2022.118188.
- [26] Senkov ON, Gorsse S, Miracle DB. High temperature strength of refractory complex concentrated alloys. Acta Mater 2019;175:394–405. https://doi.org/10.1016/j.actamat.2019.06.032.
- [27] Ghafarollahi A, Curtin WA. Screw-controlled strength of BCC non-dilute and high-entropy alloys. Acta Mater 2022;226:117617.
- [28] Eleti RR, Stepanov N, Yurchenko N, Zherebtsov S, Maresca F. Cross-kink unpinning controls the medium- to high-temperature strength of body-centered cubic NbTiZr medium-entropy alloy. Scr Mater 2022;209:114367. https://doi.org/10.1016/j.scriptamat.2021.114367.
- [29] Rao SI, Woodward C, Akdim B, Senkov ON, Miracle D. Theory of solid solution strengthening of BCC Chemically Complex Alloys. Acta Mater 2021;209: 116758. https://doi.org/10.1016/j.actamat.2021.116758.

- [30] Sheikh S, Shafeie S, Hu Q, Ahlström J, Persson C, Veselý J, et al. Alloy design for intrinsically ductile refractory high-entropy alloys. J Appl Phys 2016;120(16): 164002
- [31] Senkov ON, Miracle DB. Generalization of intrinsic ductile-to-brittle criteria by Pugh and Pettifor for materials with a cubic crystal structure. Sci Rep 2021;11: 10–3. https://doi.org/10.1038/s41598-021-83953-z.
- [32] Lu Y, Zhang YH, Ma E, Han WZ. Relative mobility of screw versus edge dislocations controls the ductile-to-brittle transition in metals. Proc Natl Acad Sci U S A 2021;118:1–6. https://doi.org/10.1073/pnas.2110596118.
- [33] Butler BG, Paramore JD, Ligda JP, Ren C, Fang ZZ, Middlemas SC, et al. Mechanisms of deformation and ductility in tungsten A review. Int J Refract Met Hard Mater 2018;75:248–61. https://doi.org/10.1016/j.ijrmhm.2018.04.021.
- [34] Ren C, Fang ZZ, Koopman M, Butler B, Paramore J, Middlemas S. Methods for improving ductility of tungsten A review. Int J Refract Met Hard Mater 2018; 75:170–83. https://doi.org/10.1016/j.ijrmhm.2018.04.012.
- [35] Gludovatz B, Wurster S, Weingartner T, Hoffmann A, Pippan R. Influence of impurities on the fracture behaviour of tungsten. Philos Mag 2011;91:3006–20. https://doi.org/10.1080/14786435.2011.558861.
- [36] G.T. Hahn, A. Gilbert, R.I. Jaffee, The Effects of Solutes on the Ductile-to-Brittle Transition in Refractory Metals, Columbus, Ohio, 1962.
- [37] Wang Z, Wu H, Wu Y, Huang H, Zhu X, Zhang Y, et al. Solving oxygen embrittlement of refractory high-entropy alloy via grain boundary engineering. Mater Today 2022;54:83–9. https://doi.org/10.1016/j.mattod.2022.02.006.
- [38] Wang R, Tang Y, Lei Z, Ai Y, Tong Z, Li S, et al. Achieving high strength and ductility in nitrogen-doped refractory high-entropy alloys. Mater Des 2022;213: 110356. https://doi.org/10.1016/j.matdes.2021.110356.
- [39] Lei Z, Liu X, Wu Y, Wang H, Jiang S, Wang S, et al. Enhanced strength and ductility in a high-entropy alloy via ordered oxygen complexes. Nature 2018;563: 546–50. https://doi.org/10.1038/s41586-018-0685-y.
- [40] Liu C, Lu W, Xia W, Du C, Rao Z, Best JP, et al. Massive interstitial solid solution alloys achieve near-theoretical strength. Nat Commun 2022;13:1–9. https://doi.org/10.1038/s41467-022-28706-w.
- [41] Iroc LK, Tukac OU, Tanrisevdi BB, El-Atwani O, Tunes MA, Kalay YE, et al. Design of oxygen-doped TiZrHfNbTa refractory high entropy alloys with enhanced strength and ductility. Mater Des 2022;223:111239.
- [42] Cui Y, Zhu Q, Xiao G, Yang W, Liu Y, Cao G-H, et al. Interstitially carbon-alloyed refractory high-entropy alloys with a body-centered cubic structure. Sci China Mater 2022;65(2):494–500.
- [43] Ye YX, Ouyang B, Liu CZ, Duscher GJ, Nieh TG. Effect of interstitial oxygen and nitrogen on incipient plasticity of NbTiZrHf high-entropy alloys. Acta Mater 2020;199:413–24. https://doi.org/10.1016/j.actamat.2020.08.065.
- [44] Zou Y, Maiti S, Steurer W, Spolenak R. Size-dependent plasticity in an Nb25Mo25Ta 25W25 refractory high-entropy alloy. Acta Mater 2014;65:85–97. https://doi.org/10.1016/j.actamat.2013.11.049.
- [45] Zou Y, Okle P, Yu H, Sumigawa T, Kitamura T, Maiti S, et al. Fracture properties of a refractory high-entropy alloy: In situ micro-cantilever and atom probe tomography studies. Scr Mater 2017;128:95–9. https://doi.org/10.1016/j.scriptamat.2016.09.036.
- [46] Lei Z, Wu Y, He J, Liu X, Wang H, Jiang S, et al. Snoek-type damping performance in strong and ductile high-entropy alloys. Sci Adv 2020;6:1–9. https://doi.org/10.1126/sciadv.aba7802.
- [47] Schulze KK, Jehn HA, Horez G. High-temperature interactions of refractory metals with gases. J Met 1988;40:25-31.
- [48] Fromm E. Gas-Metal Reactions of Refractory Metals at High Temperature in High Vacuum. J Vac Sci Technol 1970;7:S100–5. https://doi.org/10.1116/ 1.1315801
- [49] Fromm E, Jehn H. Thermodynamics and phase relations in refractory metal solid solutions containing carbon, nitrogen, and oxygen. Metall Trans 1972;3: 1685–92. https://doi.org/10.1007/BF02642547.
- [50] Grabke HJ, Horz G. Kinetics and Mechanisms of Gas-Metal Interactions. Annu Rev Mater Sci 1977;7:1057-76.
- [51] Ellingham HJT. Reducibility of Oxides and Sulphides in Metallurgical Processes. J Soc Chem Ind Trans Commun 1944;63:125–60. https://doi.org/10.1002/ictb.5000515215
- [52] Gruber H. Consumable-electrode vacuum arc melting. J Met 1958:193–8. https://doi.org/10.1201/9781315221618-6.
- [53] Knight R, Smith RW, Apelian D. Application of plasma arc melting technology to processing of reactive metals. Int Mater Rev 1991;36:221–52. https://doi.org/10.1179/imr.1991.36.1.221.
- [54] Davidson PA, He X, Lowe AJ. Flow transitions in vacuum arc remelting. Mater Sci Technol 2000;16:699-711. https://doi.org/10.1179/026708300101508306.
- [55] Reed TB. Free Energy of Formation of Binary Compounds: An Atlas of Charts for High-Temperature Chemical Calculations. Cambridge: The MIT Press: 1972.
- [56] Oh JM, Roh KM, Lim JW. Brief review of removal effect of hydrogen-plasma arc melting on refining of pure titanium and titanium alloys. Int J Hydrogen Energy 2016;41:23033–41. https://doi.org/10.1016/j.ijhydene.2016.09.082.
- [57] Suryanarayana C. Mechanical alloying and milling. Prog Mater Sci 2001;46:1-184. https://doi.org/10.1016/S0079-6425(99)00010-9.
- [58] Suryanarayana C. Mechanical Alloying: A Novel Technique to Synthesize Advanced Materials. Research 2019;2019:1–17. https://doi.org/10.34133/2019/4219812.
- [59] Smeltzer JA, Hornbuckle BC, Giri AK, Darling KA, Harmer MP, Chan HM, et al. Nitrogen-induced hardening of refractory high entropy alloys containing laminar ordered phases. Acta Mater 2021;211:116884. https://doi.org/10.1016/j.actamat.2021.116884.
- [60] Garay JE. Current-Activated, Pressure-Assisted Densification of Materials. Annu Rev Mater Res 2010;40:445–68. https://doi.org/10.1146/annurev-matsci-070909-104433.
- [61] Feng X, Utama Surjadi J, Lu Y. Annealing-induced abnormal hardening in nanocrystalline NbMoTaW high-entropy alloy thin films. Mater Lett 2020;275: 128097.
- [62] A. Behera, S. Aich, T. Theivasanthi, Magnetron sputtering for development of nanostructured materials, Elsevier Inc., 2021. https://doi.org/10.1016/B978-0-12-820558-7.00002-9.
- [63] Xu J, Duan R, Feng K, Zhang C, Zhou Q, Liu P, et al. Enhanced strength and ductility of laser powder bed fused NbMoTaW refractory high-entropy alloy via carbon microalloying. Addit Manuf Lett 2022;3:100079. https://doi.org/10.1016/j.addlet.2022.100079.
- [64] Liu C, Zhu K, Ding W, Liu Yu, Chen G, Qu X. Additive manufacturing of WMoTaTi refractory high-entropy alloy by employing fluidised powders. Powder
- [65] Zhang H, Zhao Y, Cai J, Ji S, Geng J, Sun X, et al. High-strength NbMoTaX refractory high-entropy alloy with low stacking fault energy eutectic phase via laser additive manufacturing. Mater Des 2021;201:109462. https://doi.org/10.1016/j.matdes.2021.109462.
- [66] Su B, Li J, Yang C, Zhang Y, Li Z, Zhang Y. Microstructure and mechanical properties of a refractory AlMo0.5NbTa0.5TiZr high-entropy alloy manufactured by laser-directed energy deposition. Mater Lett 2023;335:133748. https://doi.org/10.1016/j.matlet.2022.133748.
- [67] Jeong H-I, Lee C-M, Kim D-H. Manufacturing of Ti-Nb-Cr-V-Ni-Al Refractory High-Entropy Alloys Using Direct Energy Deposition. Materials (Basel) 2022;15 (19):6570.
- [68] Dobbelstein H, Gurevich EL, George EP, Ostendorf A, Laplanche G. Laser metal deposition of a refractory TiZrNbHfTa high-entropy alloy. Addit Manuf 2018; 24:386–90. https://doi.org/10.1016/j.addma.2018.10.008.
- [69] Moorehead M, Bertsch K, Niezgoda M, Parkin C, Elbakhshwan M, Sridharan K, et al. High-throughput synthesis of Mo-Nb-Ta-W high-entropy alloys via additive manufacturing. Mater Des 2020;187:108358. https://doi.org/10.1016/j.matdes.2019.108358.
- [70] Melia MA, Whetten SR, Puckett R, Jones M, Heiden MJ, Argibay N, et al. High-throughput additive manufacturing and characterization of refractory high entropy alloys. Appl Mater Today 2020;19:100560. https://doi.org/10.1016/j.apmt.2020.100560.
- [71] Xiao B, Liu H, Jia W, Wang J, Zhou L. Cracking suppression in selective electron beam melted WMoTaNbC refractory high-entropy alloy. J Alloys Compd 2023; 948:169787. https://doi.org/10.1016/j.jallcom.2023.169787.
- [72] Holden RB, Kopelman B. The Hot-Wire Process for Zirconium. J Electrochem Soc 1953;100:120. https://doi.org/10.1149/1.2781092.
- [73] J.D. Fast, Interaction of Metals and Gases Vol. 1 Thermodynamics and Phase Relations, Academic Press, New York, 1965.

- [74] van Arkel AE, de Boer JH. Darstellung von reinem Titanium-, Zirkonium-, Hafnium-. Z Anorg Allg Chem 1925;148:345-50.
- [75] Briant CL, editor. Impurities in Engineering Materials Impact, Reliability, and Control. New York: Marcel Dekker Inc; 1999.
- [76] Wang WE, Olander DR. Computational thermodynamics of the ZrN system. J Alloys Compd 1995;224:153–8. https://doi.org/10.1016/0925-8388(95)01528-
- [77] Okamoto H. N-V (Nitrogen-Vanadium). J Phase Equilibria 2001;22:362. https://doi.org/10.1361/105497101770338923.
- [78] Wang WE, Kim YS, Hong HS. Characterization of the vanadium-nitrogen system with nitrogen pressure isobars. J Alloys Compd 2000;308:147–52. https://doi.org/10.1016/S0925-8388(00)00932-4.
- [79] Jarl M. A Thermodynamic Analysis of the Chromium-Nitrogen System. Calphad 1977;1(1):91-5.
- [80] Nagai S. The N-W system. Bull Alloy Phase Diagrams 1989;10(4):416.
- [81] Naito K, Tsuneo M. Review on Phase Equilibria and Defect Structures in the Niobium-Oxygen System. Solid State Ion 1984;12:125-34.
- [82] Wriedt HA. The O-W (oxygen-tungsten) system. Bull Alloy Phase Diagrams 1989;10:368-84. https://doi.org/10.1007/BF02877593.
- [83] Okamoto H. N-Ta (Nitrogen-Tantalum). J Phase Equilibria Diffus 2008;29:291. https://doi.org/10.1007/s11669-008-9316-x.
- [84] Murray JL, Wriedt HA. The O-Ti (Oxygen-Titanium) system. J Phase Equilibria 1987;8:148-65. https://doi.org/10.1007/BF02873201.
- [85] Wang WE. Partial thermodynamic properties of the Ti-N system. J Alloys Compd 1996;233:89–95. https://doi.org/10.1016/0925-8388(96)80039-9.
- [86] Okabe TH, Suzuki RO, Oishi T, Ono K. Thermodynamic Properties of Dilute Titanium-Oxygen Solid Solution in Beta Phase. Mater Trans 1991;32(5):485-8.
- [87] Takeuchi A, Inoue A. Classification of Bulk Metallic Glasses by Atomic Size Difference, Heat of Mixing and Period of Constituent Elements and Its Application to Characterization of the Main Alloying Element. Mater Trans 2005;46:2817–29. https://doi.org/10.2320/matertrans.46.2817.
- [88] Okamoto H, Schlesinger ME, Mueller EM. N (Nitrogen) Binary Alloy Phase Diagrams. Alloy Phase Diagrams 2018;3:498–502. https://doi.org/10.31399/asm. hb.v03.a0006179.
- [89] Mah AD, Gellert NL. Heats of Formation of Niobium Nitride, Tantalum Nitride and Zirconium Nitride from Combustion Calorimetry. J Am Chem Soc 1956;78: 3261–3. https://doi.org/10.1021/ja01595a007.
- [90] Klemme S, O'Neill HSC, Schnelle W, Gmelin E. The heat capacity of MgCr2O4, FeCr2O4, and Cr2O3 at low temperatures and derived thermodynamic properties. Am Mineral 2000:85:1686–93. https://doi.org/10.2138/am-2000-11-1212.
- [91] Carlson ON, Smith JF, Nafziger RH. The vanadium-nitrogen system: a review. Metall Mater Trans A 1986;17:1647–56. https://doi.org/10.1007/BF02817263.
- [92] Jehn H, Ettmayer P. The molybdenum-nitrogen phase diagram. J Less-Common Met 1978;28:85–98. http://www.sciencedirect.com/science/article/pii/0022508878900735/pdf?md5=ed6817ec4edd1d63138ace78400e0e4b&pid=1-s2.0-0022508878900735-main.pdf.
- [93] Skołyszewska-Kühberger B, Reichmann TL, Ipse H. A thermodynamic study of the cadmium-neodymium system. Monatsh Chem 2016;147:1001-8. https://doi.org/10.1007/s00706-016-1670-5.
- [94] Garg SP, Krishnamurthy N, Awasthi A, Venkatraman M. Erratum to: The O-Ta (Oxygen-Tantalum) system. J Phase Equilibria 1997;18:407. https://doi.org/10.1007/s11669-997-0076-9.
- [95] Massalski TB, Okamoto H, Subramanian PR, Kacprzak L. Hf (Hafnium) Binary Alloy Phase Diagrams. Alloy Phase Diagrams 2018;3:410–7. https://doi.org/10.31399/asm.hb.v03.a0006167.
- [96] Messmer RP, Briant CL. The role of chemical bonding in grain boundary embrittlement. Acta Metall 1982;30:457–67. https://doi.org/10.1016/0001-6160(82) 90226-7.
- [97] Wriedt HA. The O-V (Oxygen-Vanadium) system. Bull Alloy Phase Diagrams 1989;10:271–7. https://doi.org/10.1007/BF02877512.
- [98] Abriata JP, Garcés J, Versaci R. The O-Zr (Oxygen-Zirconium) system.pdf. Bull Alloy Phase Diagrams 1986;7(2):116-24.
- [99] Tetot R, Picard C, Boureau G, Gerdanian P. High temperature thermodynamics of the titanium oxygen system for O<0/ Ti<1. J Chem PHys 1978;69.
- [100] Snoek JL. Effect of small quantities of carbon and nitrogen on the elastic and plastic properties of iron. Physica 1941;8:711–33. https://doi.org/10.1016/ S0031-8914(41)90517-7.
- [101] Okamoto H. Cr-O (chromium-oxygen). J Phase Equilibria 1997;18:402. https://doi.org/10.1007/s11669-997-0072-0.
- [102] Gribaudo L, Arias D, Abriata J. The N-Zr (Nitrogen-Zirconium) System. J Phase Equilibria 1994;15:441-9. https://doi.org/10.1007/BF02647575.
- [103] Brewer L, Lamoreaux RH. The Mo-O system (Molybdenum-Oxygen). Bull Alloy Phase Diagrams 1980;1:85–9. https://doi.org/10.1007/BF02881199.
- [104] Kolb M, Freund LP, Fischer F, Povstugar I, Makineni SK, Gault B, et al. On the grain boundary strengthening effect of boron in γ/γ' Cobalt-base superalloys. Acta Mater 2018;145:247–54. https://doi.org/10.1016/j.actamat.2017.12.020.
- [105] Leitner K, Scheiber D, Jakob S, Primig S, Clemens H, Povoden-Karadeniz E, et al. How grain boundary chemistry controls the fracture mode of molybdenum. Mater Des 2018:142:36–43. https://doi.org/10.1016/j.matdes.2018.01.012.
- [106] Y.-S. Chen, P.-Y. Liu, R. Niu, A. Devaraj, H.-W. Yen, R.K.W. Marceau, J.M. Cairney, "Atom Probe Tomography for the Observation of Hydrogen in Materials: A Review," *Microsc. Microanal.* 29 (2023) 1–15. https://doi.org/10.1093/micmic/ozac005.
- [107] McCarroll IE, Bagot PAJ, Devaraj A, Perea DE, Cairney JM. New frontiers in atom probe tomography: a review of research enabled by cryo and/or vacuum transfer systems. Mater Today Adv 2020;7:100090. https://doi.org/10.1016/j.mtadv.2020.100090.
- [108] Zhou X, Tehranchi A, Curtin WA. Mechanism and Prediction of Hydrogen Embrittlement in fcc Stainless Steels and High Entropy Alloys. Phys Rev Lett 2021; 127:175501. https://doi.org/10.1103/PhysRevLett.127.175501.
- [109] Tehranchi A, Curtin WA. The role of atomistic simulations in probing hydrogen effects on plasticity and embrittlement in metals. Eng Fract Mech 2019;216: 106502. https://doi.org/10.1016/j.engfracmech.2019.106502.
- [110] Esayed AY, Northwood DO. Metal hydrides: A review of group V transition metals-niobium, vanadium and tantalum. Int J Hydrogen Energy 1992;17:41–52. https://doi.org/10.1016/0360-3199(92)90220-Q.
- [111] Cottrell AH. Unified theory of effects of segregated interstitials on grain boundary cohesion. Mater Sci Technol (United Kingdom) 1990;6:806–10. https://doi.org/10.1179/mst.1990.6.9.806.
- [112] Simbi DJ, Scully JC. The effect of residual interstitial elements and iron on mechanical properties of commercially pure titanium. Mater Lett 1996;26:35–9. https://doi.org/10.1016/0167-577X(95)00204-9.
- [113] Chong Y, Poschmann M, Zhang R, Zhao S, Hooshmand MS, Rothchild E, et al. Mechanistic basis of oxygen sensitivity in titanium. Sci Adv 2020;6:1–11. https://doi.org/10.1126/sciadv.abc4060.
- [114] Conrad H. Effect of interstitial solutes on the strength and ductility of titanium. Prog Mater Sci 1981;26:123–403. https://doi.org/10.1016/0079-6425(81) 90001-3.
- [115] Ogden HR, Jaffee RI. The Effects of Carbon, Oxygen, and Nitrogen on the Mechanical Properties of Titanium and Titanium Alloys, Columbus, Ohio, 1955. https://medium.com/@arifwicaksanaa/pengertian-use-case-a7e576e1b6bf.
- [116] Yamaguchi S. Interstitial Order-Disorder Transformation in the Ti-O Solid Solution. I. Ordered Arrangement of Oxygen. J Phys Soc Japan 1969;27:155–63. https://doi.org/10.1143/JPSJ.27.155.
- [117] Yamaguchi S. Ordered arrangement of oxygen in the interstitial solid solution of zirconium-oxygen system. J Phys Soc Japan 1968;24:855–68. https://doi.org/10.1143/JPSJ.24.855.
- [118] Ruban AV, Baykov VI, Johansson B, Dmitriev VV, Blanter MS. Oxygen and nitrogen interstitial ordering in hcp Ti, Zr, and Hf: An ab initio study. Phys Rev B Condens Matter Mater Phys 2010;82:1–10. https://doi.org/10.1103/PhysRevB.82.134110.
- [119] Hirabayashi M, Yamaguchi S, Arai T. Superstructure and Order-Disorder Transformation of Interstitial Oxygen in Hafnium. J Phys Soc Japan 1972;35:473–81. https://doi.org/10.1143/JPSJ.35.473.
- [120] Ritchie IG, Atrens A. The diffusion of oxygen in alpha-zirconium. J Nucl Mater 1977;67:254-64. https://doi.org/10.1016/0022-3115(77)90097-6.
- [121] Cerreta E, Gray GT, Hixson RS, Rigg PA, Brown DW. The influence of interstitial oxygen and peak pressure on the shock loading behavior of zirconium. Acta Mater 2005;53(6):1751–8.
- [122] Nayak SK, Hung CJ, Sharma V, Alpay SP, Dongare AM, Brindley WJ, et al. Insight into point defects and impurities in titanium from first principles. Npj Comput Mater 2018;4. https://doi.org/10.1038/s41524-018-0068-9.

- [123] Kornilov II. Effect of oxygen on titanium and its alloys. Met Sci Heat Treat 1973;15:826-9, https://doi.org/10.1007/BF00656056.
- [124] Stráský J, Janeček M, Harcuba P, Preisler D, Landa M. Biocompatible beta-Ti alloys with enhanced strength due to increased oxygen content. Titan Med Dent Appl 2018:371–92. https://doi.org/10.1016/B978-0-12-812456-7.00017-2.
- [125] Bisogni E, Mah G, Wert C. Diffusion of gases in special interstitial sites in hafnium. J Less-Common Met 1964;7:197–204. https://doi.org/10.1016/0022-5088
- [126] Yin F, Iwasaki S, Ping D, Nagai K. Snoek-type high-damping alloys realized in β-ti alloys with high oxygen solid solution. Adv Mater 2006;18:1541–4. https://doi.org/10.1002/adma.200600128.
- [127] Maksimov YA, Kornilov II, Vavilova VV. Properties of Ti-V and Ti-V-Al Alloys with Oxygen. Titan Its Alloy 1970:28-30.
- [128] Wu HH, Trinkle DR, Solute effect on oxygen diffusion in α-titanium, J Appl Phys 2013;113(22):223504.
- [129] Umbelino dos Santos L, Campo KN, Caram R, Najar Lopes ÉS. Oxygen addition in biomedical Ti-Nb alloys with low Nb contents: Effect on the microstructure and mechanical properties. Mater Sci Eng A 2021;823:141750.
- [130] Gunda NSH, Van der Ven A. Understanding the interactions between interstitial and substitutional solutes in refractory alloys: The case of Ti-Al-O. Acta Mater 2020;191:149–57. https://doi.org/10.1016/j.actamat.2020.04.017.
- [131] Hiraga K, Onozuka T, Hirabayashi M. Locations of Oxygen, Nitrogen and Carbon Atoms in Vanadium Determined by Neutron Diffraction. Mater Sci Eng 1977; 27(1):35–8.
- [132] Donoso JR, Reed-Hill RE. Slow strain-rate embrittlement of niobium by Oxygen. Metall Trans A 1976;7A:961–5. https://doi.org/10.1007/BF02644061.
- [133] Shkama T, Ishino S, Mishima Y. The Interaction Between Interstitial Impurities and Substitutional Solutes in Vanadium. J Nucl Mater 1977;68(3):315-23.
- [134] Ulitchny MG, Gibala R. The effects of interstitial solute additions on the mechanical properties of niobium and tantalum single crystals. J Less-Common Met 1973;33:105–16. https://doi.org/10.1016/0022-5088(73)90061-1.
- [135] Smialek RL, Mitchell TE. Interstitial solution hardening in tantalum single crystals. Philos Mag 1970;22:1105–27. https://doi.org/10.1080/
- [136] Jo MG, Madakashira PP, Suh JY, Han HN. Effect of oxygen and nitrogen on microstructure and mechanical properties of vanadium. Mater Sci Eng A 2016;675: 92–8. https://doi.org/10.1016/j.msea.2016.08.040.
- [137] Zhang J, Han WZ. Oxygen solutes induced anomalous hardening, toughening and embrittlement in body-centered cubic vanadium. Acta Mater 2020;196: 122–32. https://doi.org/10.1016/j.actamat.2020.06.023.
- [138] Yang PJ, Li QJ, Tsuru T, Ogata S, Zhang JW, Sheng HW, et al. Mechanism of hardening and damage initiation in oxygen embrittlement of body-centred-cubic niobium. Acta Mater 2019;168:331–42. https://doi.org/10.1016/j.actamat.2019.02.030.
- [139] Cantelli R, Szkopiak ZC. Effects of Interstitial Oxygen and Nitrogen on the Mechanical Properties of Niobium-Titanium Alloys. Appl Phys 1976;9(3):253-7.
- [140] Spitzig WA, Owen CV, Scott TE. The effects of interstitials and hydrogen-interstitial interactions on low temperature hardening and embrittlement in V, Nb, and Ta. Metall Trans A 1986;17:1179–89. https://doi.org/10.1007/BF02665317.
- [141] Park SC, Beckerman LP, Reed-Hill RE. On the Portevin-Le Chatelier Effect Due To Snoek Strain Aging in the Niobium Oxygen System. Metall Trans A 1983;14A: 463–9. https://doi.org/10.1007/bf02644223.
- [142] Pint BA, DiStefano JR. The role of oxygen uptake and scale formation on the embrittlement of vanadium alloys. Oxid Met 2005;63:33–55. https://doi.org/10.1007/s11085-005-1950-7.
- [143] Cochardt AW, Schoek G, Wiedersich H. Interaction between dislocations and interstitial atoms in body-centered cubic metals. Acta Metall 1955;3:533–7. https://doi.org/10.1016/0001-6160(55)90111-5.
- [144] Setyawan W, Kurtz RJ. Effects of transition metals on the grain boundary cohesion in tungsten. Scr Mater 2012;66:558–61. https://doi.org/10.1016/j.
- [145] Medvedeva NI, Gornostyrev YN, Freeman AJ. Solid solution softening and hardening in the group-V and group-VI bcc transition metals alloys: First principles calculations and atomistic modeling. Phys Rev B Condens Matter Mater Phys 2007;76:3–6. https://doi.org/10.1103/PhysRevB.76.212104.
- [146] Liu G, Zhang GJ, Jiang F, Ding XD, Sun YJ, Sun J, et al. Nanostructured high-strength molybdenum alloys with unprecedented tensile ductility. Nat Mater 2013;12:344–50. https://doi.org/10.1038/nmat3544.
- [147] Krajnikov AV, Drachinskiy AS, Slyunyaev VN. Grain boundary segregation in recrystallized molybdenum alloys and its effect on brittle intergranular fracture. Int J Refract Met Hard Mater 1992;11:175–80. https://doi.org/10.1016/0263-4368(92)90060-F.
- [148] Joshi A, Stein DF. Intergranular brittleness studies in Tungsten Using Auger Spectroscopy. Metall Trans 1970;1:2543-6. https://doi.org/10.1007/BF03038381.
- [149] Brosse JB, Fillit R, Biscondi M. Intrinsic intergranular brittleness of molybdenum. Scr Metall 1981;15:619–23. https://doi.org/10.1016/0036-9748(81)90038-7.
- [150] Liu CT, Inouye H. Internal Oxidation and Mechanical Properties of TZM-Mo Alloy. Metall Trans 1974;5:2515-25. https://doi.org/10.1007/BF02643872.
- [151] Majumdar S, Raveendra S, Samajdar I, Bhargava P, Sharma IG. Densification and grain growth during isothermal sintering of Mo and mechanically alloyed Mo-TZM. Acta Mater 2009;57:4158–68. https://doi.org/10.1016/j.actamat.2009.05.013.
- [152] Prasad CVS, Baligidad RG, Gokhale AA. Chapter 12 Aerospace Materials and Material Technologies, Volume 1: Aerospace Material Technologies, Springer, 2017. https://doi.org/10.1007/978-981-10-2134-3.
- [153] Sankar M, Baligidad RG, Satyanarayana DVV, Gokhale AA. Effect of internal oxidation on the microstructure and mechanical properties of C-103 alloy. Mater Sci Eng A 2013;574:104–12. https://doi.org/10.1016/j.msea.2013.02.057.
- [154] Tien JK, Collier JP, Vignoul G. The Role of Niobium and Other Refractory Elements in Superalloys. TMS 1969:553–66. https://doi.org/10.7449/1989/superalloys 1989 553 566.
- [155] Trinkle DR, Woodward C. The Chemistry of Deformation: How Solutes Soften Pure Metals. Science 2005;80-:310. https://doi.org/10.1126/science.311.5758.177.
- [156] Wei Q, Jiao T, Ramesh KT, Ma E, Kecskes LJ, Magness L, et al. Mechanical behavior and dynamic failure of high-strength ultrafine grained tungsten under uniaxial compression. Acta Mater 2006;54:77–87. https://doi.org/10.1016/j.actamat.2005.08.031.
- [157] Kecskes LJ, Cho KC, Dowding RJ, Schuster BE, Valiev RZ, Wei Q. Grain size engineering of bcc refractory metals: Top-down and bottom-up-Application to tungsten. Mater Sci Eng A 2007;467:33–43. https://doi.org/10.1016/j.msea.2007.02.099.
- [158] Chan KS. A computational approach to designing ductile Nb-Ti-Cr-Al solid-solution alloys. Metall Mater Trans A Phys Metall Mater Sci 2001;32:2475–87. https://doi.org/10.1007/s11661-001-0037-6.
- [159] Qi L, Chrzan DC. Tuning ideal tensile strengths and intrinsic ductility of bcc refractory alloys. Phys Rev Lett 2014;112:1–5. https://doi.org/10.1103/ PhysRevLett.112.115503.
- [160] Senkov O, Gorsse S, Wheeler R, Payton E, Miracle D. Effect of re on the microstructure and mechanical properties of nbtizr and tatizr equiatomic alloys. Metals (Basel) 2021;11(11):1819.
- [161] Wan Y, Wang X, Zhang Z, Mo J, Shen B, Liang X. Structures and properties of the (NbMoTaW)100-xCx high-entropy composites. J Alloys Compd 2022;889: 161645. https://doi.org/10.1016/j.jallcom.2021.161645.
- [162] Butler TM, Senkov ON, Velez MA, Daboiku TI. Microstructures and mechanical properties of CrNb, CrNbTi, and CrNbTaTi concentrated refractory alloys. Intermetallics 2021;138:107323. https://doi.org/10.1016/j.intermet.2021.107323.
- [163] Kang B, Lee J, Ryu HJ, Hong SH. Ultra-high strength WNbMoTaV high-entropy alloys with fine grain structure fabricated by powder metallurgical process. Mater Sci Eng A 2018;712:616–24. https://doi.org/10.1016/j.msea.2017.12.021.
- [164] Huber F, Bartels D, Schmidt M. In situ alloy formation of a WMoTaNbV refractory metal high entropy alloy by laser powder bed fusion (Pbf-lb/m). Materials (Basel) 2021;14:1–12. https://doi.org/10.3390/ma14113095.
- [165] Wang M, Ma ZL, Xu ZQ, Cheng XW. Designing VxNbMoTa refractory high-entropy alloys with improved properties for high-temperature applications. Scr Mater 2021;191:131–6. https://doi.org/10.1016/j.scriptamat.2020.09.027.
- [166] Yao H, Qiao JW, Gao MC, Hawk JA, Ma SG, Zhou H. MoNbTaV medium-entropy alloy. Entropy 2016;18:1–15. https://doi.org/10.3390/e18050189.

- [167] Yao HW, Qiao JW, Gao MC, Hawk JA, Ma SG, Zhou HF, et al. NbTaV-(Ti, W) refractory high-entropy alloys: Experiments and modeling. Mater Sci Eng A 2016; 674:203–11. https://doi.org/10.1016/j.msea.2016.07.102.
- [168] Han ZD, Chen N, Zhao SF, Fan LW, Yang GN, Shao Y, et al. Effect of Ti additions on mechanical properties of NbMoTaW and VNbMoTaW refractory high entropy alloys. Intermetallics 2017;84:153–7. https://doi.org/10.1016/j.intermet.2017.01.007.
- [169] Xu Q, Wang Qi, Chen D-Z, Fu Y-A, Shi Q-S, Yin Y-J, et al. Microstructure characteristics and mechanical properties of NbMoTiVWSix refractory high-entropy alloys. China Foundry 2022;19(6):495–502.
- [170] Ding XY, Zheng HY, Zhang PP, Luo LM, Wu YC, Yao JH. Microstructure and Mechanical Properties of WTaVCrTi Refractory High-Entropy Alloy by Vacuum Levitation Melting for Fusion Applications. J Mater Eng Perform 2022. https://doi.org/10.1007/s11665-022-07688-2.
- [171] Zhang W, Jiang W, Wu S, Tao S, Zhu B, Guo S. Microstructural and Mechanical Evaluation of NbMoTiVSix(x = 0, 0.25) Refractory High-Entropy Alloys at High Temperature. Adv Eng Mater 2022;24:1–9. https://doi.org/10.1002/adem.202101248.
- [172] Yao HW, Qiao JW, Hawk JA, Zhou HF, Chen MW, Gao MC. Mechanical properties of refractory high-entropy alloys: Experiments and modeling. J Alloys Compd 2017;696:1139–50. https://doi.org/10.1016/j.jallcom.2016.11.188.
- [173] Yang C, Bian H, Aoyagi K, Hayasaka Y, Yamanaka K, Chiba A. Synergetic strengthening in HfMoNbTaTi refractory high-entropy alloy via disordered nanoscale phase and semicoherent refractory particle. Mater Des 2021;212:110248. https://doi.org/10.1016/j.matdes.2021.110248.
- [174] Tseng KK, Juan CC, Tso S, Chen HC, Tsai CW, Yeh JW. Effects of Mo, Nb, Ta, Ti, and Zr on mechanical properties of equiatomic Hf-Mo-Nb-Ta-Ti-Zr alloys. Entropy 2019;21:1–14. https://doi.org/10.3390/e21010015.
- [175] Senkov ON, Daboiku TI, Butler TM, Detor A, Payton EJ. "Effect of Mo on the microstructure and mechanical properties of (Hf0.73Ta0.27)100-XMoX (X = 0, 5, 16, 21 and 30 at.%) alloys,". Int. J. Refract. Met. Hard Mater. 2022;103:105737. https://doi.org/10.1016/j.ijrmhm.2021.105737.
- [176] Wang J, Jiang F, Wang L, Yang G, Xu M, Yi J. Cr addition-mediated simultaneous achievement of excellent strength and plasticity in non-equiatomic Nb-Ti-Zr-Ta-base refractory high-entropy alloys. J Alloys Compd 2023;946:169423. https://doi.org/10.1016/j.jallcom.2023.169423.
- [177] Rao Y, Baruffi C, De Luca A, Leinenbach C, Curtin WA. Theory-guided design of high-strength, high-melting point, ductile, low-density, single-phase BCC high entropy alloys. Acta Mater 2022;237:118132. https://doi.org/10.1016/j.actamat.2022.118132.
- [178] Senkov ON, Gild J, Butler TM. Microstructure, mechanical properties and oxidation behavior of NbTaTi and NbTaZr refractory alloys. J Alloys Compd 2021; 862:158003. https://doi.org/10.1016/j.jallcom.2020.158003.
- [179] Wei Q, Zhang A, Han J, Xin B, Su B, Wang X, et al. A novel Hf30Nb25Ta25Ti15Mo5 refractory high entropy alloy with excellent combination of strength and ductility. Mater Sci Eng A 2022;857:144035. https://doi.org/10.1016/j.msea.2022.144035.
 [180] Yurchenko N, Panina E, Tojibaey A, Novikov V, Salishchey G, Zherebtsov S, et al. Effect of B2 ordering on the tensile mechanical properties of refractory.
- [180] Yurchenko N, Panina E, Tojibaev A, Novikov V, Salishchev G, Zherebtsov S, et al. Effect of B2 ordering on the tensile mechanical properties of refractory AlxNb40Ti40V20-x medium-entropy alloys. J Alloys Compd 2023;937:168465. https://doi.org/10.1016/j.jallcom.2022.168465.
- [181] Wei S, Kim SJ, Kang J, Zhang Y, Zhang Y, Furuhara T, et al. Natural-mixing guided design of refractory high-entropy alloys with as-cast tensile ductility. Nat Mater 2020;19:1175–81. https://doi.org/10.1038/s41563-020-0750-4.
- [182] Tao S, Jiang W, Zhang W, Qiu H, Wu S, Guo S, et al. Microstructure evolution and mechanical properties of NbHfTiVCx novel refractory high entropy alloys with variable carbon content. J Alloys Compd 2022;928:166986. https://doi.org/10.1016/j.jallcom.2022.166986.
- [183] Huang W, Hou J, Wang X, Qiao J, Wu Y. Excellent room-temperature tensile ductility in as-cast Ti 37 V 15 Nb 22 Hf 23 W 3 refractory high entropy alloys. Intermetallics 2022;151:107735. https://doi.org/10.1016/j.intermet.2022.107735.
- [184] Cui D, Zhang Y, Liu L, Li Y, Wang L, Wang Z, et al. Oxygen-assisted spinodal structure achieves 1.5 GPa yield strength in a ductile refractory high-entropy alloy. J Mater Sci Technol 2023;157:11–20.
- [185] Fan XJ, Qu RT, Zhang ZF. Remarkably high fracture toughness of HfNbTaTiZr refractory high-entropy alloy. J Mater Sci Technol 2022;123:70–7. https://doi.org/10.1016/j.jmst.2022.01.017.
- [186] Ozerov M, Sokolovsky V, Nadezhdin S, Zubareva E, Zherebtsova N, Stepanov N, et al. Microstructure and mechanical properties of medium-entropy TiNbZr alloy-based composites, reinforced with boride particles. J Alloys Compd 2023;938:168512.
- [187] Jiao M, Lei Z, Wu Y, Du J, Zhou XY, Li W, et al. Manipulating the ordered oxygen complexes to achieve high strength and ductility in medium-entropy alloys. Nat Commun 2023;14:1–11. https://doi.org/10.1038/s41467-023-36319-0.
- [188] Gou S, Gao M, Shi Y, Li S, Fang Y, Chen X, et al. Additive manufacturing of ductile refractory high-entropy alloys via phase engineering. Acta Mater 2023;248: 118781. https://doi.org/10.1016/j.actamat.2023.118781.
- [189] Lai W, Liu H, Yu X, Yi Y, Li W, Zhou S, et al. A design of TiZr-rich body-centered cubic structured multi-principal element alloys with outstanding tensile strength and ductility. Mater Sci Eng A 2021;813:141135. https://doi.org/10.1016/j.msea.2021.141135.
- [190] Wu SJ, Di Wang X, Lu JT, Qu RT, Zhang ZF. Room-Temperature Mechanical Properties of V20Nb20Mo20Ta20W20 High-Entropy Alloy. Adv Eng Mater 2018; 20:1–8. https://doi.org/10.1002/adem.201800028.
- [191] Zou Y, Ma H, Spolenak R. Ultrastrong ductile and stable high-entropy alloys at small scales. Nat Commun 2015;6. https://doi.org/10.1038/ncomms8748.
- [192] Wang X, Maresca F, Cao P. The hierarchical energy landscape of screw dislocation motion in refractory high-entropy alloys. Acta Mater 2022;234:118022
- [193] Han ZD, Luan HW, Liu X, Chen N, Li XY, Shao Y, et al. Microstructures and mechanical properties of TixNbMoTaW refractory high-entropy alloys. Mater Sci Eng A 2018;712:380–5. https://doi.org/10.1016/j.msea.2017.12.004.
- [194] Bai L, Hu Y, Liang X, Tong Y, Liu J, Zhang Z, et al. Titanium alloying enhancement of mechanical properties of NbTaMoW refractory high-Entropy alloy: First-principles and experiments perspective. J Alloys Compd 2021;857:157542. https://doi.org/10.1016/j.jallcom.2020.157542.
- [195] Bhandari U, Zhang C, Zeng C, Guo S, Yang S. Computational and experimental investigation of refractory high entropy alloy mo15nb20re15ta30w20. J Mater Res Technol 2020;9:8929–36. https://doi.org/10.1016/j.jmrt.2020.06.036.
- [196] Wan Y, Wang Q, Mo J, Zhang Z, Wang X, Liang X, et al. WReTaMo Refractory High-Entropy Alloy with High Strength at 1600 °C. Adv Eng Mater 2022;24:1–8. https://doi.org/10.1002/adem.202100765.
- [197] Wei Q, Luo G, Tu R, Zhang J, Shen Q, Cui Y, et al. High-temperature ultra-strength of dual-phase Re0.5MoNbW(TaC)0.5 high-entropy alloy matrix composite. J Mater Sci Technol 2021;84:1–9. https://doi.org/10.1016/j.jmst.2020.12.015.
- [198] Tong Y, Bai L, Liang X, Hua M, Liu J, Li Y, et al. Mechanical performance of (NbTaW)1–xMox (x = 0, 0.05, 0.15, 0.25) refractory high entropy alloys: Perspective from experiments and first principles calculations. J Alloys Compd 2021;873:159740. https://doi.org/10.1016/j.jallcom.2021.159740.
- [199] Samin AJ. A computational investigation of the interstitial oxidation thermodynamics of a Mo-Nb-Ta-W high entropy alloy beyond the dilute regime. J Appl Phys 2020;128(21):215101.
- [200] Zhang C, MacDonald BE, Guo F, Wang H, Zhu C, Liu X, et al. Cold-workable refractory complex concentrated alloys with tunable microstructure and good room-temperature tensile behavior. Scr Mater 2020;188:16–20. https://doi.org/10.1016/j.scriptamat.2020.07.006.
- [201] Huang YC, Lai YC, Lin YH, Wu SK. A study on the severely cold-rolled and annealed quaternary equiatomic derivatives from quinary HfNbTaTiZr refractory high entropy alloy. J Alloys Compd 2021;855:157404. https://doi.org/10.1016/j.jallcom.2020.157404.
- [202] Zhang R, Zhao S, Ding J, Chong Y, Jia T, Ophus C, et al. Short-range order and its impact on the CrCoNi medium-entropy alloy. Nature 2020;581:283–7. https://doi.org/10.1038/s41586-020-2275-z.
- [203] Geiger I, Luo J, Lavernia EJ, Cao P, Apelian D, Rupert TJ. Influence of chemistry and structure on interfacial segregation in NbMoTaW with high-throughput atomistic simulations. J Appl Phys 2022;132(23):235301.
- [204] Aksoy D, McCarthy MJ, Geiger I, Apelian D, Hahn H, Lavernia EJ, et al. Chemical order transitions within extended interfacial segregation zones in NbMoTaW. J Appl Phys 2022;132(23):235302.
- [205] Yuan X, Wu Y, Zhou M, Liu X, Wang H, Jiang S, et al. Effects of trace elements on mechanical properties of the TiZrHfNb high-entropy alloy. J Mater Sci Technol 2023;152:135–47. https://doi.org/10.1016/j.jmst.2022.12.025.